E84-10042

CR-171 715
C.1

AgRISTARS

SR-K3-04438

A Joint Program for
Agriculture and
Resources Inventory
Surveys Through
Aerospace
Remote Sensing

Supporting Research

AUGUST 1983

A SIMULATION STUDY OF SCENE CONFUSION FACTORS IN SENSING SOIL MOISTURE FROM ORBITAL RADAR

M. C. DOBSON, S. MOEZZI, R. ROTH
F. T. ULABY, PRINCIPAL INVESTIGATOR

REMOTE SENSING LABORATORY
THE UNIVERSITY OF KANSAS CENTER FOR RESEARCH, INC.
LAWRENCE, KANSAS

Lyndon B. Johnson Space Center
Houston, Texas 77058

(E84-10042) A SIMULATION STUDY OF SCENE CONFUSION FACTORS IN SENSING SOIL MOISTURE FROM ORBITAL RADAR Final Report (Kansas Univ. Center for Research, Inc.) 138 p HC A07/MF A01 CSCL 08M G3/43

N84-13635

Unclas
00042

1. Report No.	2. Government Accession No.	3. Recipient's Catalog No.
SR-K3-04438		

4. Title and Subtitle
A SIMULATION STUDY OF SCENE CONFUSION FACTORS IN SENSING SOIL MOISTURE FROM ORBITAL RADAR

5. Report Date August 1983

6. Performing Organization Code

7. Author(s)
M. C. Dobson, S. Moezzi, F. T. Ulaby, and E. Roth

8. Performing Organization Report No. RSL 601-1

9. Performing Organization Name and Address
Remote Sensing Laboratory
University of Kansas Center for Research, Inc.
2291 Irving Hill Drive - Campus West
Lawrence, Kansas 66045-2969

10. Work Unit No.

11. Contract or Grant No. NCC 9-6

12. Sponsoring Agency Name and Address
Dale Browne
NASA/Johnson Space Center
Houston, Texas 77058

13. Type of Report and Period Covered Final Report

14. Sponsoring Agency Code

15. Supplementary Notes

16. Abstract

Simulated C-band radar imagery for a 124-km by 108-km test site in eastern Kansas is used to classify soil moisture. Simulated radar resolutions are 100 m by 100 m, 1 km by 1 km, and 3 km by 3 km; all images are processed with greater than 23 independent samples. The simulated radar operates at 4.75 GHz with HH polarization and over 7° and 17° angles of incidence.

Distributions of actual near-surface soil moisture are established daily for a 23-day accounting period using a water budget model dependent upon precipitation, potential evaporation, crop-canopy cover, crop development stage, surface slope, antecedent soil moisture, and soil hydrologic properties. Within the 23-day period, three orbital radar overpasses are simulated roughly corresponding to generally moist, wet, and dry soil moisture conditions. The radar simulations are performed by a target/sensor interaction model dependent upon a terrain model, land-use classification, and near-surface soil moisture distribution. Rayleigh fading, layover, and shadow are accounted for by the model. For each overpass date and each radar resolution, the received power and range position of a given pixel is used to classify near-surface soil moisture via a generalized algorithm requiring no ancillary data about scene characteristics.

The accuracy of soil-moisture classification is evaluated for each single-date radar observation and also for multi-date detection of relative soil moisture change. In general, the results for single-date moisture detection show that 70% to 90% of cropland can be correctly classified to within +/- 20% of the true percent of field capacity. For

17. Key Words (Suggested by Author(s))
Radar, Soil Moisture, Orbital, Simulation, Classification

18. Distribution Statement

19. Security Classif. (of this report)	20. Security Classif. (of this page)	21. No. of Pages	22. Price*
Unclassified	Unclassified	127	

*For sale by the National Technical Information Service, Springfield, Virginia 22161

Abstract continued:

a given radar resolution, the expected classification accuracy is shown to be dependent upon both the general soil moisture condition and also the geographical distribution of land-use (field-size distribution and dispersion of categories) and topographic relief. An analysis of cropland, urban, pasture/rangeland, and woodland subregions within the test site indicates that multi-temporal detection of relative soil moisture change is least sensitive to classification error resulting from scene complexity and topographic effects.

The 100 m by 100 m radar resolution is found to yield the most robust classification results, and it is concluded that further degradation of image resolution should be implemented in post-detection processing when and where coarse resolution analysis is warranted.

TABLE OF CONTENTS

LIST OF FIGURES

LIST OF TABLES

A SIMULATION STUDY OF SCENE CONFUSION FACTORS IN SENSING SOIL MOISTURE FROM ORBITAL RADAR

M. C. Dobson, S. Moezzi, F. T. Ulaby, and E. Roth
Remote Sensing Laboratory
University of Kansas Center for Research, Inc.
Lawrence, Kansas 66045-2969

ABSTRACT

Simulated C-band radar imagery for a 124-km by 108-km test site in eastern Kansas is used to classify soil moisture. Simulated radar resolutions are 100 m by 100 m, 1 km by 1 km, and 3 km by 3 km; all images are processed with greater than 23 independent samples. The simulated radar operates at 4.75 GHz with HH polarization and over 7° to 17° angles of incidence.

Distributions of actual near-surface soil moisture are established daily for a 23-day accounting period using a water budget model dependent upon precipitation, potential evaporation, crop-canopy cover, crop development stage, surface slope, antecedent soil moisture, and soil hydrologic properties. Within the 23-day period, three orbital radar overpasses are simulated roughly corresponding to generally moist, wet, and dry soil moisture conditions. The radar simulations are performed by a target/sensor interaction model dependent upon a terrain model, land-use classification, and near-surface soil moisture distribution. Rayleigh fading, layover, and shadow are accounted for by the model. For each overpass date and each radar resolution, the received power and range position of a given pixel is used to classify near-surface soil moisture via a generalized

algorithm requiring no ancillary data about scene characteristics.

The accuracy of soil-moisture classification is evaluated for each single-date radar observation and also for multi-date detection of relative soil moisture change. In general, the results for single-date moisture detection show that 70% to 90% of cropland can be correctly classified to within +/- 20% of the true percent of field capacity. For a given radar resolution, the expected classification accuracy is shown to be dependent upon both the general soil moisture condition and also the geographical distribution of land-use (field-size distribution and dispersion of categories) and topographic relief. An analysis of cropland, urban, pasture/rangeland, and woodland subregions within the test site indicates that multi-temporal detection of relative soil moisture change is least sensitive to classification error resulting from scene complexity and topographic effects.

The 100 m by 100 m radar resolution is found to yield the most robust classification results, and it is concluded that further degradation of image resolution should be implemented in post-detection processing when and where coarse resolution analysis is warranted.

1.0 INTRODUCTION

Simulation techniques have been employed to study the relationship between spatial resolution and the accuracy at which soil moisture can be estimated from orbital C-band radar imagery [1,2]. These studies were based upon the land-use and crop-canopy-cover distributions present within a relatively small agricultural test site (18 km x 19 km) adjacent to the Kansas River in eastern Kansas. Image simulation techniques were used to generate synthetic-aperture radar (SAR) images at a frequency of 4.75 GHz with HH polarization and with angles of incidence between 7° and 22° from nadir. SAR images were produced at three different spatial resolutions: 20 m by 20 m with 12 looks, 93 m by 100 m with 23 looks, and 1 km by 1 km with 230 looks. In addition, simulated real-aperture radar (RAR) imagery was produced with a spatial resolution of 2.6 km x 3.1 km with 363 looks. Analysis of these images demonstrated that for relatively flat agricultural portions of the test site about 90% of the 20-m by 20-m pixel elements can be correctly classified to within +/- 20 percent of field capacity using a generalized soil moisture algorithm. In general, moisture classification accuracy was found to be greatest for coarser resolution imagery due to the increased number of looks; however, the results also showed a distinct classification-accuracy dependence on the complexity of the "true" soil moisture distribution and also upon the spatial distribution of land-use elements within the test site.

As a consequence, the current study is designed to examine further the effects of the spatial distribution of land-use categories, the agricultural field-size distribution, the crop-canopy mix, and the variability of local topographic relief on the soil-moisture classification accuracy achievable by various orbital radar resolutions at 4.75 GHz, HH polarization, and angles of incidence from 7° to 17°. An area of 124 km by 108 km, including most of the Lawrence, Kansas USGS quadrangle (1:250,000), serves as the test site. The area includes large subregions dominated by urban features, mixed cropland, rangeland and pasture, or deciduous woodland. Simulated radar imagery of this test site at resolutions of 100 m by 100 m, 1 km by 1 km, and 3 km by 3 km are used to classify soil moisture, which is subsequently compared to the input "true" soil moisture. Classification accuracies of each radar resolution are compared for the whole test site and also for each of four subregions related to different mixtures of land-use. Since the number of processed looks for all resolutions is large ($N \geq 23$), the relative classification accuracies of each resolution should be only minimally biased by fading statistics.

The dynamic behavior of each 100 m by 100 m grid cell within the simulation test site is modeled over a 23 day time period with respect to near surface soil moisture, crop canopy cover, crop stage-of-growth, and soil surface roughness. The input parameters to this model include static conditions such as topography and soil association and also dynamic components consisting of cropping practices and daily meteorological conditions. The cropping parameters are based upon a stochastic treatment of average crop calendar, field size distribution, and crop development while the meteorological data includes daily rainfall and potential evaporation. The output of this model consists of daily updates of near surface (0-5 cm) soil moisture and radar backscatter category which is approximately equivalent to a Level III land-use category [3]. The model is run for a 23 day period and the outputs are saved on 3 dates corresponding to hypothetical orbital overpasses each nine days apart. The overpass dates were selected independent of any consideration of orbital mechanics but rather to represent three distinctive soil moisture distributions over the test site: very wet, moist, and dry. The above moisture classifications are very general, however, since the large size of the data base and the late spring time frame of the simulations leads to highly variable regional soil moisture distributions on any given date.

For each orbital overpass, a target-sensor interaction model produces simulated radar imagery for each of the three radar resolutions. The simulation model accounts for the effects of Rayleigh fading and geometric properties such as layover and shadowing [22]. Each simulated radar image is then subjected to a generalized algorithm (requiring only the amplitude of received power and the range position of a given pixel) which classifies the image into estimated soil moisture. These distributions of estimated soil moisture are subsequently compared with the distributions of actual near-surface soil moisture on a grid-cell basis for each date.

In addition to testing the absolute classification accuracies of each radar resolution for each of the three overpass dates in an instantaneous sense, multi-temporal data from two of the overpasses is used to evaluate the merits of relative change detection of near surface soil moisture as estimated from each of the three simulated radar resolutions. The above process is shown schematically in Figure 1.

2.0 TEST-SITE DATA BASE

In order to quantify the radar backscattering from a given terrain element, certain geometric and dielectric properties of the target scene must be known. First, the three-dimensional cartographic coordinates of each element must be specified relative to the orbital radar in order to compute range, area, and local incidence angle. Secondly, the radar backscattering category must be established; this is roughly equivalent to a level-III land-use classification category [3]. Finally, many land-use categories have backscattering properties that vary as a function of crop-canopy cover, row directionality, and near-surface soil

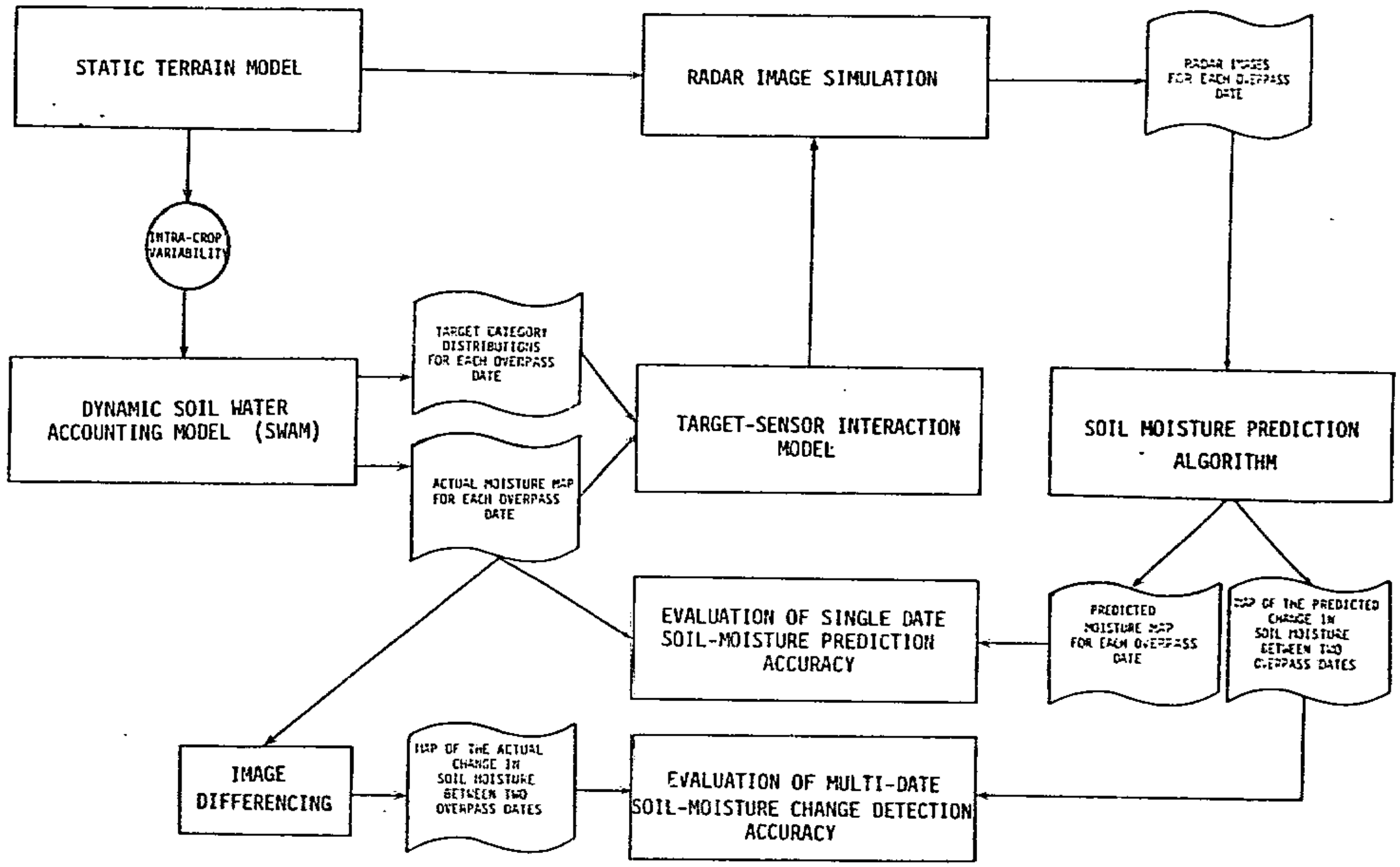

Figure 1. Flowchart of simulation approach.

moisture. A three-tiered digital data base is constructed to describe the spatial distribution of category elements and a dynamic model acts upon this distribution to vary target dielectric and backscattering properties as a function of time. It is assumed that all target properties are laterally homogeneous within a given 100 m by 100 m terrain element.

2.1 Terrain Model and Radar Backscattering Categories

Digital elevation data from the Defense Mapping Agency provide a static model of the terrain geometry. These data are corrected for scanning errors and resampled to yield a mean elevation for each 100-m by 100-m grid element within the 124-km by 108-km test site. An image-format presentation of the digital elevation data is shown in Figure 2.

The specification of radar backscattering category for each 100-m by 100-m grid element involves a three-step process that accurately describes the spatial distribution of the categories shown in Table 1 in a stochastic sense. A two-dimensional digital matrix of Level-II land-use classification is given by USGS land-use and land-cover digital data (LUDA) for the Lawrence, Kansas quadrangle. Level-II categories with similar radar backscattering properties (such as lakes and rivers) are redefined as equivalent backscattering categories. The Level-II LUDA category of cropland is insufficient to specify unique backscattering characteristics; thus a stochastic process is

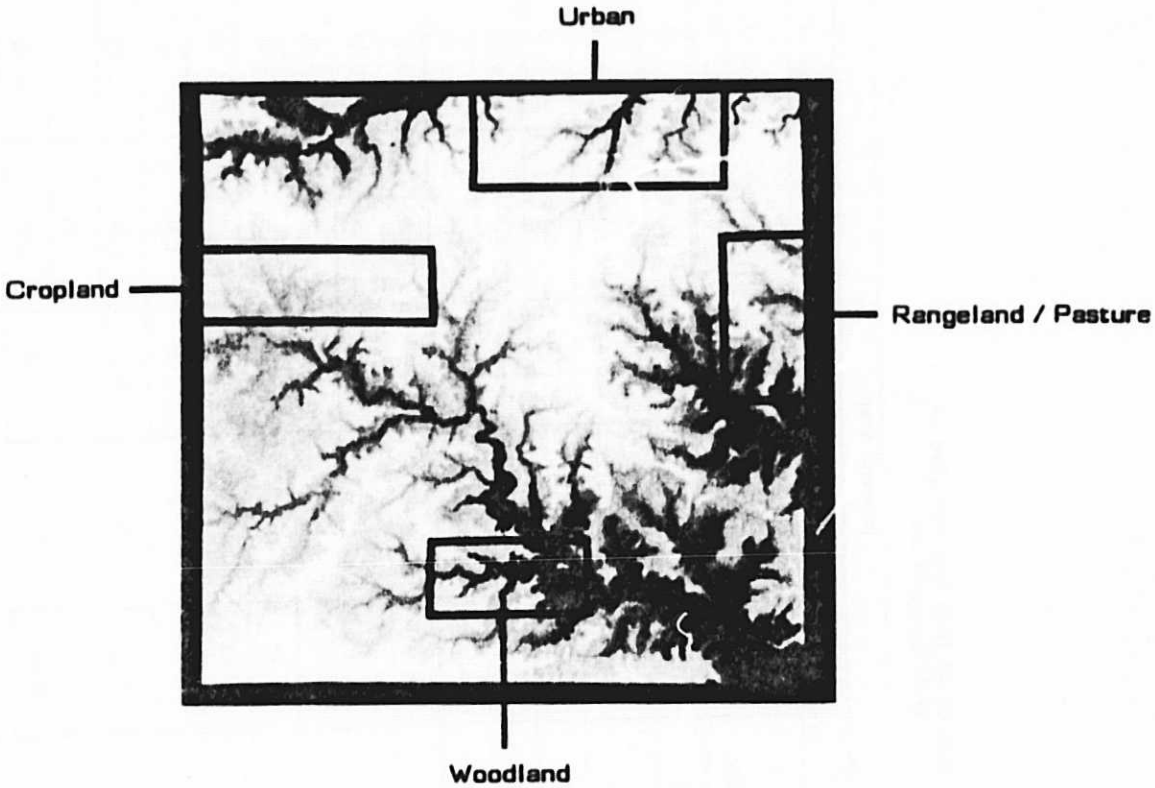

Figure 2. Digital terrain data of the test site showing the positions of the four subregions.

TABLE 1. Area Percent of Data Base Assigned to Each Target Class

Backscattering Category	Percent Area						
	Day 141					Day 150	Day 160
	Whole Test Site	Cropland	Urban	Rangeland and Pasture	Forest	Whole Test Site	Whole Test Site
Residential	2.00	0.25	23.32	0.42	0.07	2.00	2.00
Buildings (Commercial and Industrial)	0.28	0.04	2.77	0.06	0.00	0.28	0.28
Roads	0.88	0.82	5.35	0.08	0.00	0.88	0.88
Woodland (Deciduous)	6.44	2.62	3.22	3.22	26.41	6.44	6.44
Water	1.71	0.03	0.12	0.12	13.25	1.49	0.53
Smooth Bare Soil	0.05	0.04	0.06	0.09	0.10	0.05	0.05
Medium Rough Bare Soil*	24.32	27.89	11.61	21.31	17.96	21.43	18.47
Rough Bare Soil	0.54	0.08	2.42	0.07	0.38	0.55	0.56
Pasture / Rangeland	48.61	50.83	36.77	61.53	30.24	48.61	49.30
Wheat	5.25	5.81	2.63	4.02	4.26	5.26	5.33
Corn	0.50	0.79	0.29	0.50	0.20	1.43	1.46
Soybeans	0.0	0.0	0.0	0.0	0.0	1.36	2.63
Sorghum	0.0	0.0	0.0	0.0	0.0	0.01	0.02
Oats	0.50	0.43	0.03	0.38	0.46	0.49	0.50
Alfalfa	8.92	10.37	4.77	8.23	6.67	8.93	9.06

*10% of corn, 0% of soybeans, and 0% of sorghum emergent on Julian day 141; non-emergent cropland is classified as medium rough bare soil.

used to further define the spatial distribution of particular agricultural crops. A random sample of U-2 high-altitude color IR images is used to generate statistics on agricultural field-size distribution for each of the twelve counties within the test site. These statistics are then used to assign random field-boundary networks within each county. The distribution of field sizes is given by county in Table 2.

Specific crop categories and row directions are randomly assigned to each field within a county, based upon an historical enumeration of crop acreage for each county provided by the Kansas State Board of Agriculture and the Missouri Department of Agriculture. These acreages are given by county in Table 3. In addition, since all crops are not grown concurrently, crop calendar data [4] is used to factor planting and harvest into the time history of each field. Within a given crop, planting and crop-development stages established for this area are used to change a given field's backscatter category from bare soil to that of the crop after emergence in a stochasitc fashion. The fields of each crop type are subdivided into ten subgroups each with a distinctive cropping history. Thus, the crop-type distribution will vary locally as a function of time within the 23 day simulation period. The land-use and crop-type distributions for the entire 124 km by 108 km test site are shown in Table 1 for each of the hypothetical orbital overpass dates. The simulation period runs from May 18

ORIGINAL PAGE IS
OF POOR QUALITY

TABLE 2. Field-Size Distributions for the Agricultural Portions of the Land-Use Subregions

Subregion	Percent of Agricultural Area									
	Field Size in Acres									
	10	20	30	40	60	80	100	120	140	160
Urban (Kansas City)	20	18	10	15	7	16	3	2	2	7
Pasture/Rangeland	4	11	6	18	8	28	3	5	3	14
Cropland	20	23	12	19	11	6	2	2	2	3
Woodland	20	23	12	19	11	6	2	2	2	3

TABLE 3. Relative Percent of County Cropland Devoted to a Given Crop or Pasture/Range [9,10]

Group A = Anderson County
Group B = Bates, Douglas, Franklin, Linn, and Miami Counties
Gropu C = Cass, Jackson, and Johnson Counties

Group	Percent of Total Agricultural Land						
	Wheat	Sorghum	Corn	Oats	Soybeans	Alfalfa	Pasture Hay & Range
A	8.6	7.4	5.7	0.5	21.1	13.7	43.0
B	6.3	9.6	5.5	0.5	15.2	10.3	52.0
C	4.1	5.2	5.8	0.4	11.6	8.2	64.7

Note: Urban Subregion consists of most of Jackson and Johnson Counties

Cropland Subregion consists of parts of Douglas, Franklin, Johnson, and Miami Counties

Pasture/Rangeland Subregion consists of most of Cass County

Woodland Subregion consists of a large part of Linn County

(Julian day 138) until June 9 (Julian day 160) during which time corn and soybeans are emerging and this is reflected in Table 1. Examples of land-use and crop-category distribution are shown in Figure 3 for Julian day 141.

2.2 Dynamics of Soil Moisture Distribution

The above two components of the data base define the geometric properties of the test site and the distribution of backscattering categories. In addition, it is necessary to model certain dynamic conditions that largely determine the dielectric properties of the scene elements. Of major importance is the near-surface soil moisture of each 100-m by 100-m pixel element as a function of time.

The soil moisture is governed by soil type, local slope, crop canopy cover and stage of growth, antecedent soil moisture, precipitation, and potential evaporation. The distribution of soil types as generalized by soil associations from USDA/SCS county soil surveys is shown in Figure 4. The local crop calendar is derived for this area from historical records [4] and used to establish the daily transpiration rate for a given crop. Daily weather records from each of 25 reporting stations are used to generate digital overlays of daily precipitation (Figure 5) and potential evaporation. A water-budget model is used to update near-surface soil moisture on a daily basis for each grid cell. Finally, a normally distributed random-noise

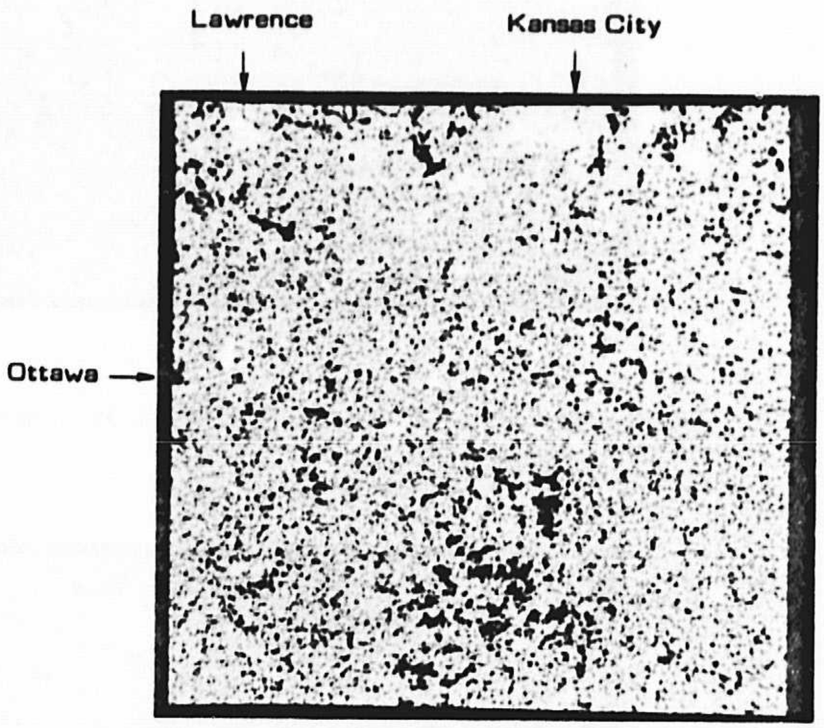

(a) Land-use: urban features are bright while water and woods are darkest.

Figure 3. Land-use and crop-category distributions on Julian day 141.

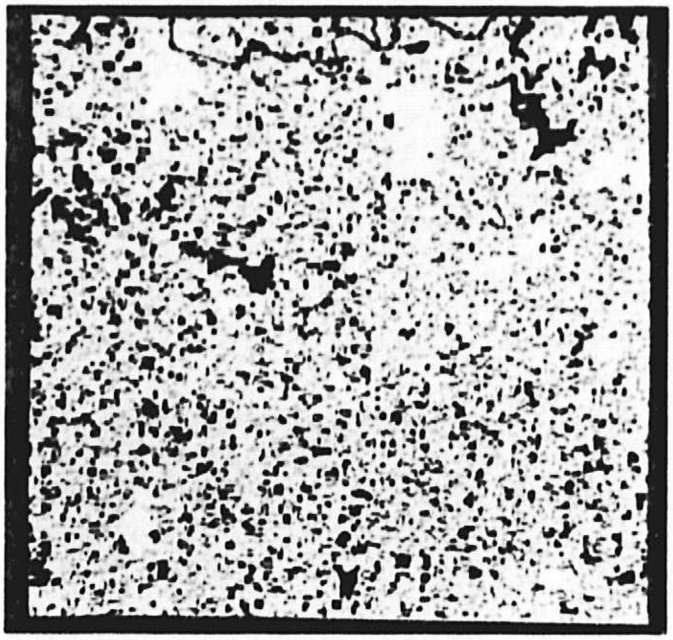

(b) Enlargement of upper-left corner shows 51.2 km by 51.2 km of total scene.

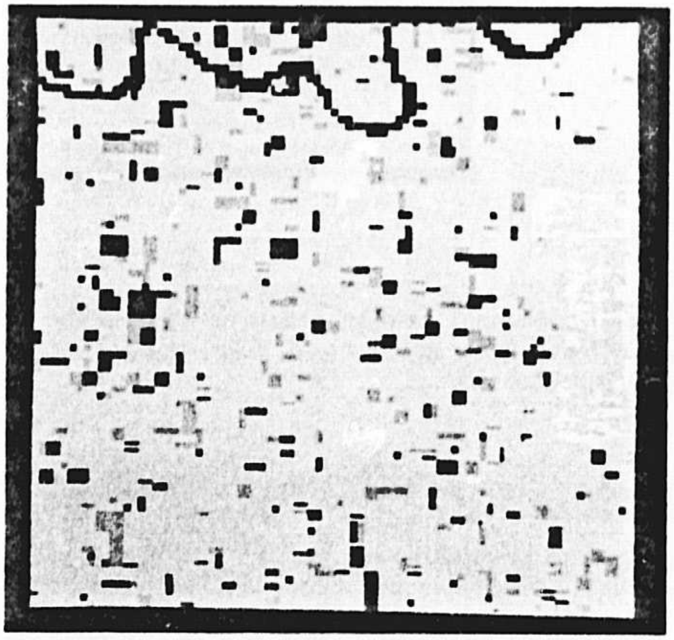

(c) Enlargement of 2b shows Kansas River and trees as black, urban features as white, the remainder of the image shows cropland of which soybeans are emphasized to show the presence of both north-south and east-west row directions.

Figure 4. Map of soil associations for test site.

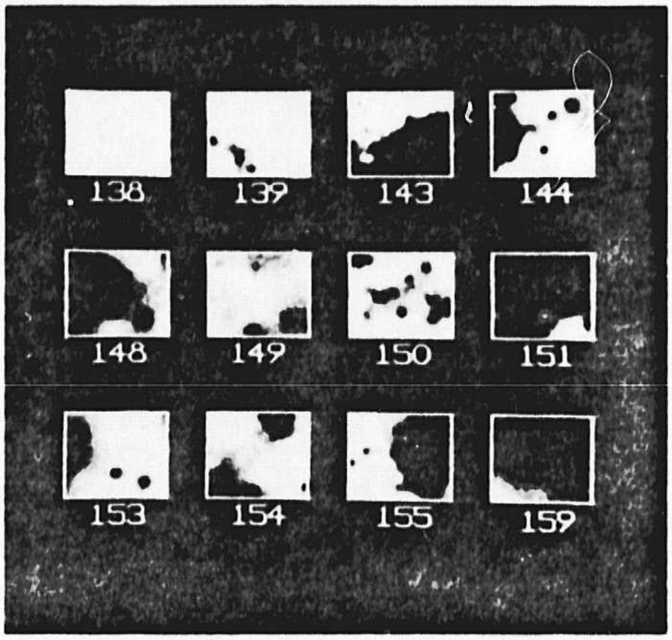

Figure 5. Image presentation of the areal distribution of rainfall within the test site on each Julian date.

component is added to the modeled soil moisture in order to simulate local, within-field variance in true soil moisture [2]. The details of the soil water accounting model and a listing of the computer program are given in Appendix A.

Examples of the 0-5 cm soil moisture distributions produced by the model are shown in Figure 6 for Julian days 141, 150, and 160 in image format. The corresponding cumulative areal distributions are shown in Figure 7a for each date. The influence of crop cover on soil moisture distribution is shown in Figure 7b for Julian day 150. These distributions when combined with the terrain model and the spatial distribution of radar backscatter categories collectively drive the radar image simulations discussed below.

3.0 RADAR IMAGE GENERATION

The average return power $\bar{P}_r$ reradiated from each laterally homogeneous grid cell is given by the radar equation

$$\bar{P}_r = \frac{P_T \, G^2 \, \lambda^2 \, \sigma^0 \, A}{(4\pi)^3 \, R^4} \tag{1}$$

where P_T is the average transmitted power, G^2 is the two-way antenna gain, λ is the wavelength, σ^0 is the radar cross section per unit area, A is the grid-cell area, and R is the range. For a given sensor configuration, P_T, G, and λ are

ORIGINAL PAGE IS
OF POOR QUALITY

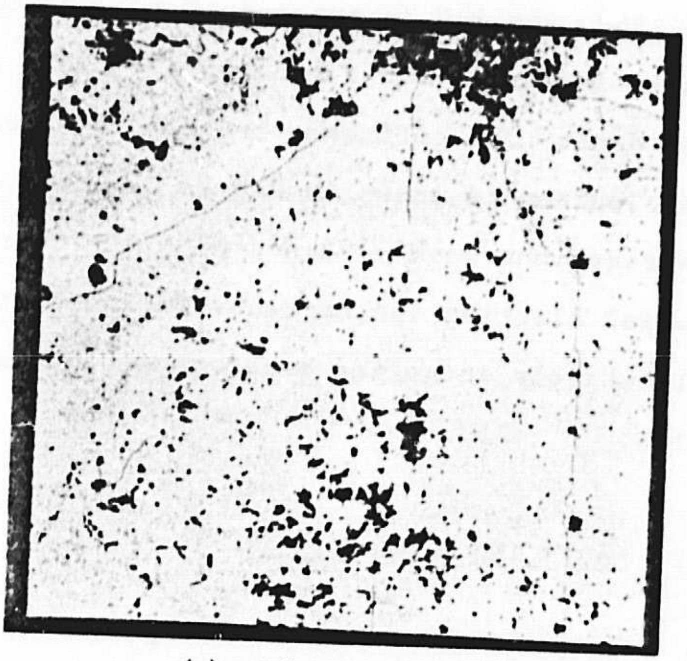

(a) Julian day 141.

Figure 6. Distribution of 0-5 cm soil moisture across the test site. Black represents undefined (zero) soil moisture.

ORIGINAL PAGE IS
OF POOR QUALITY

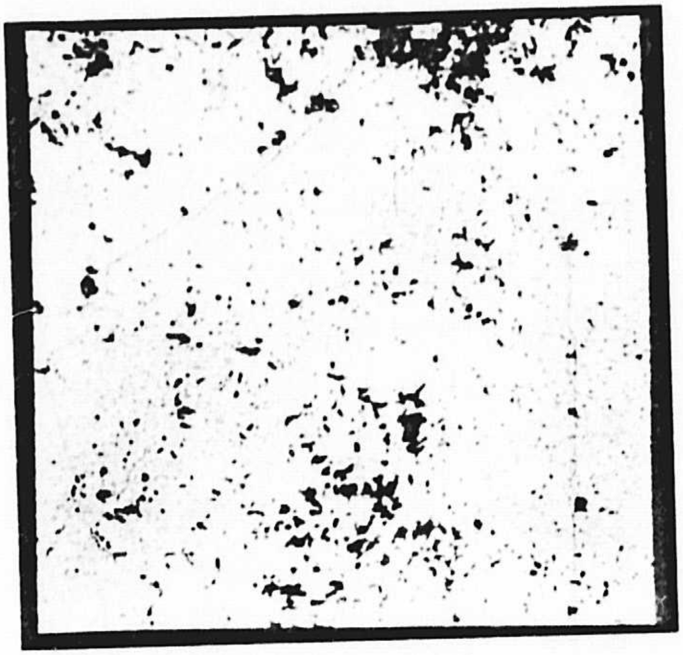

(b) Julian day 150.

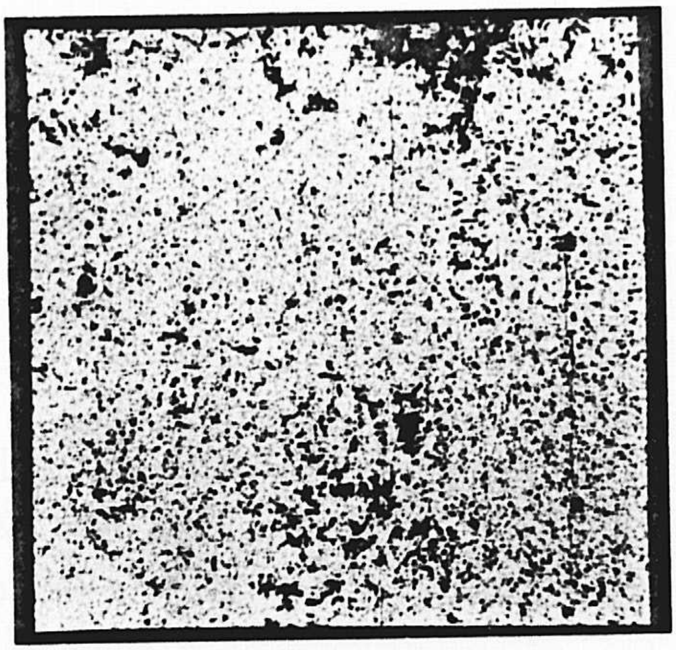

(c) Julian day 160.

ORIGINAL PAGE IS
OF POOR QUALITY

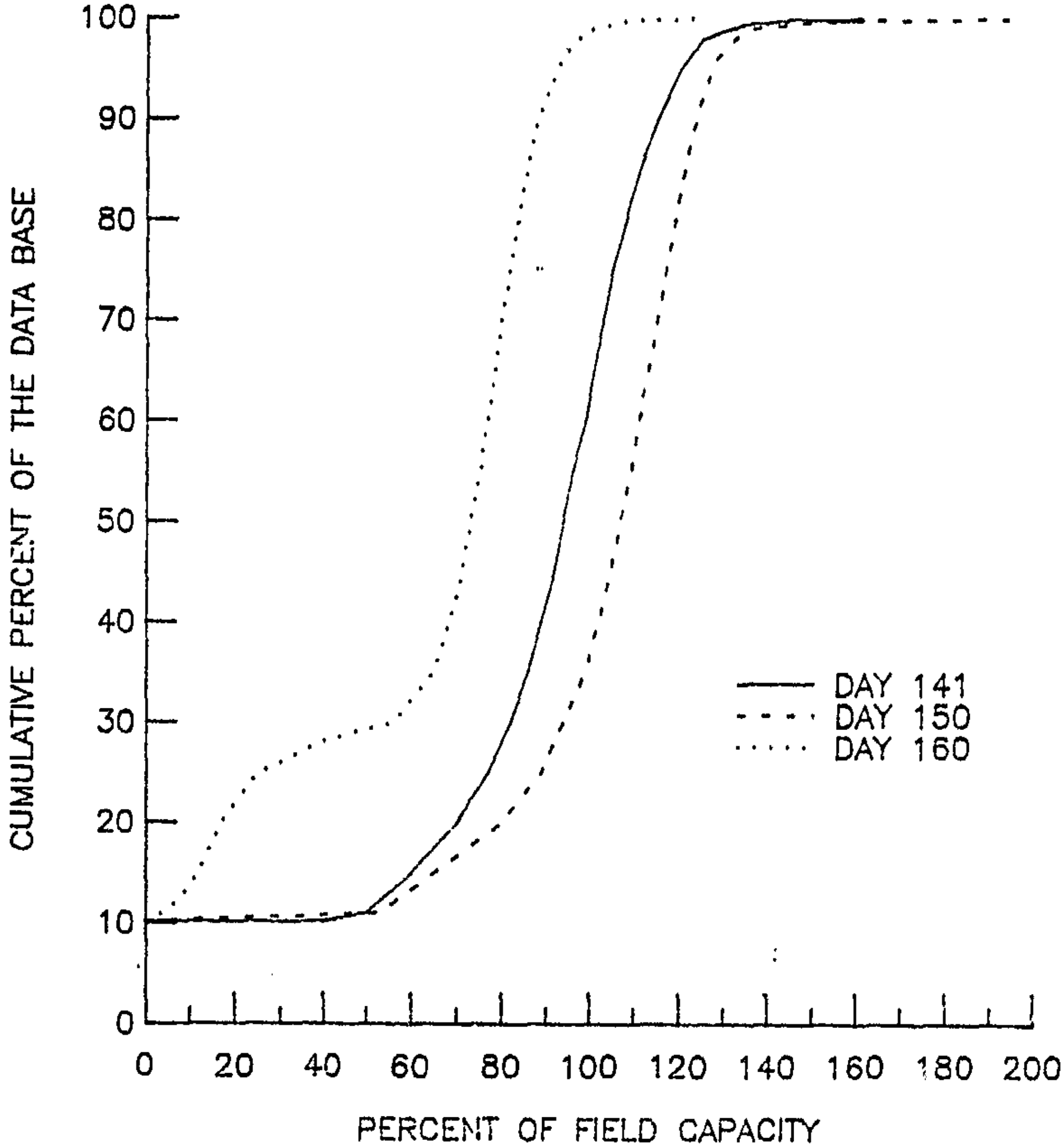

(a) Net distribution for each date.

Figure 7. Cumulative distributions of soil moisture on satellite overpass dates.

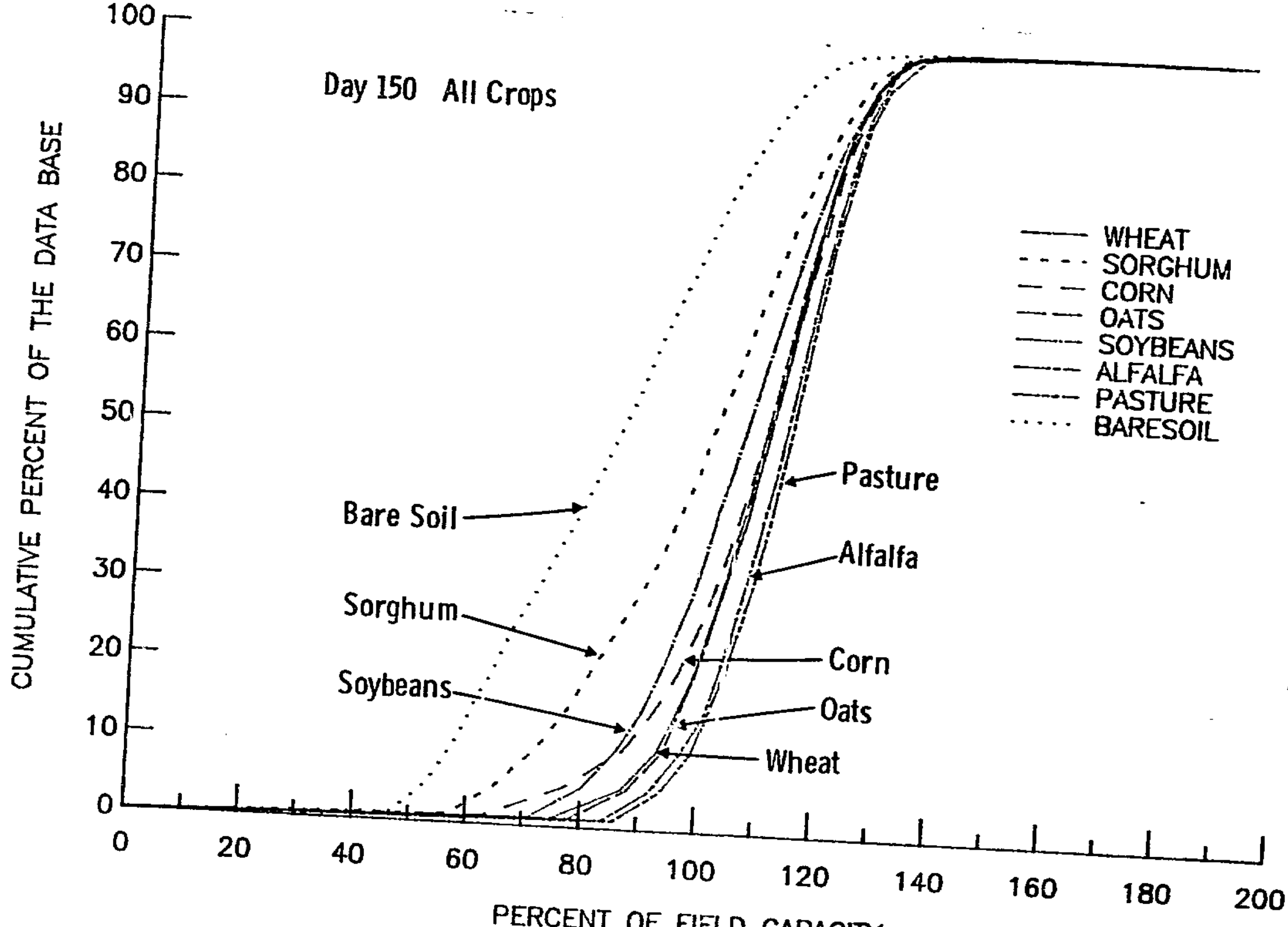

(b) Effect of crop canopy cover on Julian day 150.

constant. For each grid cell element, area and range are determined from the static terrain model. In addition, σ^o varies as a function of local angle of incidence, backscattering category, and near-surface soil moisture; and for the purpose of radar simulation, σ^o is given by empirical fits to experimental airborne and truck-mounted scatterometer data [6]. Examples of empirical radar backscatter dependence on target category, incidence angle and near-surface soil moisture are given in Table 4. Radar backscattering coefficient σ^o is shown graphically in Figure 8 as a function of local incidence angle θ for selected categories and soil moisture conditions.

The power actually received at the antenna P_r is dependent upon signal fading and atmospheric scattering and adsorption. At 4.75 GHz the atmospheric losses are assumed to be negligible for most conditions. In addition, signal fading is assumed to be χ-square distributed with 2 N degrees of freedom where N is the number of independent samples for a given range and azimuth radar resolution [7]. Hence,

$$P_r = \left(\frac{\overline{P}_r}{2N}\right) Y \tag{2}$$

where Y is a random variable with χ-squared distribution and 2 N degrees of freedom.

The radar image simulation model accounts for the geometric effects of layover and shadowing. Examples of simulated orbital radar imagery are shown in Figure 9 for the

TABLE 4. Examples of Class Specific Empirical Backscatter Models Used in Radar Simulations at 4.75 GHz and HH Polarization

A. Targets Modeled as a Function of Soil Moisture

Target Class	Roughness Class or Row Direction	Algorithm Coefficients							
		$f(\theta)$				$g(\theta)$			
		f_1	f_2	$f_3 \times 10^{-2}$	$f_4 \times 10^{-3}$	g_1	$g_2 \times 10^{-2}$	$g_3 \times 10^{-3}$	$g_4 \times 10^{-5}$
Wheat	NA	- 1.932	-2.000	9.336	-1.287	0.114	0.931	-0.914	1.575
Milo	Parallel	- 9.753	-0.262	0.365	-0.002	0.124	-0.492	0.124	-0.101
	Perpendicular	- 9.753	-0.246	0.865	-0.169	0.124	-0.492	0.125	-0.101
Corn	Parallel	- 7.748	-0.395	0.281	-0.054	0.129	-0.330	0.409	-0.029
	Perpendicular	- 7.748	-0.378	0.781	-0.113	0.129	-0.330	0.409	-0.029
Soybeans	Parallel	-10.064	-0.408	0.986	-0.089	0.182	-0.772	0.210	-0.175
	Perpendicular	-10.064	-0.391	1.486	-0.256	0.182	-0.772	0.210	-0.175
Alfalfa	NA	- 1.932	-2.000	9.336	-1.287	0.114	0.931	-0.914	1.575
Pasture	NA	- 1.932	-2.000	9.336	-1.287	0.114	0.931	-0.914	1.575
Bare	Smooth	- 5.191	-1.556	4.617	-0.477	0.182	-0.163	-0.085	0.205
	Medium Rough	-11.705	-0.434	0.767	-0.033	0.137	0.282	-0.231	0.366
	Rough	-15.154	0.338	-3.160	0.506	0.158	-0.379	0.225	-0.317

$\sigma^0(\theta) = f(\theta) + g(\theta)\, M_{fs}$ for $\theta \leq 30°$

$f(\theta) = f_1 + f_2\theta + f_3\theta^2 + f_4\theta^3$

$g(\theta) = g_1 + g_2\theta + g_3\theta^2 + g_4\theta^3$

B. Targets Modeled with no Dependence on Soil Moisture

Target Class	$f(\theta)$
Residential Areas	$13.019 - 1.755\theta + 0.640 \times 10^{-1}\ \theta^2 - 0.755 \times 10^{-3}\ \theta^3$
Water Bodies	$22.820 - 5.126\theta + 2.370 \times 10^{-1}\ \theta^2 - 3.973 \times 10^{-3}\ \theta^3$
Roads	$20.000 - 5.550\theta + 2.800 \times 10^{-1}\ \theta^2 - 4.500 \times 10^{-3}\ \theta^3$
Deciduous Trees	$10 \log (10^{-1.143} \times \cos\theta)$
Buildings	Constant value 5 dB

ORIGINAL PAGE IS
OF POOR QUALITY

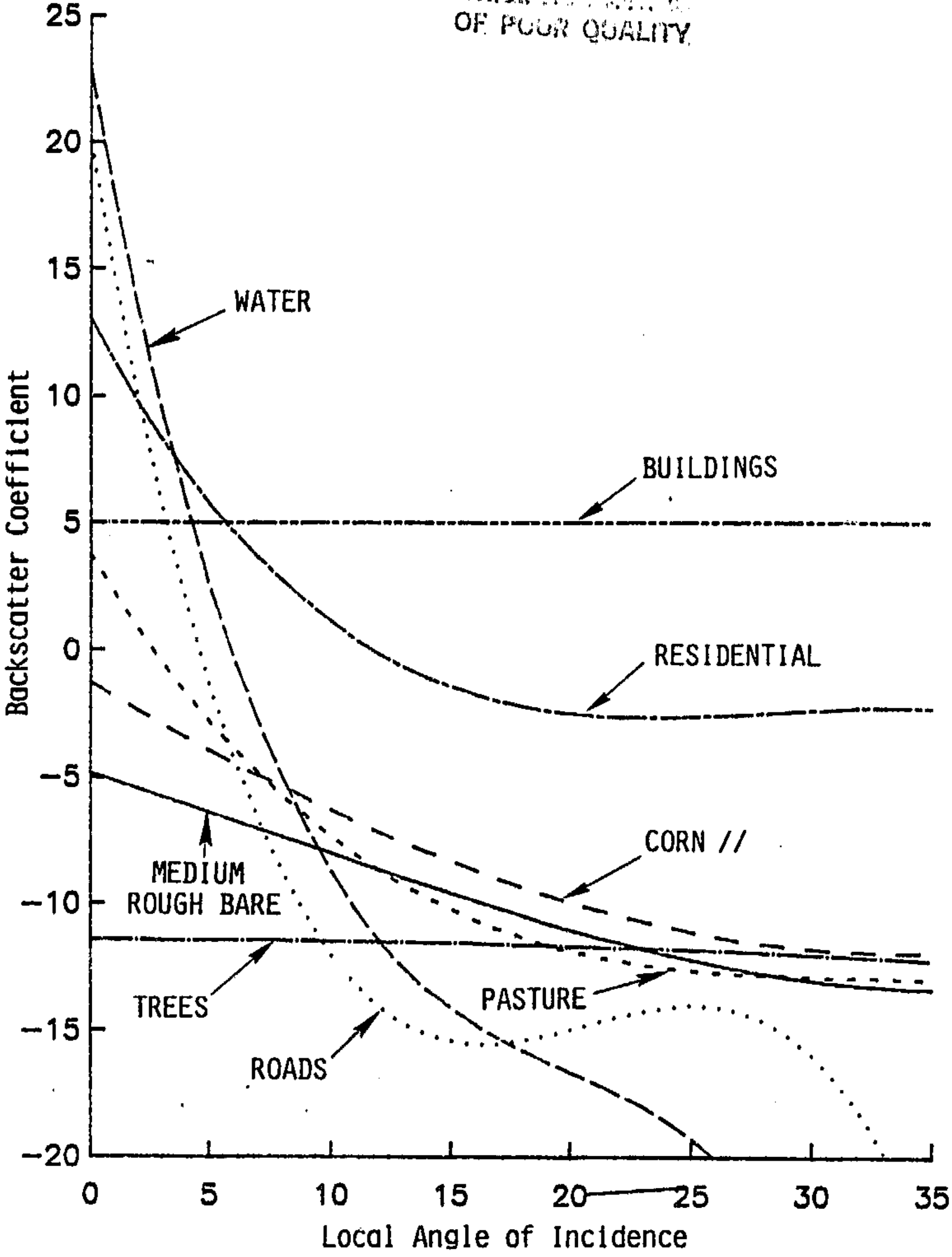

(a) Soil moisture is 50% of field capacity.

Figure 8. Radar backscattering σ^{0} at 4.75 GHz with HH polarization as a function of local incidence angle for selected moisture conditions.

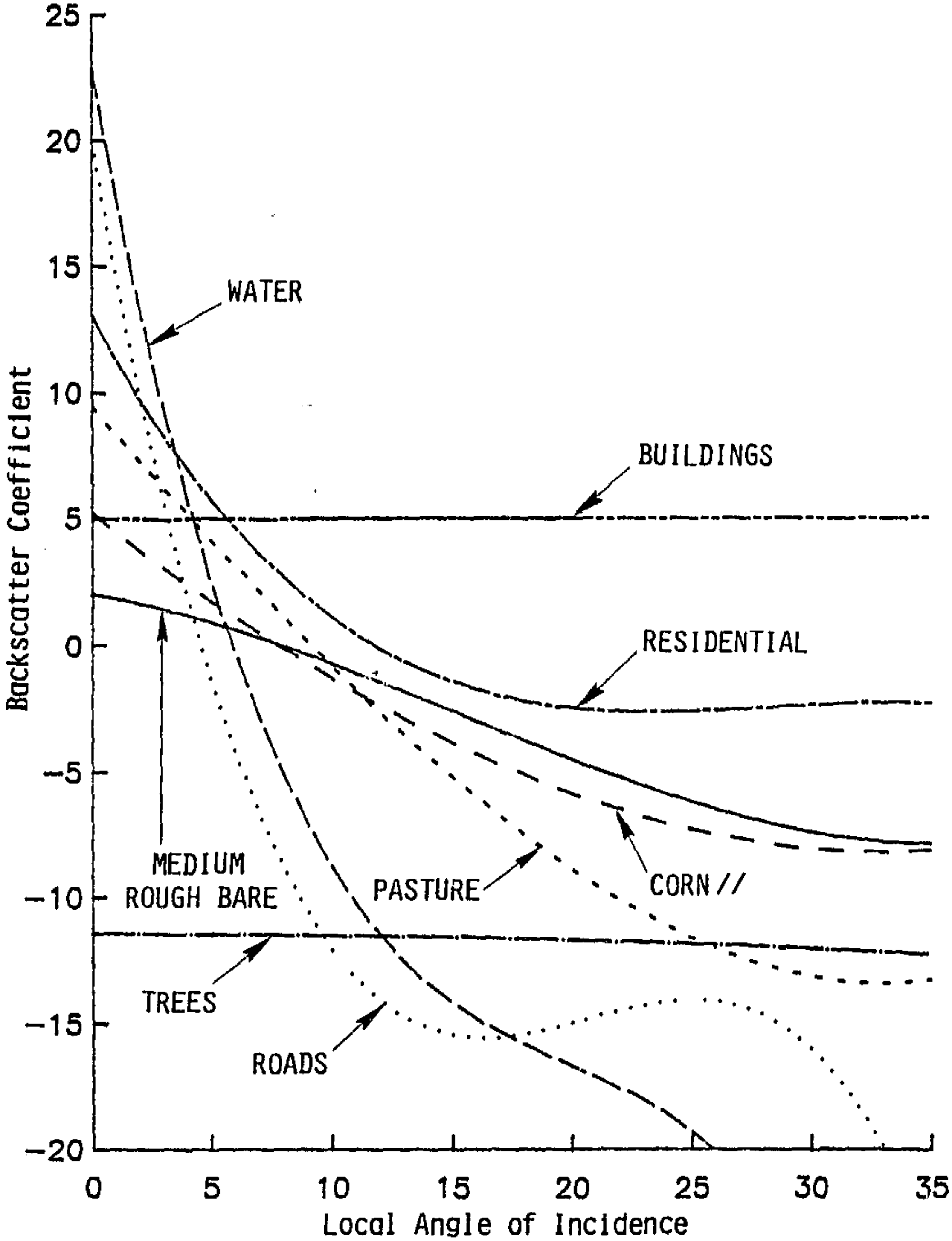

(b) Soil moisture is 100% of field capacity.

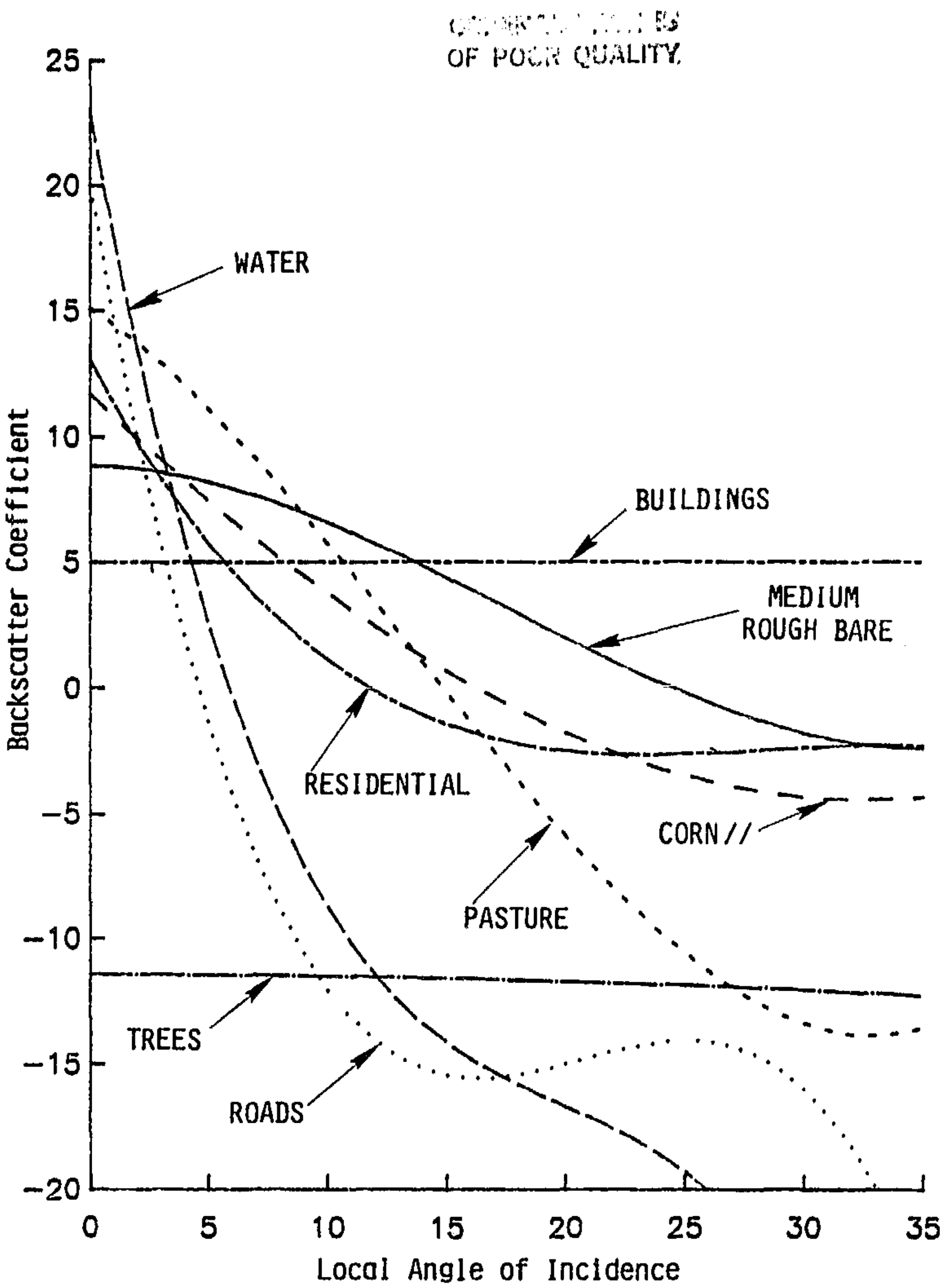

(c) Soil moisture is 150% of field capacity.

ORIGINAL PAGE IS
OF POOR QUALITY

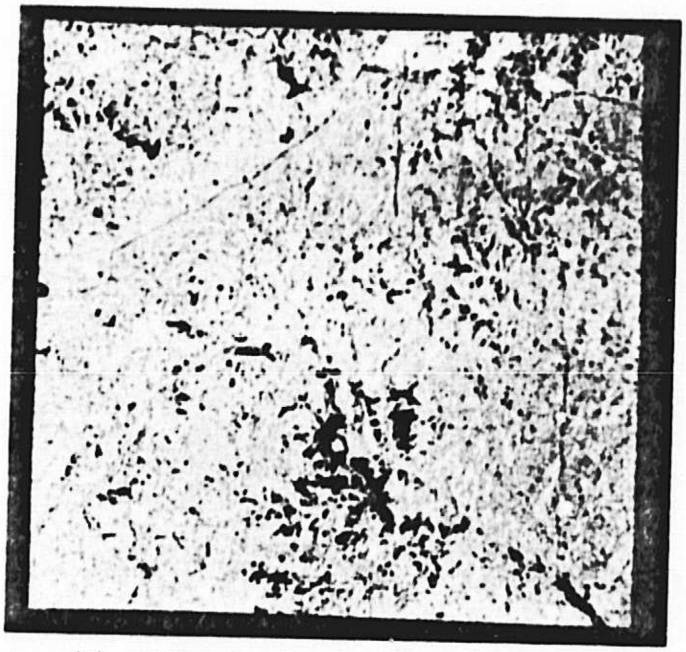

(a) 100 m by 100 m radar resolution.

Figure 9. Simulated radar imagery of the test site on Julian day 141.

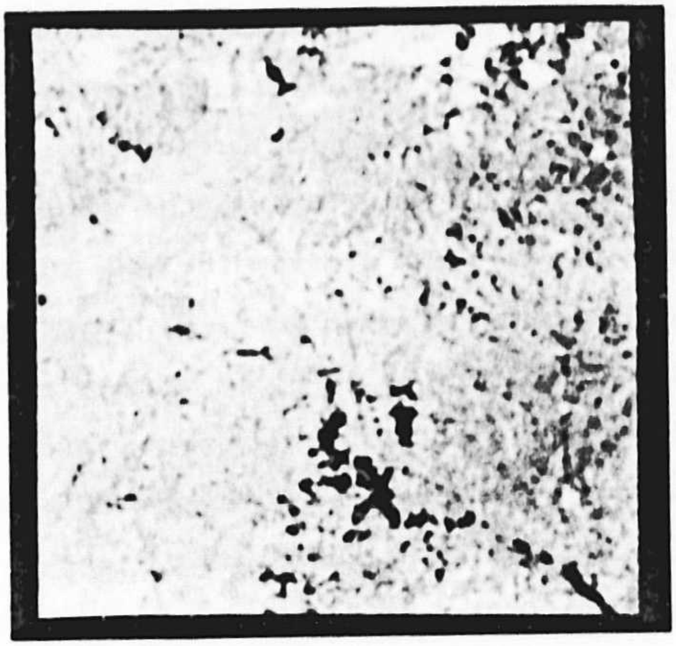

(b) 1 km by 1 km radar resolution.

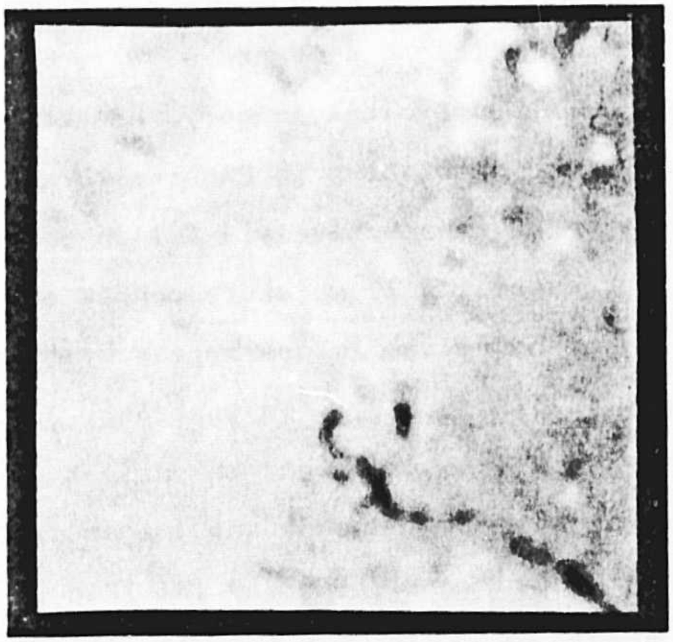

(c) 3 km by 3 km radar resolution.

soil moisture distribution present on Julian day 141 (Figure 5a) at radar resolutions of 100 m by 100 m, 1 km by 1 km and 3 km by 3 km. These images are ground-range presentations and P_r is scaled in dB to facilitate the presentation of the large dynamic range in P_r across the image swath ($\approx$ 48 dB). The radar illumination is from the west (left side of images). Due to the relatively steep incidence angles (7° - 17°), the angular decay in P_r is readily apparent across the swath from left to right. In general, areas of higher near-surface soil moisture as related to antecendent precipitation appear brighter on the images, and this is most apparent as diagonal stripes related to storm tracks. Also, areas of tree canopy cover and water bodies tend to be dark on the imagery simulated for Julian day 141, while urban features tend to appear bright and are especially noticeable in the far range (right side of images).

The simulated orbital imagery for the three radar resolutions are also shown in Figures 10 and 11 for Julian days 150 and 160, respectively. Julian day 150 represents the wettest overall soil moisture conditions as indicated in Figure 7, and hence the images appear brighter than those for Julian day 141 (Figure 9). In contrast, Julian day 160 is shown by Figure 7 to represent the driest overall soil moisture conditions, and thus the images in Figure 11 appear darker than those for Julian day 141 (Figure 9).

It should be noted that for all of the above simulated images (Figures 9, 10, 11), the number of independent looks

ORIGINAL PAGE IS
OF POOR QUALITY

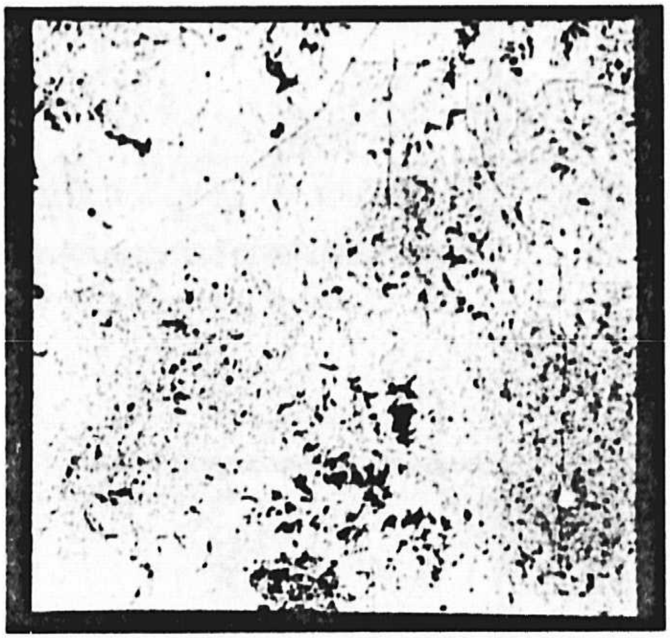

(a) 100 m by 100 m radar resolution.

Figure 10. Simulated radar imagery of the test site on Julian day 150.

ORIGINAL PAGE IS
OF POOR QUALITY

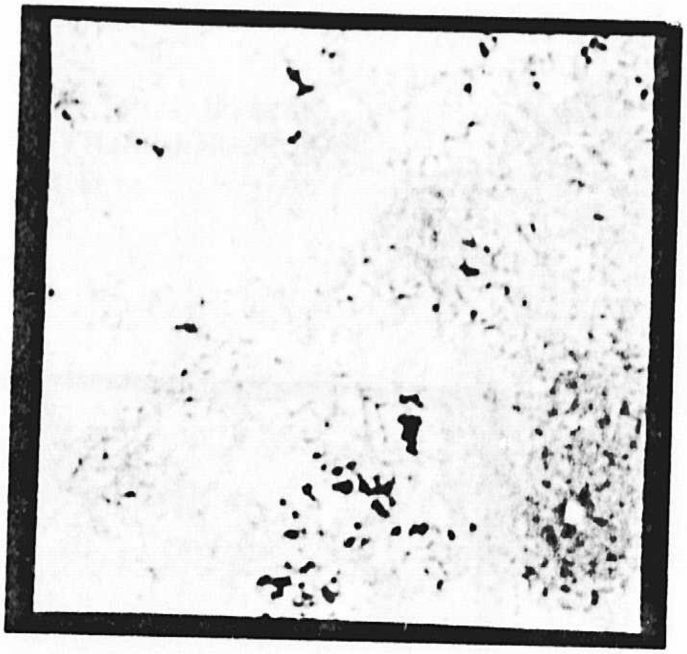

(b) 1 km by 1 km radar resolution.

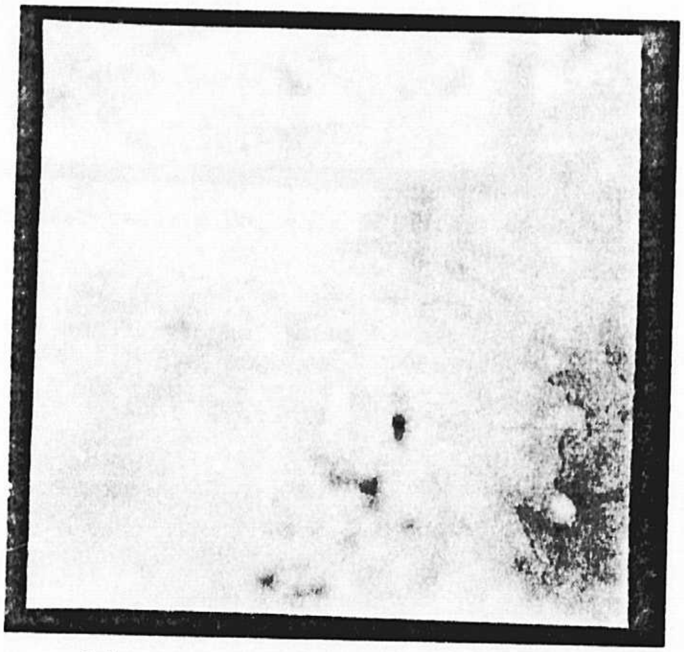

(c) 3 km by 3 km radar resolution.

ORIGINAL PAGE IS
OF POOR QUALITY

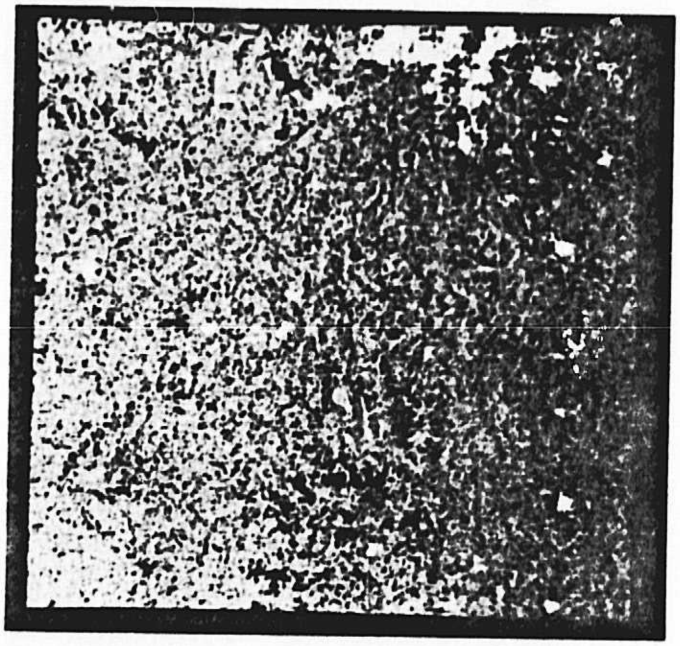

(a) 100 m by 100 m radar resolution.

Figure 11. Simulated radar imagery of the test site on Julian day 160.

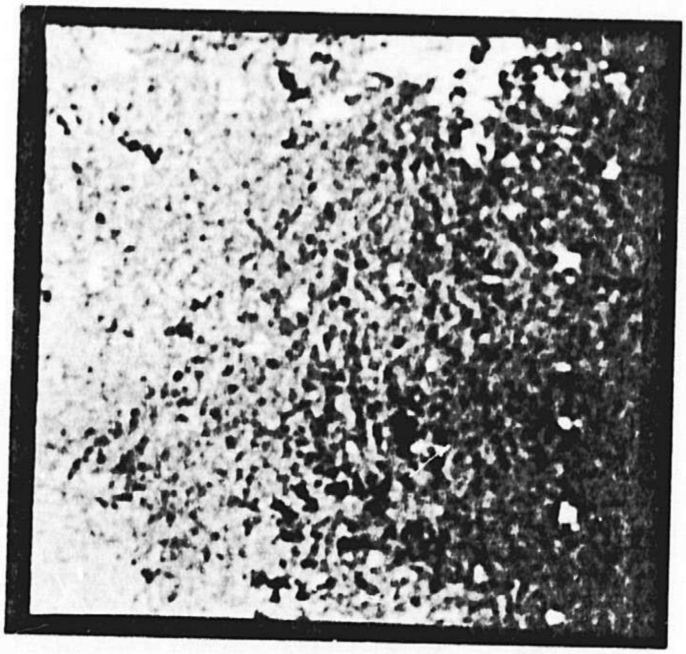

(b) 1 km by 1 km radar resolution.

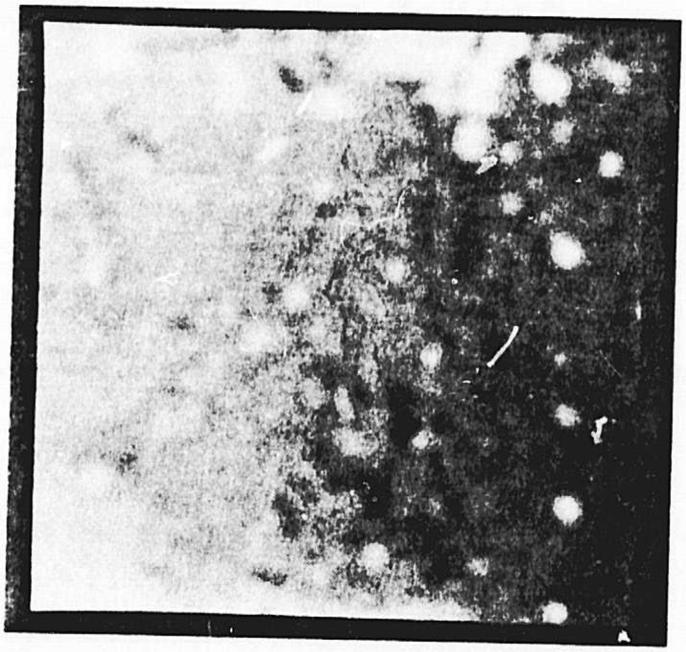

(c) 3 km by 3 km radar resolution.

is large ($N \geq 23$). Hence, the variance in P_r within a given portion of the scene is only minimally dependent upon signal fading and is mostly the result of variance in local topographic relief, radar backscatter category, and near-surface soil moisture. In a visual sense, the interaction of relief, category, and moisture yield quite different spatial patterns of P_r on each of the three simulation dates. This is best seen in the 100 m by 100 m radar resolution imagery. Figure 12 shows enlargements of the northwest (upper-left) quadrant of the 100 m by 100 m imagery for each of the three overpass dates. This quadrant encompasses the test site used in previous orbital radar simulations [1, 2, and 6]. These images illustrate the following:

1) For nearly uniform soil moisture conditions, the variance in P_r is dominated by local topographic relief and radar backscatter category. This condition is most closely approximated by Julian day 150 in Figure 12b.

2) For variable soil moisture conditions, the scene variance in P_r is most closely related to local soil moisture and radar backscatter category which tends to mask variance in P_r related to local topographic effects. This condition is best seen on Julian day 160 (Figure 12c) since an extended period of evapotranspirative losses in soil moisture has enhanced the relative difference in P_r from each radar backscatter category.

The above indicates the potential for achieving certain

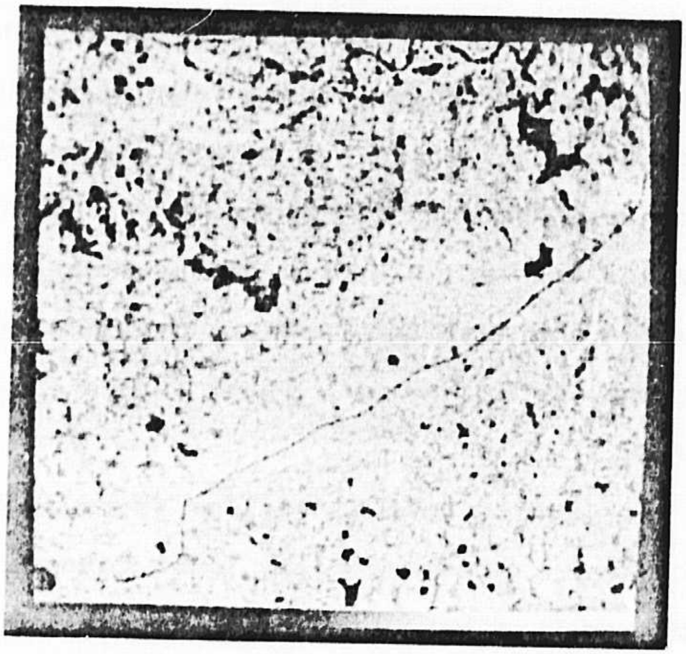

(a) Julian day 141

Figure 12. Enlargements of the northwest corner of the simulated 100 m by 100 m resolution radar imagery on each overpass date.

ORIGINAL PAGE IS
OF POOR QUALITY

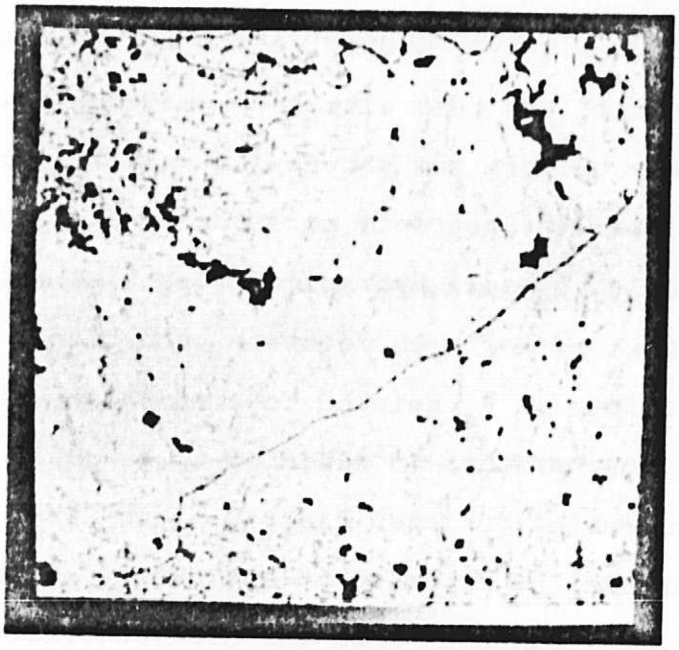

(b) Julian day 150

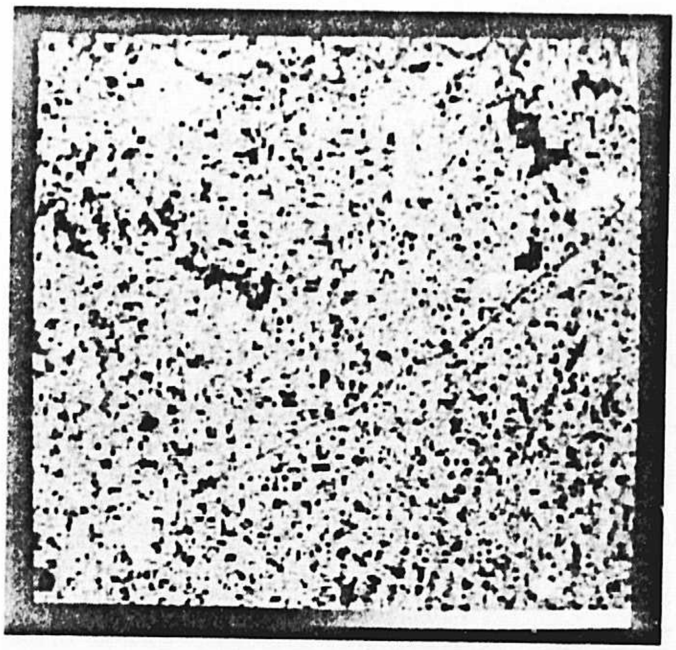

(c) Julian day 160

mapping objectives not rigorously addressed within the confines of this study. First, the potential exists to classify soil type within relatively flat agricultural portions of the test site from imagery acquired shortly after a nearly uniform and saturating rainfall event. In this case, near-surface soil moisture is high and largely controlled by soil hydraulic properties related to soil type. In addition, for high moisture conditions, the relative uncertainty in P_r related to crop-canopy attenuation and canopy backscatter is expected to be small [5]. Secondly, the potential for crop discrimination from orbital radar imagery can be expected to maximize (for this frequency and angle of incidence) when the differential evapotranspirative dry-down of each crop has enhanced the inter-crop variance in P_r. This condition would exist five or more days after a rainfall event.

4.0 SOIL MOISTURE CLASSIFICATION

In order to classify soil moisture using the simulated radar imagery, a generalized soil-moisture algorithm is derived from all experimental data for bare and vegetation-covered soil conditions (excluding woodlands). The classification algorithm relates estimated soil moisture $\hat{M}_{fs}$ to received power P_r as a function of incidence angle θ.

$$\hat{M}_{fs} = [P_r - \alpha(\theta)]/\beta(\theta) \quad (3)$$

where

$$\alpha(\theta) = 9.67 + 0.84\theta - 4.59 \times 10^{-2}\theta^2 + 8.27 \times 10^{-4}\theta^3, \text{ and}$$

$$\beta(\theta) = 0.161 + 9.38 \times 10^{-4}\theta - 4.97 \times 10^{-4}\theta^2 + 1.21 \times 10^{-5}\theta^3.$$

In this case, θ is estimated from the range position of a pixel on the radar image, assuming spherical earth geometry and a constant mean elevation of the test site above sea level. Thus, the classification algorithm is "blind" with respect to true local incidence angle and to the actual backscattering category of any given pixel [6]. Application of this algorithm to the received power images yields maps of estimated soil moisture, an example of which is shown in Figure 13 for a radar resolution of 100 m by 100 m on Julian day 141.

Given the above algorithm, orbital radar imagery can be used to classify soil moisture in two ways. First, the imagery obtained at any given radar resolutin on any single overpass date can be pssed through the general algorithm (Equation 3) to yield estimates of the absolute soil moisture distribution for that date. The second approach is to make use of the multi-temporal coverage provided by an orbital system to yield estimates of the relative change in soil moisture. The radiometric and geometric stability of the Seasat-A L-band imaging radar has shown that such a procedure is feasible and relatively uncomplicated from the standpoint of image registration [8]. The two approaches are not

ORIGINAL PAGE IS
OF POOR QUALITY

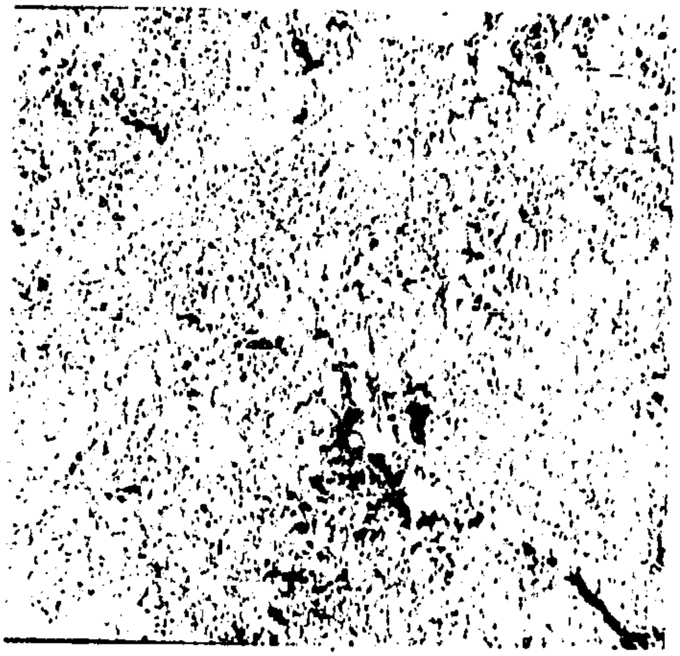

Figure 13. Near-surface soil moisture as estimated for Julian day 141 from simulated radar imagery with a 100 m by 100 m resolution.

mutually exclusive and both will be explored in the ensuing sections with respect to soil moisture classification error as a function of radar resolution and the geographic distributions of local relief and backscatter category.

4.1 Single Date Soil-Moisture Classification Accuracy

The accuracy of soil-moisture classification is examined by evaluating the difference between the true soil moisture M_{fs} and the estimated soil moisture $\hat{M}_{fs}$. This is accomplished through registration of the two images (such as Figures 6 and 13) and computation of the difference. Due to the geometric distortion inherent in the radar image-forming process, image registration by simple coordinate translation is only accurate to within about +/- 1.3 pixels (130 meters), and this registration error is proportional to changes in local elevation across the image swath. Hence, a procedural error is introduced into the comparative process which is not related to true classification error. Also, the magnitude of this procedural error is proportional to the local variance in the "true" soil moisture distributions as shown in Figure 6.

In order to examine the effects of various land-use and field-size distributions, four subregions are identified within the test site and relate to an urban area, mixed cropland, pasture and rangeland, or woodland. Figure 2 shows the spatial locations of these subregions, and their land-use and field-size distributions are tabulated in Tables 1 and 2, respectively. All subregions contain more than 30% pasture, grass, and rangeland, and are distinctive primarily in terms of the percent area occupied by cultural features (residential, buildings, and roads), water, woodland, and crops. In addition, the rangeland/pasture subregion is characterized by a greater percentage of large fields as compared to the other subregions. Finally, Figure 2 shows that the woodland and the rangeland/pasture subregions are located in areas of relatively large local relief.

An example of soil-moisture classification error is shown in Figure 14 for the 100-m by 100-m resolution radar on Julian day 141. Classification error E_m is defined by

$$E_m = M_{fs} - \hat{M}_{fs} \tag{4}$$

where

M_{fs} = true soil moisture, and

$\hat{M}_{fs}$ = estimated soil moisture.

Figure 14a shows the category classification map for the woodland subregion where wooded areas are black, water is dark gray, cultural features are white, and agricultural land and pasture/rangeland are generally light gray. The difference between actual soil moisture M_{fs} and classified soil moisture $\hat{M}_{fs}$ is mapped in Figure 14b. E_m is linearly represented by graytone and thus, dark and white areas represent overestimation and underestimation of soil moisture, respectively. The large P_r from cultural features

ORIGINAL PAGE IS
OF POOR QUALITY

(a) Backscatter category map: woods are black, water bodies are dark gray, cultural features are white, and agricultural areas are light gray.

(b) Soil moisture estimate error E_m: overestimates of soil moisture are dark, underestimates of soil moisture are white, areas with small estimate errors are gray.

Figure 14. Soil moisture classification error E_m on Julian day 141 within the woodland subregion resulting from use of the "blind" classifier on 100 m by 100 m radar imagery.

at A leads to an overestimation of moisture, while the low P_r from woodland at B and water at C yields a low estimate of soil moisture. Median gray tones in Figure 14b relate to small estimate errors. A comparison of Figures 14a and 14b shows moisture-estimate errors to be highly correlated with the spatial location of specific land-use categories, especially cultural features, trees, and water. Image registration errors yield white or black rings around specific features. Hence, the spatial organization of such confusion categories largely determines the moisture classification accuracy of a given radar resolution for a given geographic land-use setting.

The single date soil moisture classification error can be examined as a function of radar resolution, general soil moiture condition (overpass date), and geographic subregion.

The soil moisture classification error E_m resulting from radar resolutions of 100 m by 100 m, 1 km by 1 km, and 3 km by 3 km is shown for the entire 124-km by 108-km test site on each overpass date in Figure 15. For all general soil moisture conditions (overpass dates), the distributions of E_m resulting from classification of the 100-m resolution imagery are more peaked and yet have longer tails than the corresponding distributions of E_m for the coarser resolutions. These long tails are related to the presence of confusion categories such as urban features, woodland, and water. The effects of these confusion categories at the coarser resolutions (1 km by 1 km and 3 km by 3 km) are to

ORIGINAL PAGE IS
OF POOR QUALITY

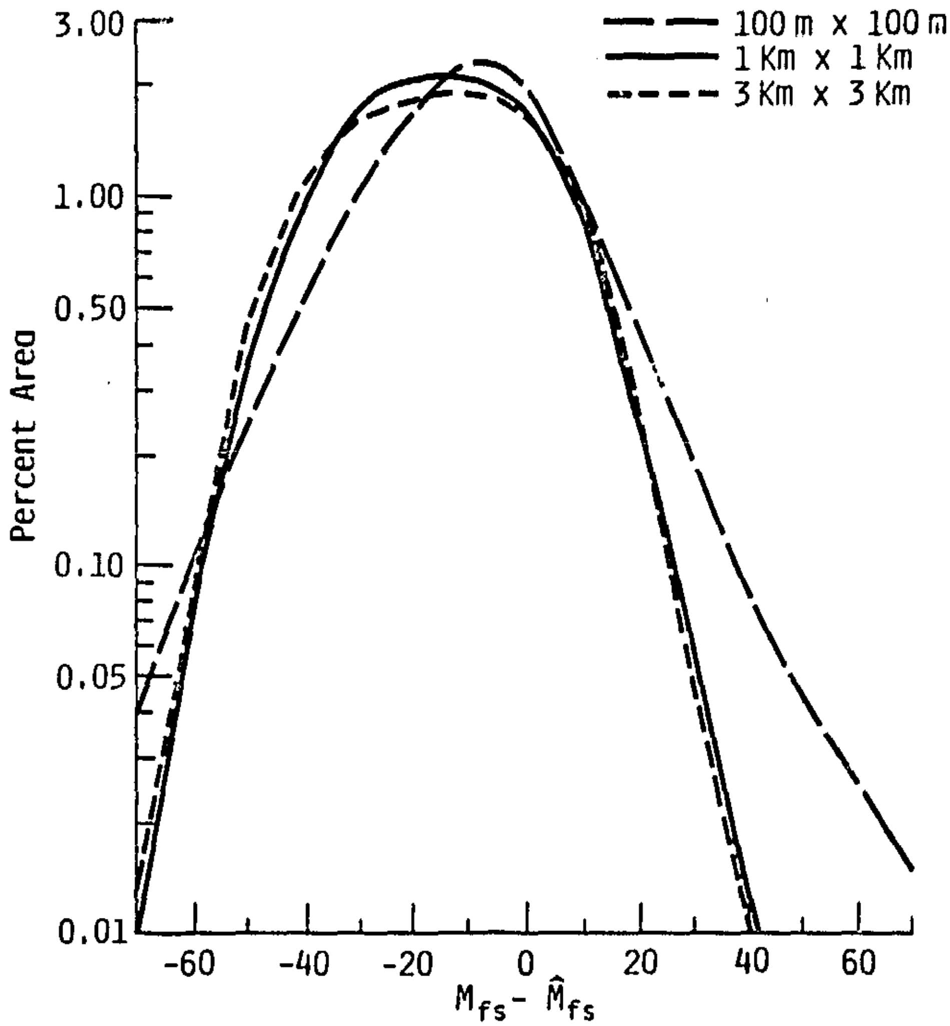

(a)

Figure 15. Soil moisture classification error E_m resulting from each radar resolution for all moisture dependent pixels in the test site (excluding woods) on a) Julian day 141, b) Julian day 150, and c) Julian day 160.

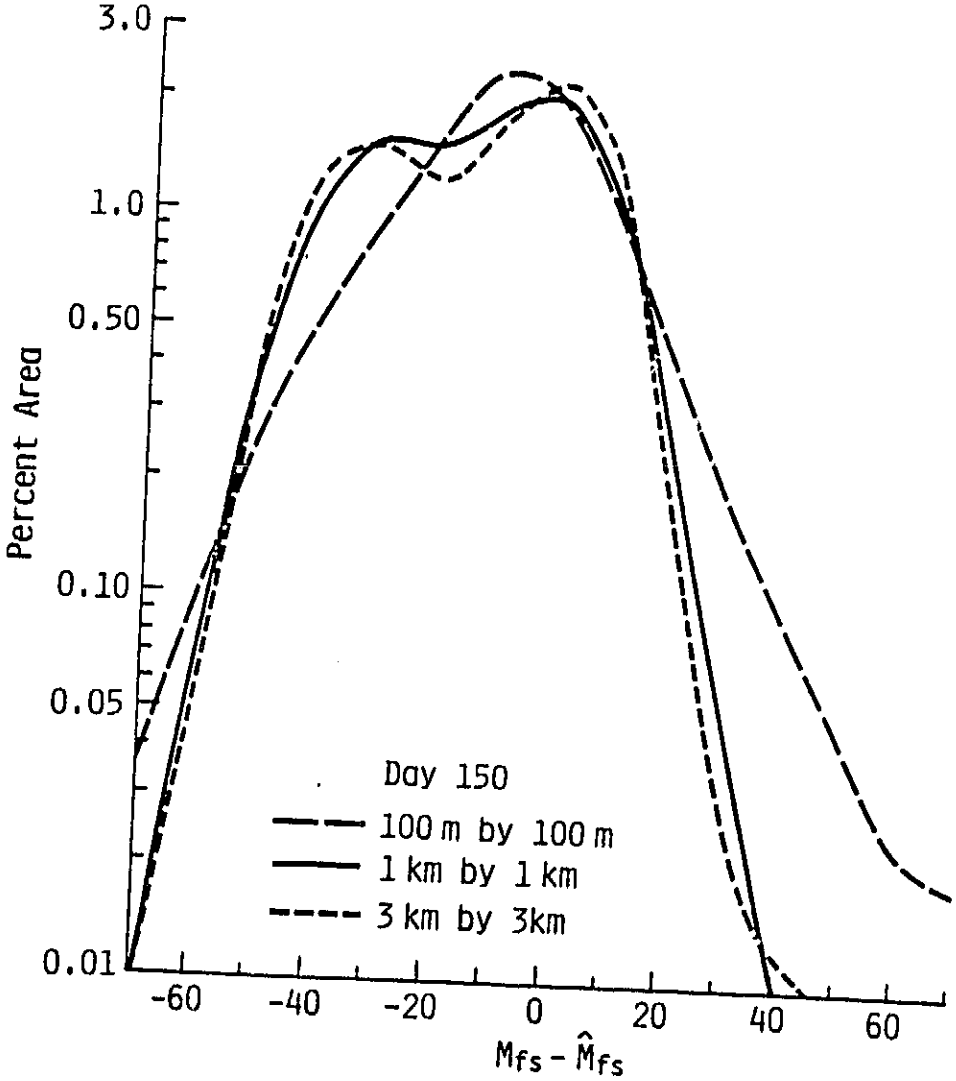
3.0
1.0
0.50
0.10
0.05
0.01
Percent Area
Day 150
100 m by 100 m
1 km by 1 km
3 km by 3km
-60
-40
-20
0
20
40
60
$M_{fs} - \hat{M}_{fs}$

(b)

ORIGINAL PAGE IS
OF POOR QUALITY

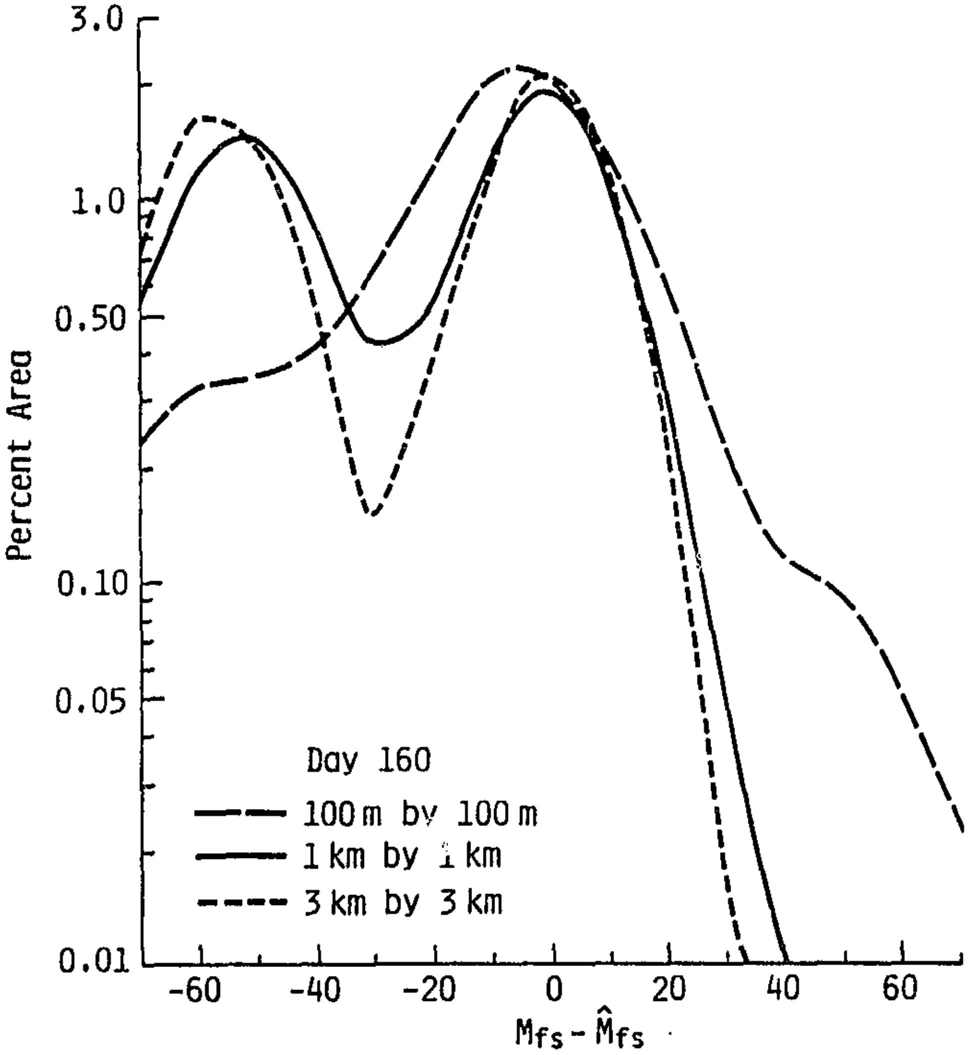

(c)

broaden the error distribution.

The tendency of the coarser resolutions (1 km by 1 km and 3 km by 3 km) to yield bimodal distributions of E_m in Figure 15 with a secondary peak ranging from -30% to -50% is primarily related to the presence of cultural features which have large scattering cross-sections relative to agricultural and rangeland areas. These overestimates of local soil moisture result from averaging the large P_r from cultural targets over a larger area. Hence, the magnitude of this secondary peak is proportional to both the net area occupied by cultural features and the dispersion of such features within the total scene, and the size of E_m at this peak is proportional to the ratio of P_r cultural to P_r agricultural.

The associated absolute moisture classification accuracies of the three radar resolutions are shown in Figure 16. In general, the 100-m by 100-m resolution is shown to yield the most accurate estimates of soil moisture. For example, use of the "blind" generalized moisture algorithm on Julian day 141 yields $\hat{M}_{fs}$ within +/- 20% of true moisture M_{fs} for 68% of the area using a radar with a 100-m resolution, while only 60% and 58% of the area is classified within this error limit using radar resolutions of 1 km and 3 km, respectively. In Figures 14 and 15, this result is shown to be related to the spatial distribution of land-use confusion categories.

The differences in absolute classification accuracy between the three radar resolutions are also dependent upon

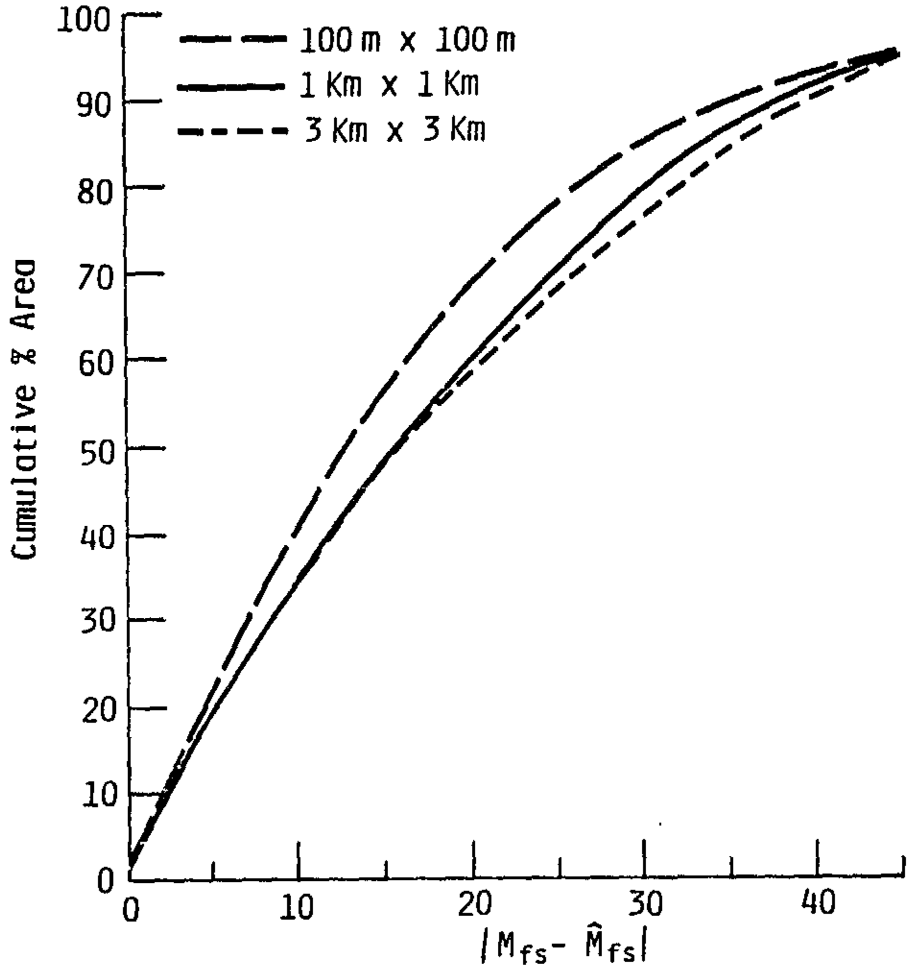

(a)

Figure 16. Cumulative percent area of all moisture dependent pixels in the test site (excluding woods) as a function of absolute moisture classification error for each radar resolution.

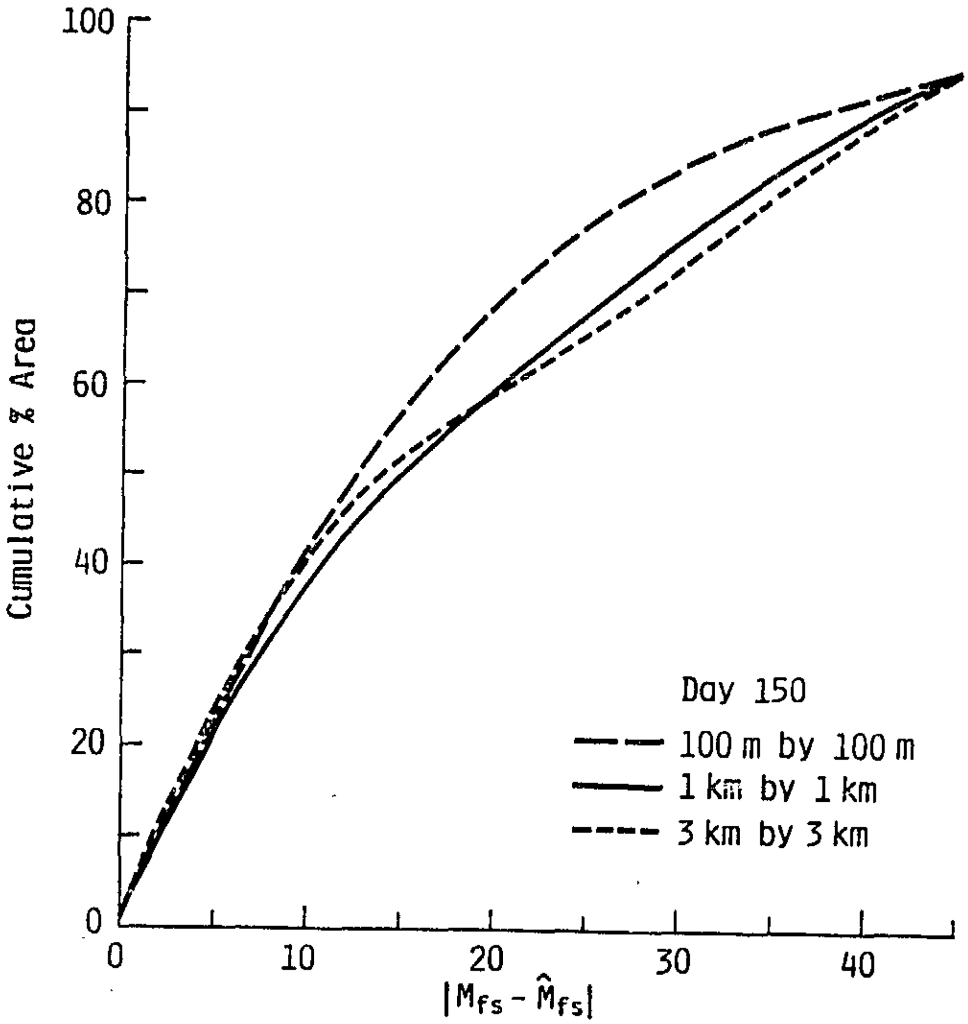
Cumulative % Area
100
80
60
40
20
0
0
10
20
30
40
$|M_{fs} - \hat{M}_{fs}|$
Day 150
100 m by 100 m
1 km by 1 km
3 km by 3 km

(b)

ORIGINAL PAGE IS
OF POOR QUALITY

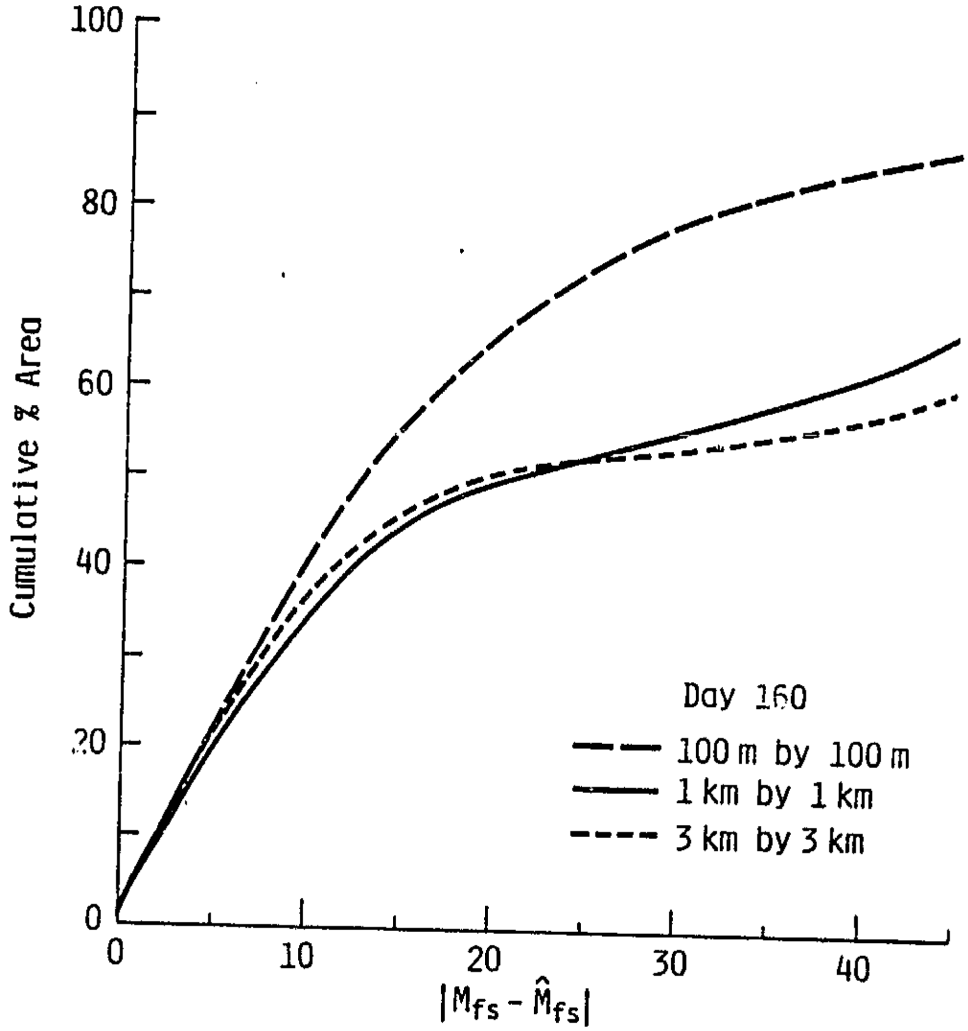

(c)

general soil moisture condition. This effect is seen by comparing the results achieved for different overpass dates in Figure 16a, b, and c for overpasses on Julian days 141, 150, and 160, respectively. The classification accuracy of the coarse resolution sensors (1 km by 1 km and 3 km by 3 km) is seen in Figure 16c to be significantly reduced relative to the classification accuracy achieved with the 100 m resolution radar. The local variance in true soil moisture M_{fs} and local received power P_r are seen to be greatest on Julian day 160 in Figures 6 and 12, respectively. As previously stated, this is largely the result of the differential evapotranspirative dry-down rates of the various crop canopies constituting the scene. Thus, the within-scene variance in soil moisture M_{fs} is highly correlated with the crop distribution given in Table 1 which is dispersed in agregates given by the field size distribution (Table 2). Hence, at radar resolutions coarser than field size a serious degradation in moisture classification accuracy can be expected for imagery acquired during periods of protracted evapotranspirative loss.

The effects on moisture classification error of varying the local distribution of land-use confusion categories are demonstrated by comparing the error distributions for the four land-use subregions. The error distributions for the urban, pasture/rangeland, cropland, and woodland subregions are compared in Figure 17, based upon the 100-m resolution radar imagery for Julian day 141. When the error

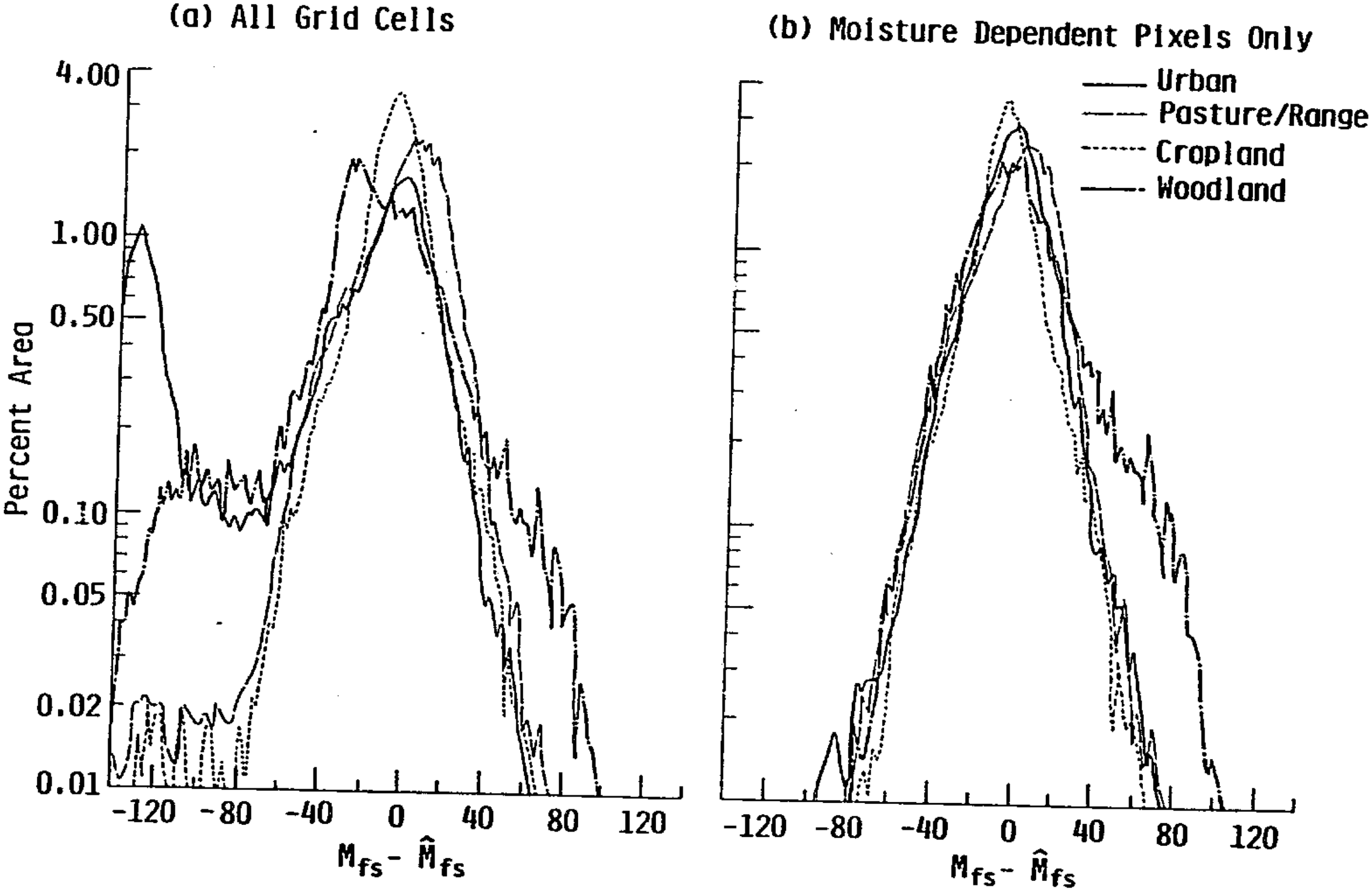

Figure 17. Distribution of the difference between actual and classified soil moisture for the subregions of the test site as computed from 100-m resolution radar imagery for Julian day 141.

ORIGINAL PAGE IS OF POOR QUALITY

distribution is plotted for all 100-m by 100-m grid cells within each region (Figure 17a), large overestimates of moisture, primarily in the urban and woodland subregions, are related to the presence of cult al features such as buildings and roads and also related to the presence of water bodies since for these categories soil moisture is undefined and any moisture estimate for these categories is therefore an overestimate. In a similar fashion, large underestimates of M_{fs}, best exemplified by the woodland subregion, are largely related to the presence of deciduous trees, which are assumed to fully attenuate backscattering from the soil at 4.75 GHz.

The exclusion of nonagricultural categories (cultural features, water, and woodland) from the grid-cell comparisons of $\hat{M}_{fs}$ to M_{fs} yields highly peaked distributions centered around $\simeq 0$ error as shown for each subregion in Figure 17b. The woodland still exhibits a larger area where soil moisture is underestimated than the other subregions and this is largely the result of locally saturated to flooded soil moisture conditions. The radar backscatter model treats fully saturated soil as a near specular surface similar to a water body, and hence P_r is low at off nadir indicence angles. As a consequence, soil moisture M_{fs} is generaliy underestimated. Similar results are obtained for the other two overpass dates.

The absolute classification accuracy for Julian day 141 within each of the four land-use subregions is shown in

Figures 18a and 18b from simulated radar resolutions of 100 m by 100 m and 1 km by 1 km respectively. As expected from the above and from the distributions of land-use categories and field-size given in Tables 1 and 2, Figure 18a shows that the greatest classification accuracy is achieved for the cropland subregion and the poorest for the woodland subregion. Based upon land-use and field-size distributions alone, one would expect a greater absolute classification accuracy for the pasture/rangeland subregion than for the urban subregion in Figure 18a; however, the greater local topographic variation present within the pasture/rangeland subregion (Figure 1) leads to moisture classification errors related to the variance in local slope, which is unknown to the "blind" classification algorithm. This same effect also suppresses the absolute classification accuracy for the woodland subregion which is also "hilly" in nature.

For a 1-km by 1-km resolution radar, the combined effects of the spatial distribution of land-use categories (the relative mix of categories and their respective size distributions) and topographic relief upon absolute classification accuracy yield the results shown in Figure 18b. For areas where local topographic relief varies over spatial dimensions of hundreds of meters, the 1-km by 1-km radar resolution will tend to average local slope-related variance in P_r, and thus yield absolute classification accuracies greater than those achieved by a finer resolution sensor (such as 100 m by 100 m). This appears to be the case

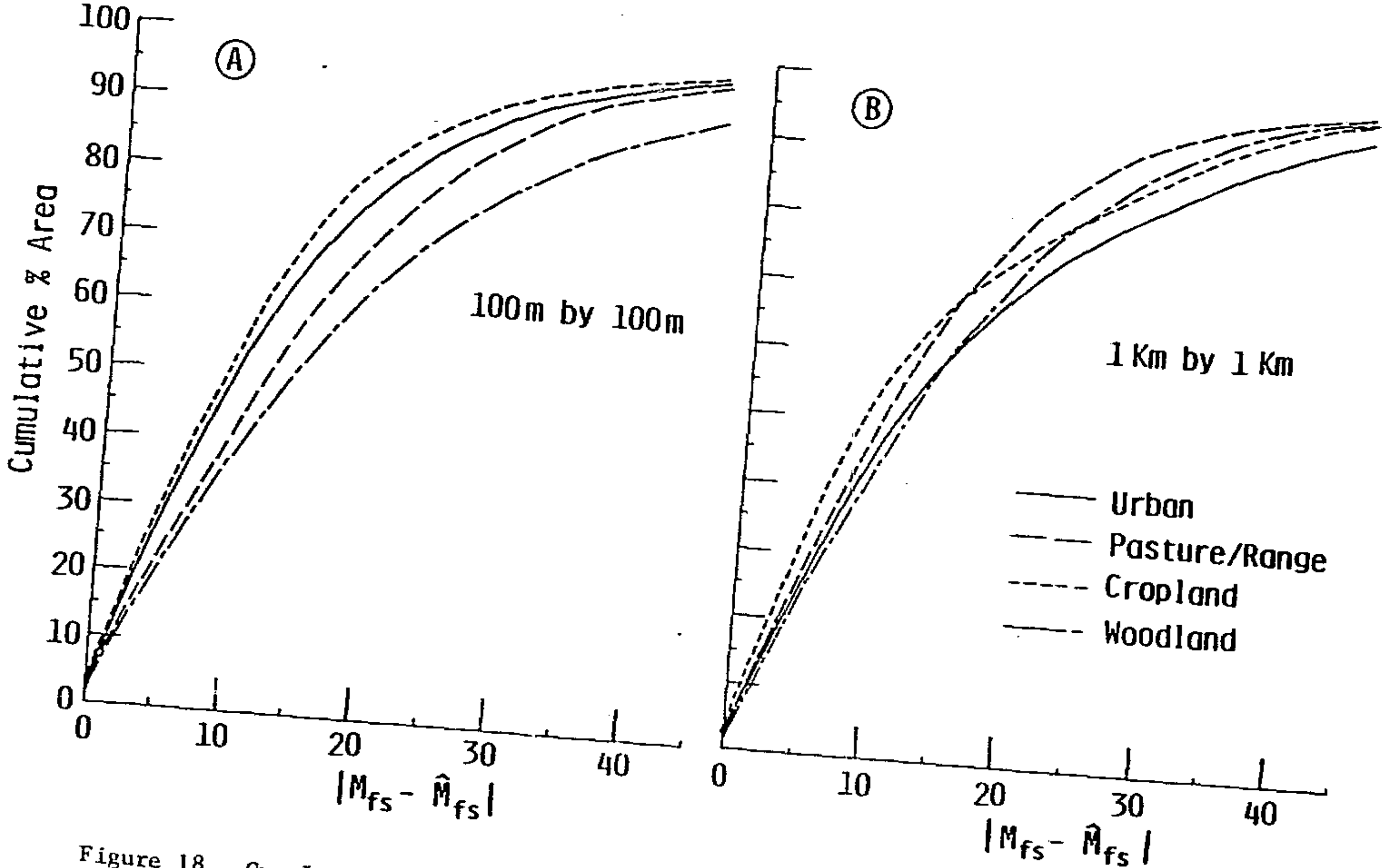

Figure 18. Cumulative percent area correctly classified as to soil moisture versus maximum classification error (only moisture-dependent grid cells are compared).

for the pasture/rangeland and woodland subregions of the test site. For example, at an absolute accuracy level of +/- 20% of field capacity, Table 5 shows that the percent area correctly classified within this limit from the 100-m resolution radar is 71.3% and 64.1% for the pasture/rangeland and woodland subregions, respectively; and the percent area correctly classified from the 1-km resolution radar increases to 79.4% and 73.3% for the two subregions, respectively.

Conversely, for areas characterized by a large number of dispersed cultural targets (with generally large P_r), the use of a coarse-resolution radar, such as 1 km by 1 km, is shown to degrade absolute moisture classification accuracy relative to that achievable by a 100-m by 100-m resolution sensor; this effect is demonstrated by the urban and cropland subregions. For example, in Figure 18 the effect of dispersed cultural features and field size distribution leads to a decrease in percent of the urban subregion which is correctly classified to within +/- 20% of field capacity from 77.9% (100-m radar resolution) to 70.1% (1-km radar resolution). In a similar fashion, the percent area correctly classified to within +/- 20% of field capacity for the cropland subregion decreases from 82.0% to 75.6% for the 100-m and 1-km radar resolutions, respectively.

The above results for Julian day 141 are not independent of general soil moisture condition and the spatial variability of soil moisture. The absolute soil moisture classification accuracies for each of the four subregions are

TABLE 5. Percent of Moisture Variant Area Correctly Classified to Within +/-20 of True Soil Moisture ($|E_m| \leq 20\%$)

Julian Day	141			150			160		
Radar Resolution	100 m	1 km	3 km	100 m	1 km	3 km	100 m	1 km	3 km
Subregions									
Cropland	82.0	75.6	74.3	87.5	91.0	91.8	77.4	73.9	75.6
Urban	77.9	70.1	65.0	75.3	83.6	86.9	76.2	63.7	58.5
Rangeland/Pasture	71.3	79.4	80.4	72.5	80.4	82.3	77.0	74.6	77.4
Woodland	64.1	73.3	72.7	72.6	83.6	86.0	68.3	68.5	68.4

shown for Julian days 150 and 160 in Figures 19 and 20, respectively. In addition, the percent area correctly classified to within +/- 20% of field capacity are also given for each date and radar resolution in Table 5.

For the generally wet soil conditions prevalent on Julian day 150, comparison of the results shown in Figure 19 and Table 5 as a function of orbital radar resolution indicates that estimate accuracy increases with the additional spatial averaging provided by the coarse resolution radars for all subregions. This is explained by the distribution of soil moisture for this date which is primarily governed by the antecedent rainfall pattern. Since a large quantity of rain fell within most of the test site just prior to the simulated orbital overpass, the local properties of slope, soil texture, and crop canopy condition have not had sufficient time to exert a large influence and vary local soil moisture distributions. As a result, the added spatial averaging provided by the coarser radar resolutions acts to increase classification accuracy by averaging small spatial scale noise effects related to local relief and variance in local radar backscattering category. This is true even for the urban scene; since at very high soil moisture conditions, the P_r from wet agricultural fields approaches that from the cultural features.

Within the four subregions, the dependence of soil moisture classification accuracy upon radar resolution is shown in Figure 20 and Table 5 for the generally dry and

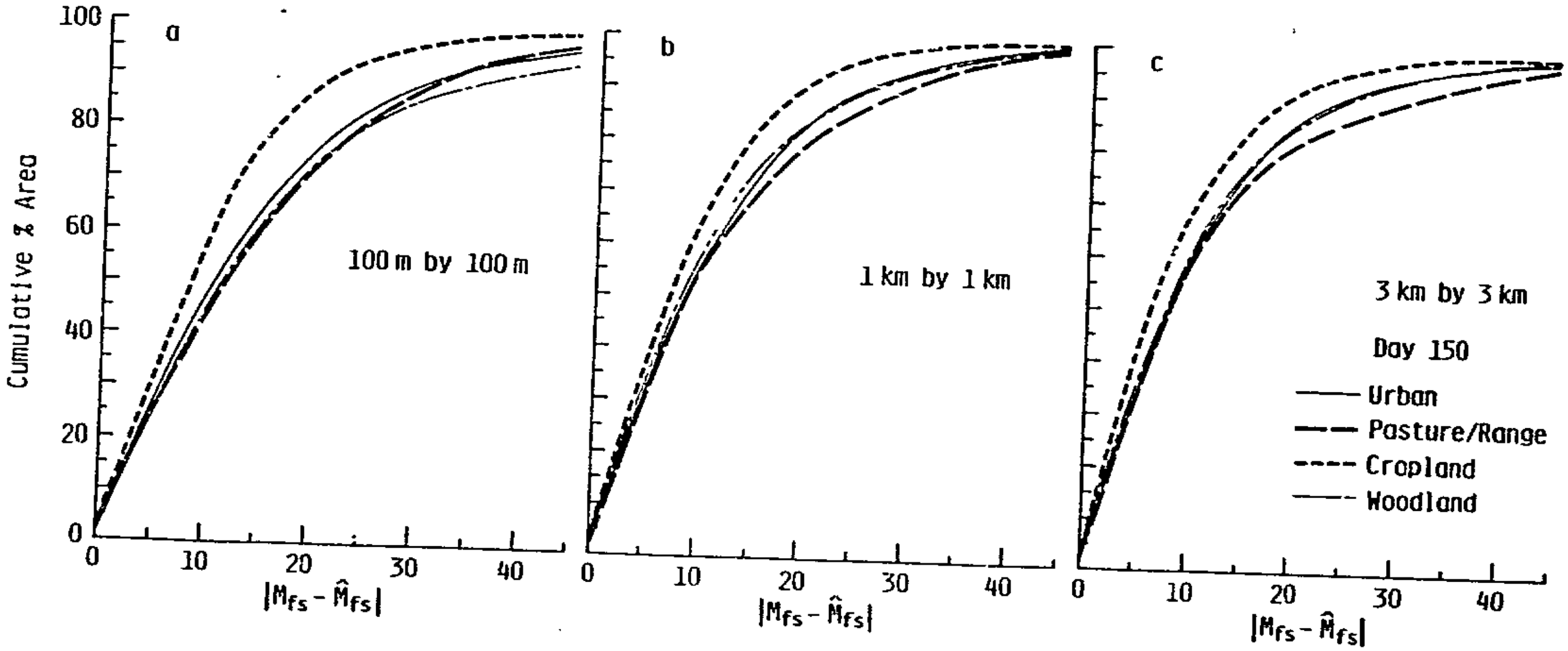

Figure 19. Cumulative percent area of all moisture dependent pixels in each subregion as a function of absolute moisture classification error on Julian day 150.

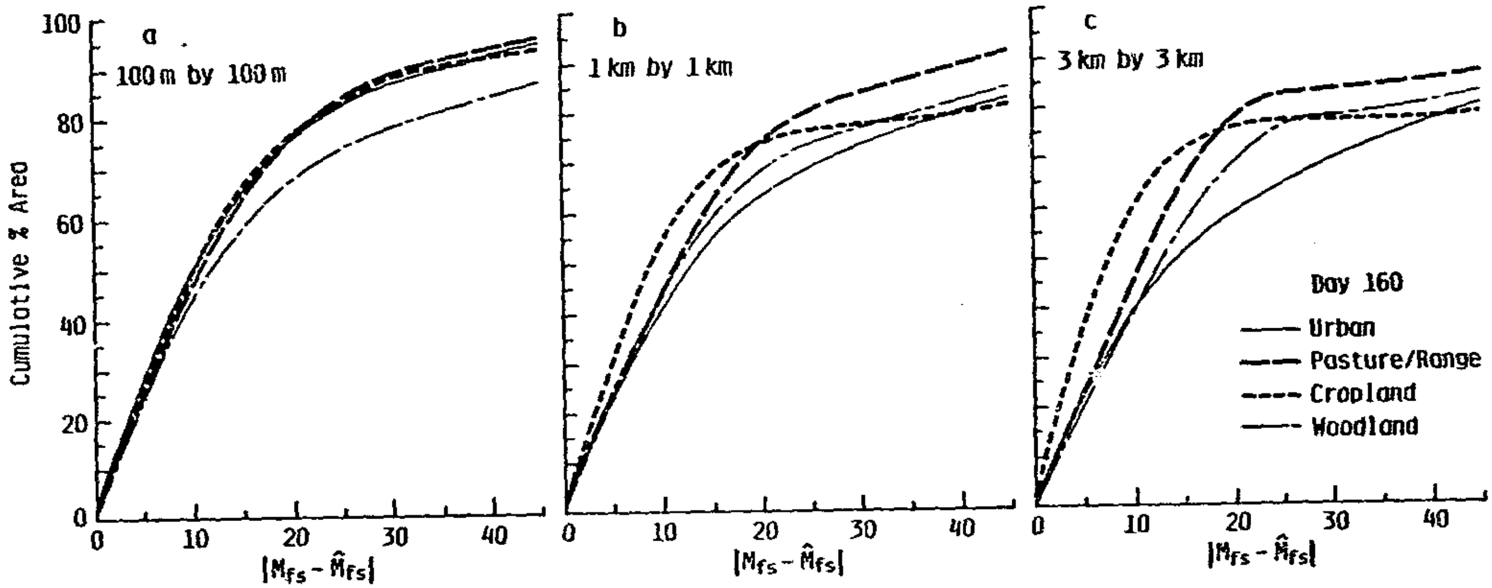

Figure 20. Cumulative percent area of all moisture dependent pixels in each subregion as a function of absolute moisture classification error on Julian day 160.

spatially variable soil moisture conditions prevalent on Julian day 160. Classification accuracy is shown to be independent of radar resolution for absolute estimate error $|M_{fs} - \hat{M}_{fs}|$ less than 20% of field capacity for the cropland, rangeland/pasture, and woodland subregions. However, as radar resolution is degraded the areal percentage of the cropland and woodland subregions with large absolute estimate errors, $|M_{fs} - \hat{M}_{fs}| \geq 30$, does increase significantly. This is attributed to the large local variance in true soil moisture M_{fs} within these subregions on Julian day 160. The most extreme example of local variance in M_{fs} is given by the urban subregion which exhibits a pronounced decrease in classification accuracy as radar resolution is degraded.

4.2 Multidate Change Detection of Soil Moisture

The preceeding section shows that absolute moisture classification accuracy from a single date orbital radar observation is limited by the presence of scene confusion factors within the imagery and their size and spatial dispersion relative to the radar resolution. Within the present discussion, scene confusion factors are defined both as the presence of scene elements for which soil moisture is unidentified such as buildings, roads, water bodies, etc. and also the occurance of variability in $P_r(\theta)$ from scene elements possessing equivalent soil moisture. The latter results from natural variability in topographic slope, crop canopy type and stage of growth, row direction, and surface roughness.

In single date sensing and classification of soil moisture, the confusion effects of cultural features and water bodies can be minimized (but not eliminated) by spatial filtering. Two approaches are feasible. First a simple intensity slice of the received power $P_r(\theta)$ could be used to roughly define water (dark) and point targets such as buildings (bright) within the image, the remainder of the image could then be subjected to the "blind" moisture classification algorithm. However, this approach cannot be expected to yield consistent results since for very dry soil moisture conditions many agricultural targets can appear similar to water (Figure 8a) or the water may be roughened by wind. In addition, for very wet soil conditions, many agricultural targets will be characterized by P_r near nadir similar to that from the point targets (Figure 8c). A second, more satisfactory approach would be to incorporate _a priori_ knowledge of the spatial distribution of such features and filter them from moisture classification. This, of course, assumes the availability of a Level I land-use classification which could be scaled and rectified to the orbital radar imagery.

In a similar fashion, the moisture classification error related to natural variability within the agricultural portions of the scene could be reduced if the radar data can be registered to topographic and crop distribution data. This would assume a mechanism for crop discrimination and classification. In this case, each pixel element in the radar image could be classified as to soil moisture using an algorithm tailored to be crop specific. Obviously, this approach is not currently feasible.

However, since most of the confusion factors are spatially fixed and relatively invariant over short periods of time (excepting wind conditions), their effects on moisture classification accuracy can be minimized more economically by the multi-temporal change detection approach. In this technique, the radar imagery acquired at two dates are coregistered and their ratio yields a map of scene change. This process has been shown to be relatively simple to implement with L-band orbital imagery obtained by Seasat-A [8]. For a constant imaging geometry on the two dates (angle of incidence and azimuth view angle), the backscattered power received from cultural targets should remain approximately constant and that received from water bodies should remain nearly constant depending upon local wind conditions. Hence, these features should display little or no change in the multidate ratio images. On the other hand, all scene elements subject to change in backscatter category (such as planting, harvest, and tillage of agricultural fields) and/or subject to change in near-surface soil moisture status will yield a corresponding change in the multidate ratio images. If the time separation in multi-date observation is short relative to changes in crop development, then changes apparent in the ratio images will reflect relative moisture change and/or field status change related to tillage operations. Since surface slope is constant over the time interval, row direction is time constant in the absence of tillage, and surface roughness decays only slowly with time, the impact of these confusion factors upon the ratio of multidate received power should be negligible.

The soil moisture distributions and the radar imagery simulated for Julian days 150 and 160 (wet and dry, respectively) are used to evaluate the utility of change detection for monitoring relative change in near-surfce soil moisture. The change in actual soil moisture ΔM_{fs} between the two dates is shown in Figure 21. The graytone values in the image are linearly scaled to the difference function given as:

$$\Delta M_{fs} = M_{fs}(150) - M_{fs}(160) \tag{5}$$

where the value in parentheses refers to Julian date. In producing Figure 21, a constant value of 128 (of 256 maximum) was added to ΔM_{fs}, hence medium gray values such as those for the Kansas City area denote no change in soil moisture, bright areas denote considerable drying over the 10 day period, and dark areas denote an increase in near-surface (0-5 cm) soil moisture. In general, Figure 21 shows that drying conditions are prevalent over most of the test site except for scattered areas located primarily in the western portion (left side) due to rainfall (see Figure 5).

Multidate registration of the radar imagery simulated at

ORIGINAL PAGE IS
OF POOR QUALITY

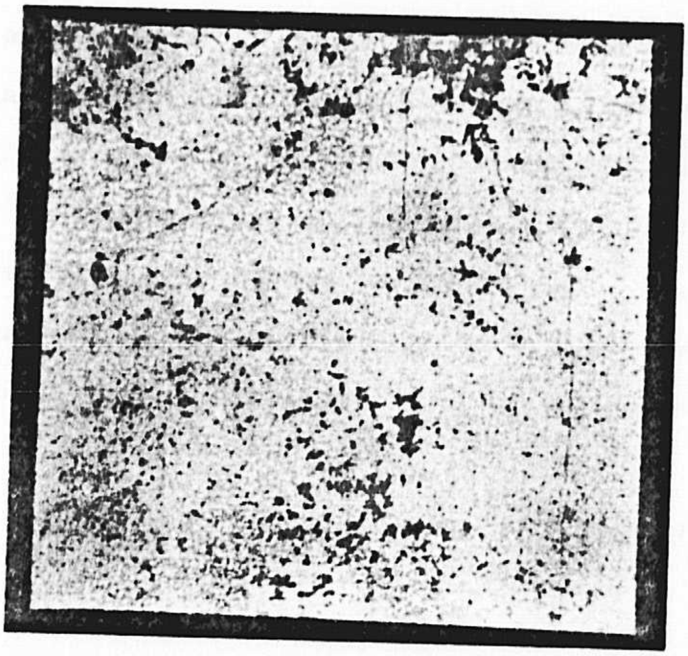

Figure 21. Change in actual soil moisture between Julian days 150 and 160; medium gray indicates no change in soil moisture, bright areas indicate drying over the period, and black areas indicate an increase in soil moisture.

each of the three resolutions yields difference images which are scaled to $\Delta\hat{M}_{fs}$ via the blind classification algorithm (Equation 2). Image presentations of predicted change in soil moisture $\Delta\hat{M}_{fs}$ are shown for each radar resolution in Figure 22. In general, the direction (wetting or drying) and the magnitude of the true change in soil moisture observed in Figure 21 are faithfully reproduced for all radar resolutions. A noteable exception to this can be observed at the bottom center of each image in Figure 22. The black area denotes a predicted increase in soil moisture which is not observed in Figure 21. This discrepancy is the consequence of saturated to partially flooded soil conditions on Julian day 150 and moist conditions on Julian day 160 for this area. Hence, actual soil moisture has decreased while that predicted shows an increase since under flooded conditions the radar backscatter models generally yield low values of P_r comparable to that from a water body.

The area distributions of actual moisture change ΔM_{fs} and that predicted from the radar imagery $\Delta\hat{M}_{fs}$ are plotted in Figure 23. The sharp spike in the ΔM_{fs} distribution at zero change is related to cultural features and water bodies. In general, it is apparent that the distribution of predicted moisture change $\Delta\hat{M}_{fs}$ as derived from the 100 m resolution radar most closely approximates the actual ΔM_{fs} distribution. The spatial averaging of the coarser radar resolutions causes them to be less sensitive to relatively large local change in ΔM_{fs} and thus the magnitude and extent of such changes tends

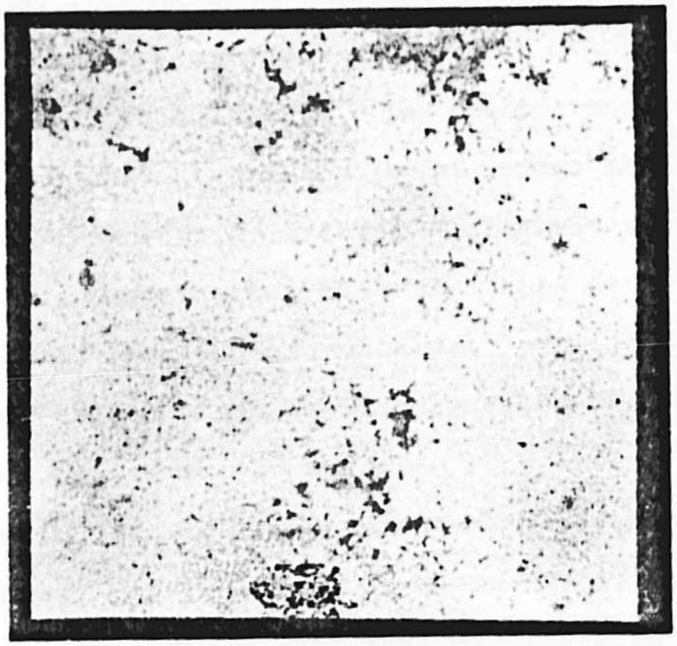

(a) 100 m by 100 m radar resolution.

Figure 22. Predicted change in soil moisture between Julian days 150 and 160 based on multidate radar imagery.

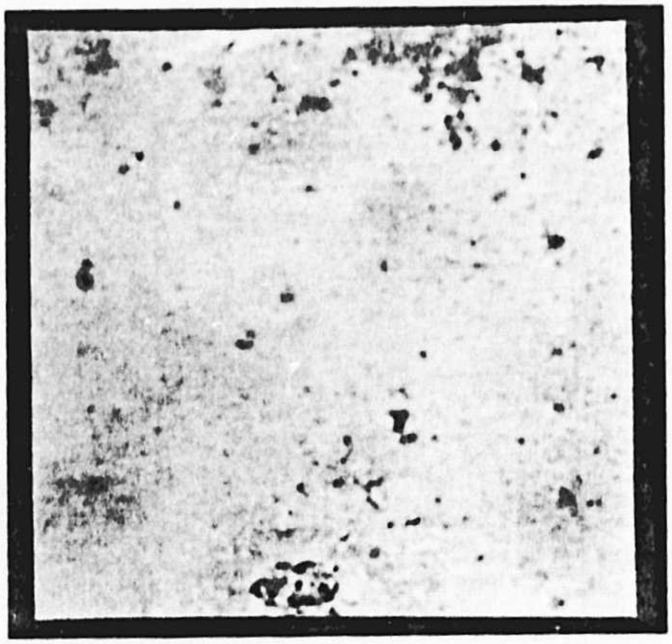

(b) 1 km by 1 km radar resolution.

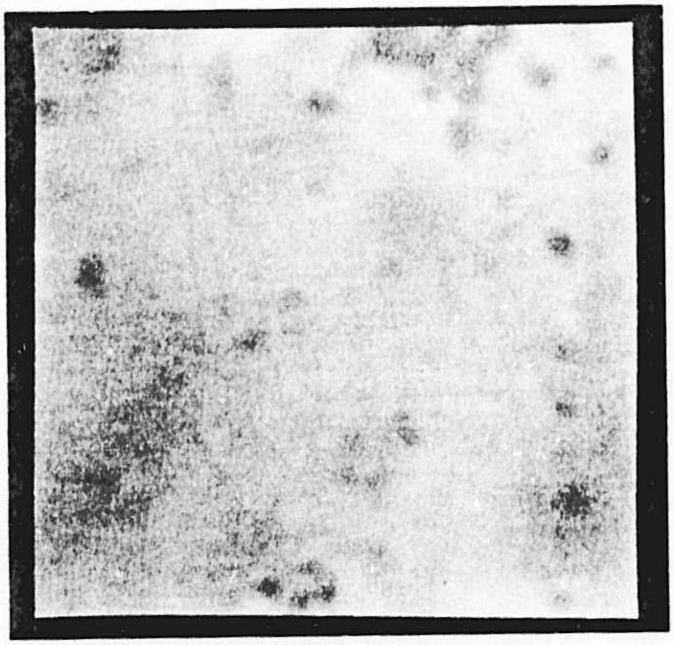

(c) 3 km by 3 km radar resolution.

ORIGINAL PAGE IS
OF POOR QUALITY

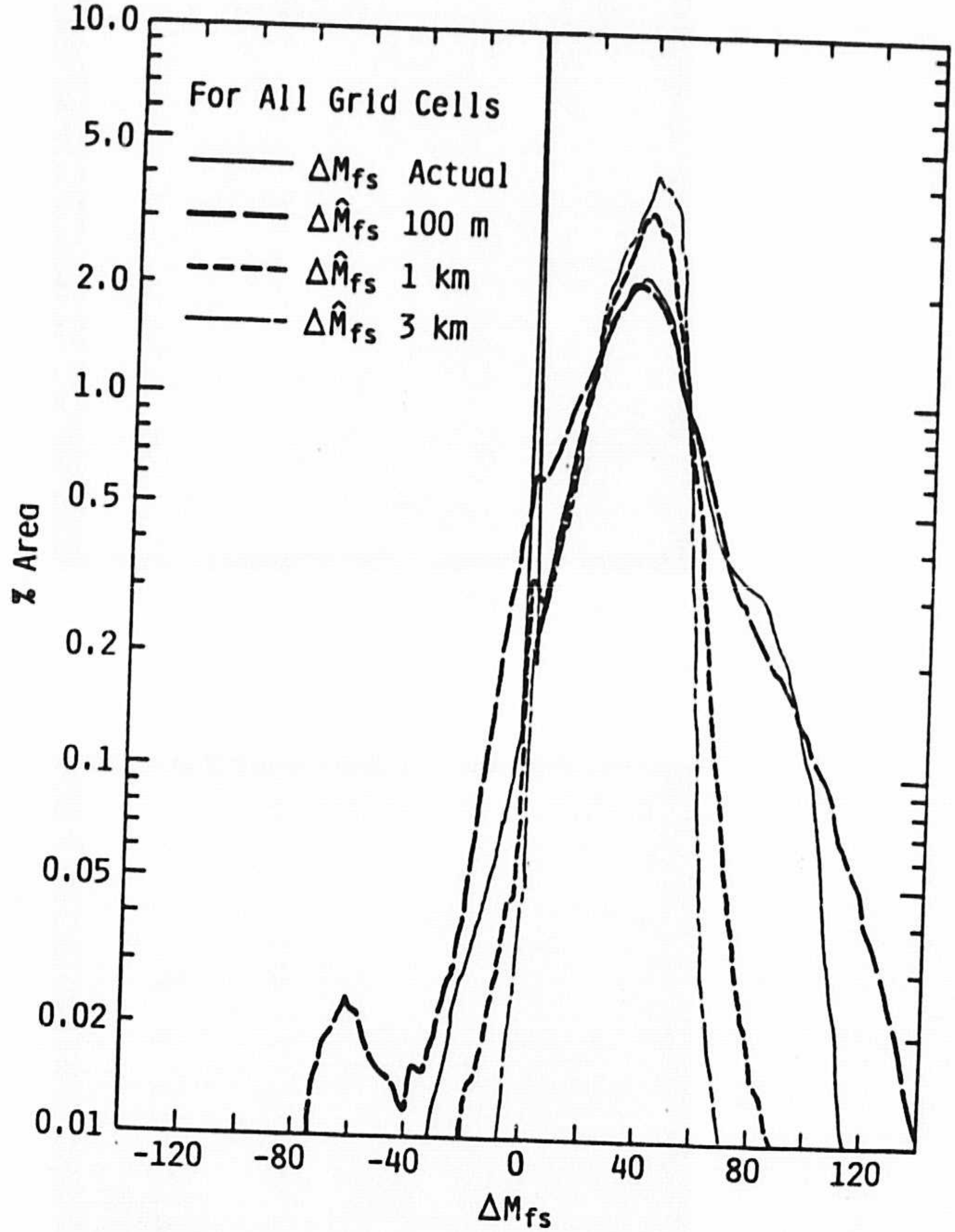

Figure 23. Distributions of actual ΔM_{fs} and predicted $\Delta \hat{M}_{fs}$ change in soil moisture.

to be underpredicted.

The actual and predicted change in soil moisture can be compared on a grid cell basis by registration of the images in Figures 21 and 22. This procedure is, of course, subject to the registration errors discussed earlier for single date moisture classification due to changes in image geometry and position. For each pixel, the error in predicting relative moisture change can be defined as:

$$E_{\Delta M} = \Delta M_{fs} - \Delta\hat{M}_{fs} \qquad (6)$$

The spatial distribution of $E_{\Delta M}$ is shown for each radar resolution in Figure 24. The brightest area on the scale bar denotes regions where the absolute magnitude of $E_{\Delta M}$ is within +/- 10% of ΔM_{fs} and as graytone decreases the areas correspond to $|E_{\Delta M}|$ limits of +/- 20%, +/- 30%, and +/- 40% respectively as shown on the scale bar. For the 100 m resolution radar, 80% of the area is correctly classified to within +/- 20% of ΔM_{fs} and greater than 90% of the area to within +/- 30% of ΔM_{fs}. In addition, most of the residual error is randomly distributed except for some classification error of large magnitude which is related to offsets in mechanical image registration as exemplified by linear features such as roads. For degraded radar resolutions of 1 km and 3 km, the magnitude of classification errors increase and are spatially associated with edges between backscatter categories.

The comparative error in moisture-change extimates $E_{\Delta M}$

ORIGINAL PAGE IS
OF POOR QUALITY

(a) 100 m by 100 m radar resolution.

Figure 24. Spatial distribution of difference between actual change in soil moisture and that predicted from multidate radar observation.

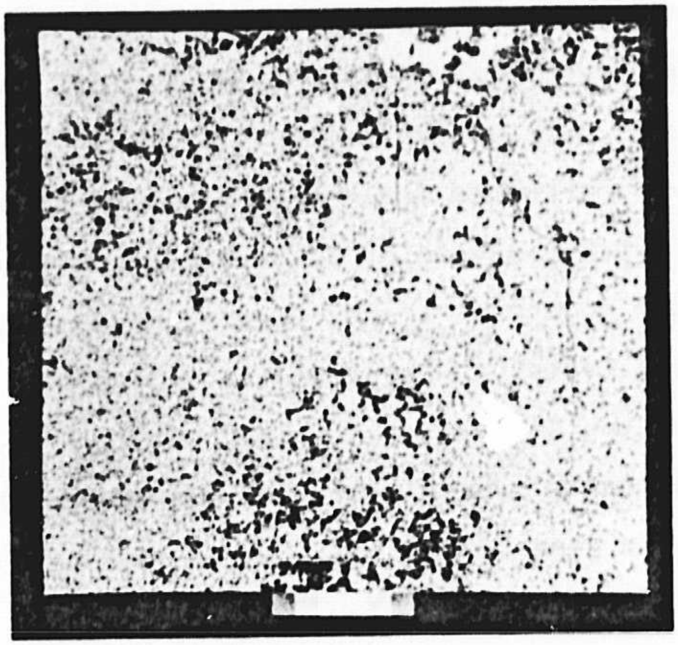

(b) 1 km by 1 km radar resolution.

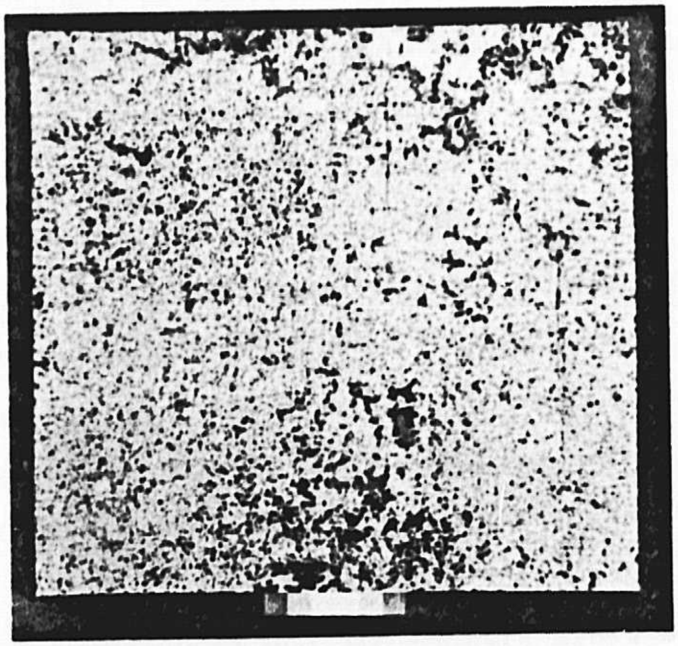

(c) 3 km by 3 km radar resolution.

for the three radar resolutions is shown in Figure 25 for all 1.34 million grid cell comparisons within the test site. The corresponding percent of total area (124 km by 108 km) with absolute classification error less than a given magnitude is plotted in Figures 26a. Obviously, the 100 m resolution radar exhibits superior classification accuracy. However, if only the moisture variant pixels are compared (excludes cultural features, water bodies, and woodland) the distinction between resolutions shown in Figure 26b is not statistically significant; 78% and 89% of the area is correctly classified to within +/- 20% and +/- 30% of ΔM_{fs}, respectively.

The effect of geographic subregion on the above results is shown in Figure 27. For the 100 m resolution radar, the change detection analysis results in superior classification accuracies for areas characterized by gentle topographic relief (cropland and urban subregions). For the coarser radar resolutions shown in Figure 27b and c, two effects are noted. First the influence of edges related to variance in the magnitude of ΔM_{fs} between adjacent backscatter categories causes classification accuracy for all subregions to decrease relative to that for the rangeland/pasture subregion which is characterized by large field sizes. Secondly, the absolute classification accuracy decreases as a function of resolution for all subregions except rangeland/pasture. The large relative field size within the rangeland/pasture subregion and the large percent area occupied by range and pasture

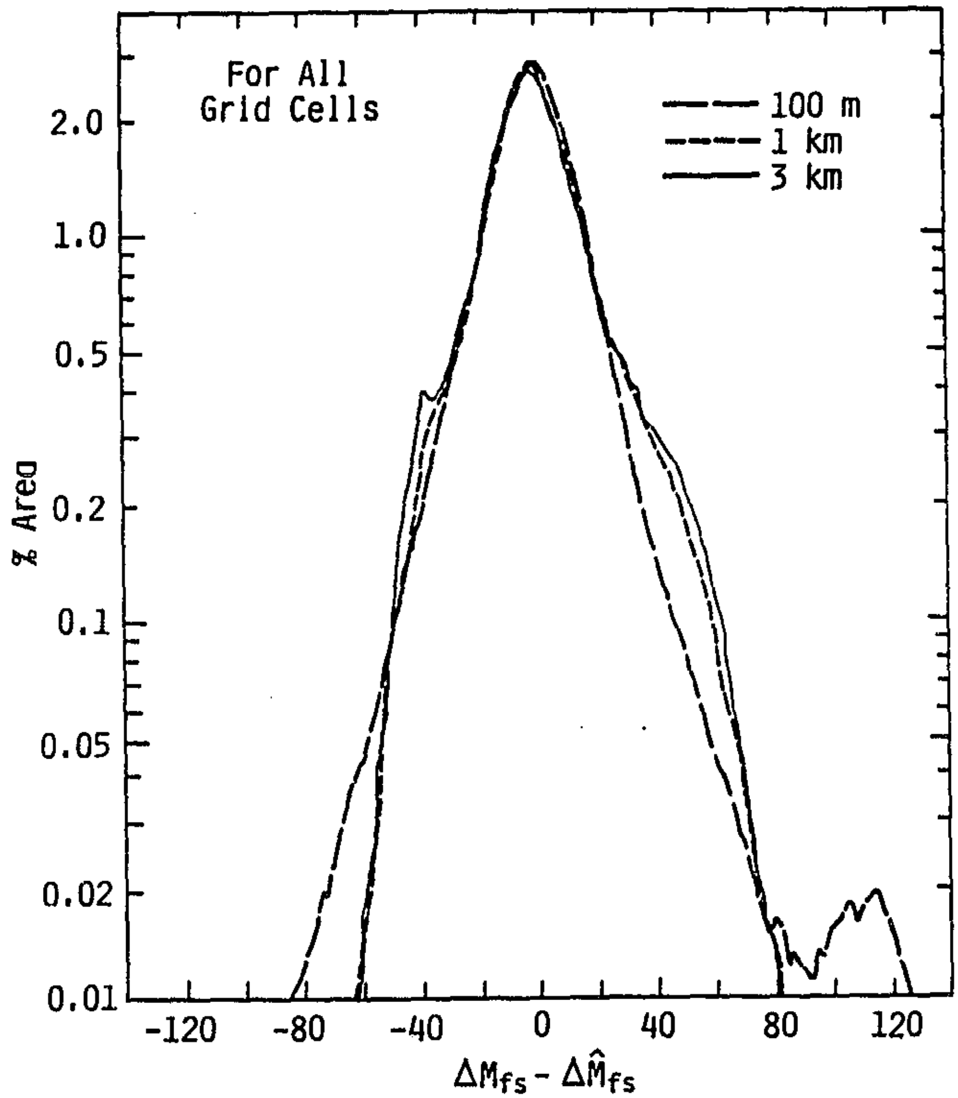

Figure 25. Magnitude of error in estimates of relative soil moisture change as a function of test site area.

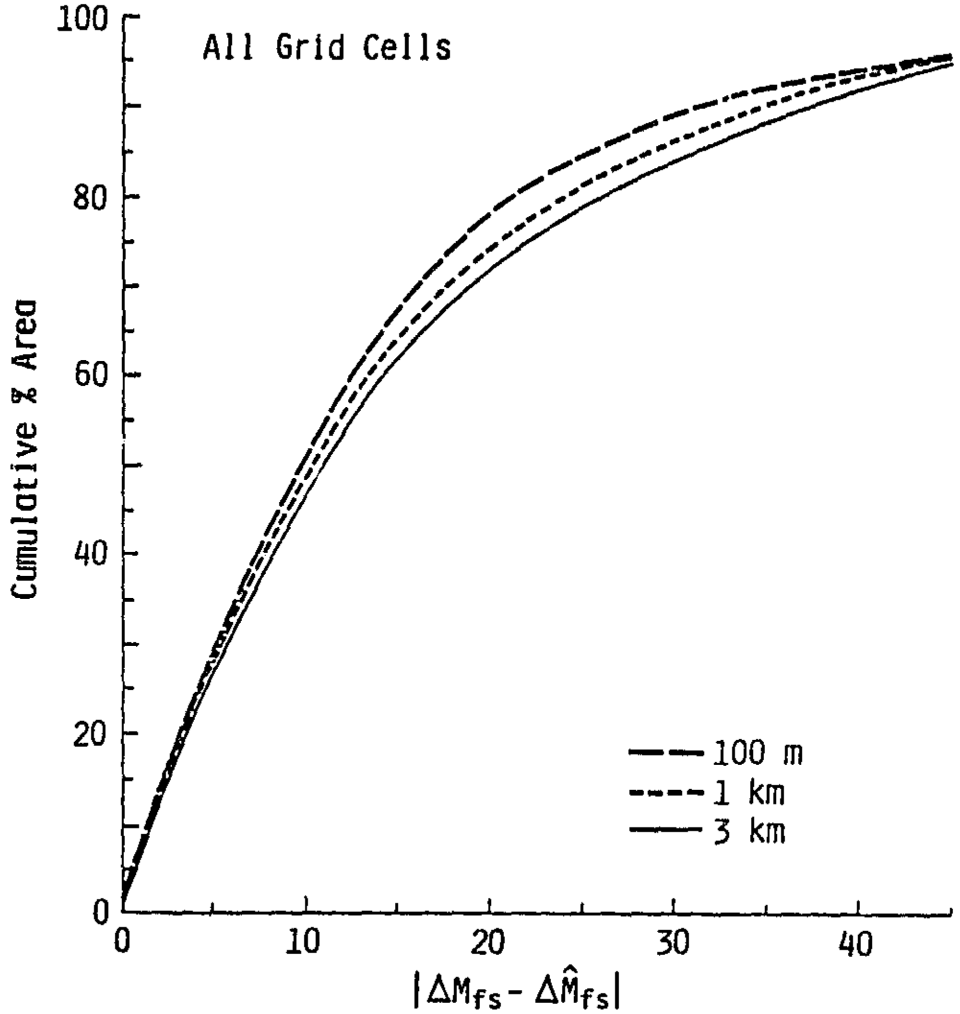

(a) Full test site, 1.34 million grid cell comparisons.

Figure 26. Percent of test site area wherein relative change in soil moisture is correctly classified versus magnitude of classification error.

ORIGINAL PAGE IS
OF POOR QUALITY

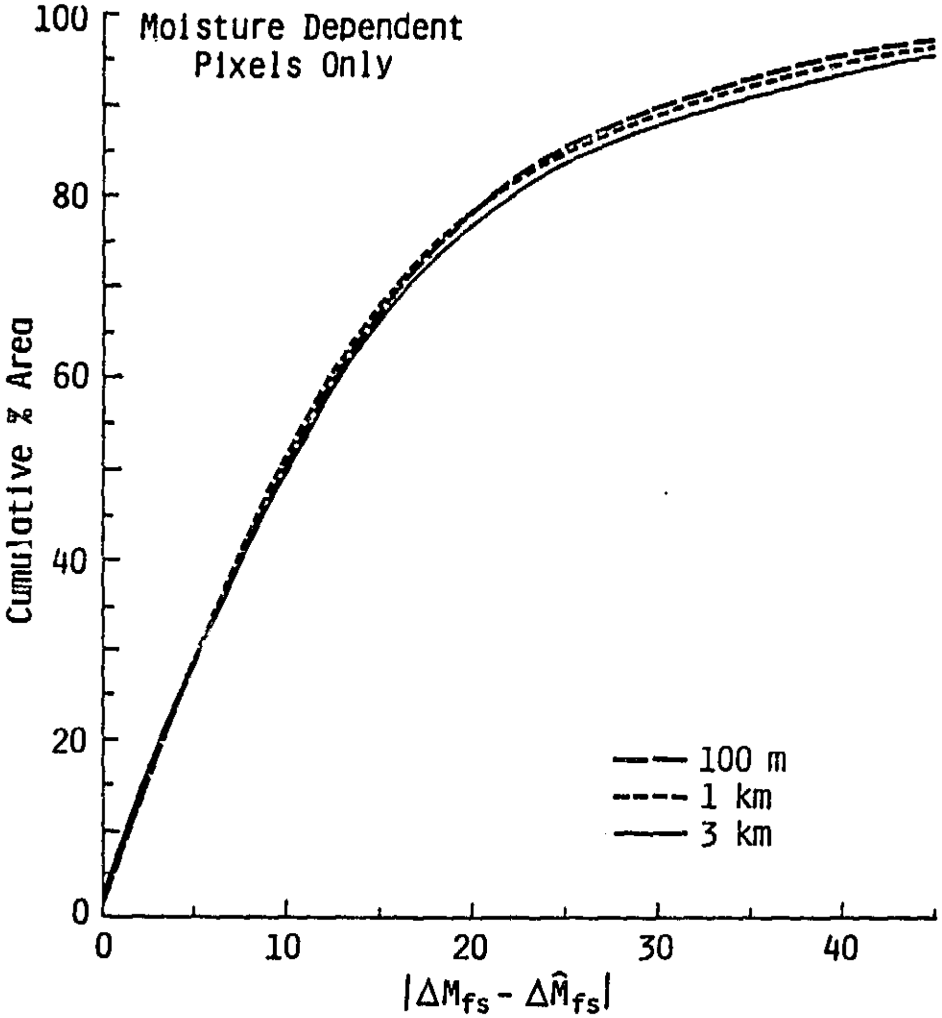

(b) Moisture dependent categories only, 1.20 million grid cell comparisons, excludes cultural features, water bodies, and woods.

ORIGINAL PAGE IS
OF POOR QUALITY

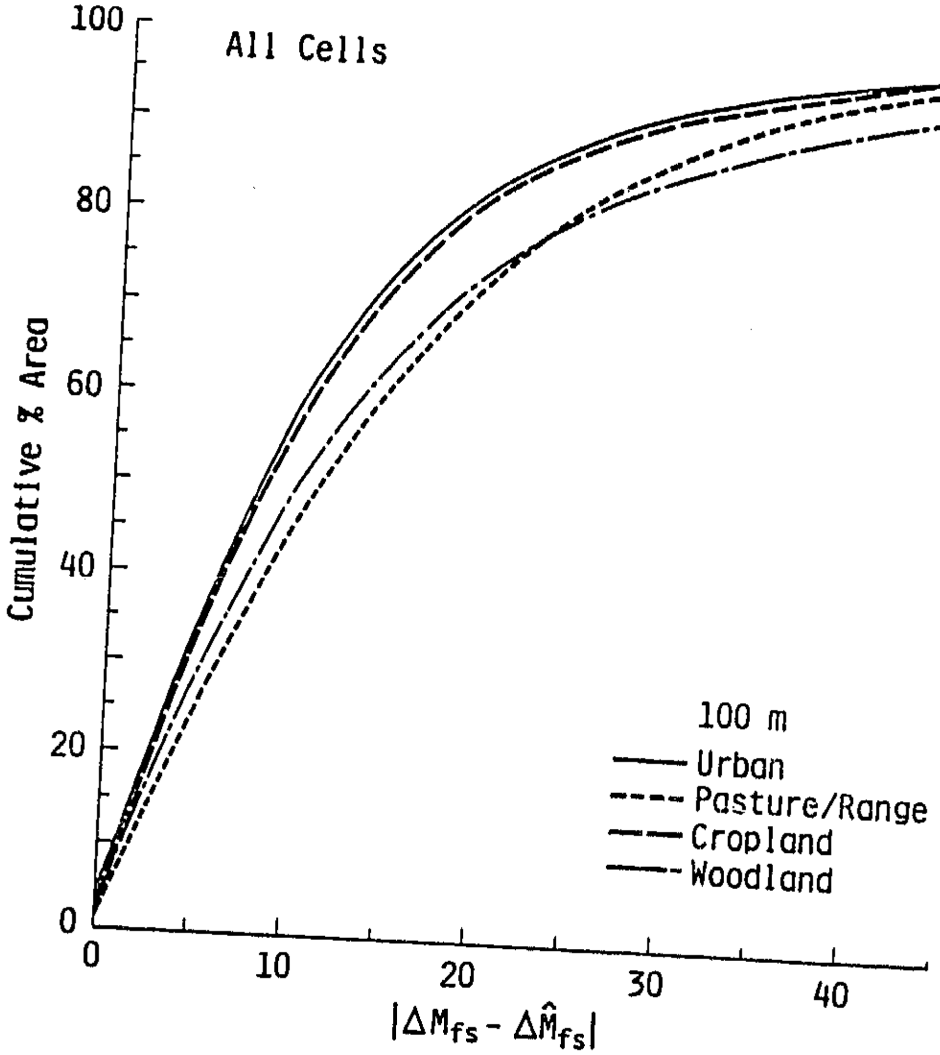

(a) 100 m by 100 m radar resolution

Figure 27. Percent of each subregion wherein relative change in soil moisture is correctly classified versus magnitude of classification error.

ORIGINAL PAGE IS
OF POOR QUALITY

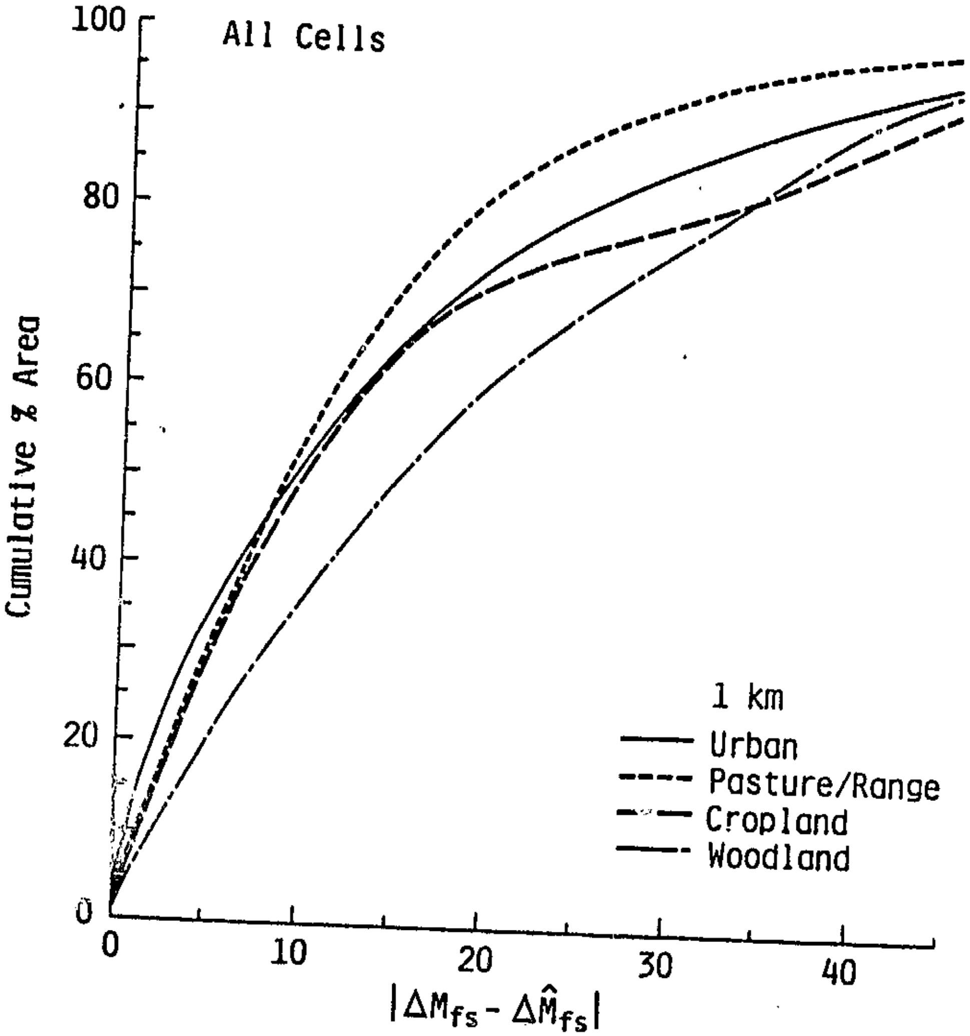

(b) 1 km by 1 km radar resolution

ORIGINAL PAGE IS
OF POOR QUALITY

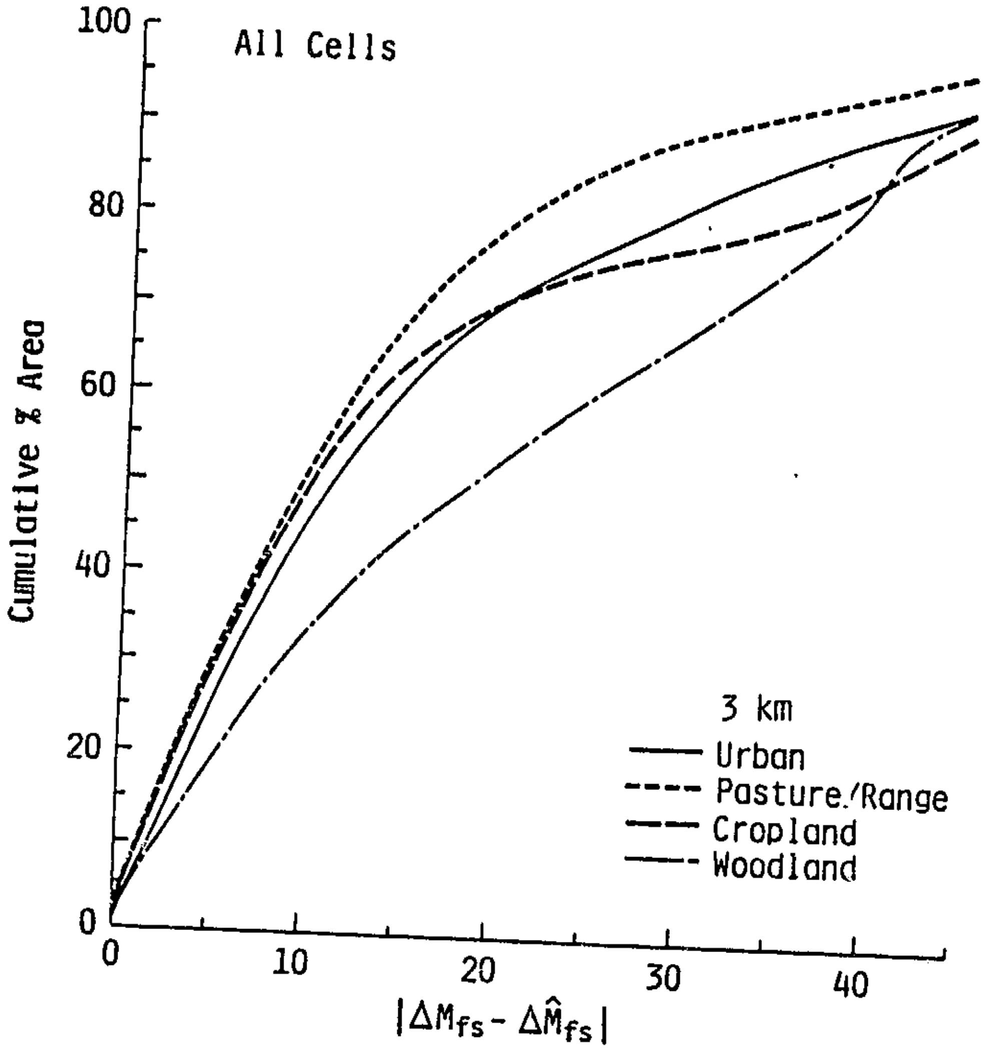

(c) 3 km by 3 km radar resolution

(61.5%) is largely responsible for the increase in classification accuracy using 1 km by 1 km radar data relative to that obtained using 100 m by 100 m radar data.

Representative values of classification accuracy within each subregion for an error magnitude of +/- 20% of ΔM_{fs} are shown in Table 6. These values show that 73% to 83% of the area within any subregion can be correctly classified as to within +/- 20% of actual soil moisture change for 100 m by 100 m resolution radar imagery. In addition, these values are generally superior to those obtained for single date moisture classification shown in Table 5.

5.0 CONCLUSIONS

This simulation study reconfirms prior results that relatively high single-date moisture-classification accuracies can be achieved from orbital radar operating at 4.75 GHz with HH polarization and at incidence angles of 7° to 17° relative to nadir. Furthermore, this study shows that classification accuracy is optimized for radar resolutions smaller than the expected field-size distribution of extended targets; a nominal sensor resolution on the order of 100 m by 100 m is found to yield the most robust classification results for the majority of tested conditions. In addition, prior results have been extended to show that expected moisture-classification accuracy for a given sensor resolution is not independent of general soil moisture

TABLE 6. Percent Area Correctly Classified to Within +/- 20% of the True Change in Soil Moisture ΔM_{fs} from Julian Day 150 to Julian Day 160

Subregions	All Pixels 100 m	1 km	3 km	Moisture Dep. Pixels 100 km	1 km	3 km
Cropland	82.4	71.4	70.8	83.3	74.0	73.6
Urban	83.4	73.9	70.5	80.4	69.8	64.2
Rangeland/Pasture	73.7	81.77	79.1	74.1	84.8	82.3
Woodland	74.7	60.7	52.6	72.8	73.5	73.5
Full Scene	78.3	74.6	72.0	78.3	78.3	76.8

condition or of the geographical mix of land-use, field-size distribution, and local topography. Finally, the use of multi-date radar imagery to estimate relative change in near-surface soil moisture status is shown to substantially reduce classification errors related to the presence of cultural features and water bodies, the presence of variable crop-canopy covers, and local variability in topographic relief.

Based upon this study, a reasonable approach for the purposes of soil-moisture sensing would be to obtain the data at a sensor resolution on the order of 100 m (with a large number of independent looks) and then degrade the resolution where necessary by post-detection processing to average the moisture classification errors associated with local slope in regions of variable topographic relief. In addition, multi-temporal change-detection analyses could also minimize classification errors controlled by topographic relief as well as those errors that are related to intra- and inter-crop variance in radar backscattering [8].

6.0 ACKNOWLEDGMENTS

This research was supported by the National Aeronautics and Space Administration, Johnson Space Flight Center, Houston, Texas, Grant NCC 9-6.

REFERENCES

[1] Ulaby, F. T., M. C. Dobson, J. Stiles, R. K. Moore, and J. Holtzman, 1982, "A Simulation Study of Soil Moisture Estimation by a Space SAR," Photo. Eng. Rem. Sens., Vol. 48, No. 4, pp. 645-660.

[2] Dobson, M. C., F. T. Ulaby, and S. Moezzi, 1982, "Assessment of Radar Resolution Requirements for Soil Moisture Estimation from Simulated Satellite Imagery," RSL Technical Report 551-2, University of Kansas Center for Research, Inc., Lawrence, Kansas.

[3] Anderson, J. R., et al., 1976, "A Land Use and Land Cover Classification System for Use with Remote Sensor Data," Geol. Surv. Prof. Paper 964, U.S. Government Printing Office, Washington, D.C.

[4] Hodges, T., 1981, "U.S. Crop Calendars in Support of the Earlier Warning Project," LEMSCO-14674, Lockheed Eng. and Management Services Co., Inc.

[5] Ulaby, F. T., M. C. Dobson, and D. R. Brunfeldt, 1983, "Improvement of Moisture Estimation Accuracy of Vegetation-Covered Soil by Combined Active/Passive Microwave Remote Sensing," IEEE Trans. Geosc. and Rem. Sens., accepted for publication 1983.

[6] Ulaby, F. T., M. C. Dobson, J. Stiles, R. K. Moore, and J. Holtzman, 1981, "Evaluation of the Soil Moisture Prediction Accuracy of a Space Radar Using Simulation Techniques," RSL Technical Report 429-1, University of Kansas Center for Research, Inc., Lawrence, Kansas.

[7] Holtzman, J. C., V. S. Frost, J. L. Abbott, and V. H. Kaupp, 1978, "Radar Image Simulation," IEEE Trans. Geo. Elect., Vol. GE-16, No. 5, pp. 296-303.

[8] Brisco, B., F. T. Ulaby, and M. C. Dobson, 1983, "Spaceborne SAR Data for Land-Cover Classification and Change Detection," Digest of the 3rd IEEE Intl. Geoscience and Remote Sensing Symp., San Francisco, CA, August 31 - September 2.

[9] Kansas State Board of Agriculture, 62nd Annual Report and Farm Facts, Topeka, Kansas, 1979.

[10] Missouri Farm Facts, Missouri Crop and Livestock Reporting Service, Columbia, Missouri, April 1982.

[11] Peck, A. J., R. J. Luxmoore, and J. L. Stolzy, 1977, "Effects of Spatial Variability of Soil Hydraulic Properties in Water Budget Modeling," Water Resources

Research, Vol. 13, No. 2, pp. 348-354.

[12] Peak, A. J., R. McQuivey, T. Keefer, E. R. Johnson, and J. Erekson, 1981, "Review of Hydrologic Models for Evaluating Use of Remote Sensing Capabilities," NASA CR 166674, Hydrex Corp., Fairfax, Virginia.

[13] Hildreth, W. W., 1981, "Comparison of the Characteristics of Soil Water Profile Models," NASA - 15700, Lockheed Eng. and Management Services Co., Inc.

[14] Jackson, R. D., 1972, "On the Calculation of Hydraulic Conductivity," Soil Sci. Soc. Amer. Proc. Vol. 36, pp. 380-382.

[15] Armstrong, B. L., 1978, "Derivation of Initial Soil Moisture Accounting Parameters from Soil Properties for the National Weather Service River Forecast System," NOA Technical Memorandum NWS HYDRO 37, National Weather Service.

[16] Eagleman, J. R., 1971, "An Experimentally Derived Model for Actual Evapotranspiration," Agr. Met., Vol. 8, pp. 385-394.

[17] Clapp, R. B., and G. M. Hornberger, 1978, "Empirical Equations for Some Soil Hydraulic Properties," Water Res., Vol. 14, No. 4, pp. 601-605.

[18] Doorenbos, J., and W. O. Pruitt, 1977, "Guidelines for Predicting Crop Water Requirements," FAO Irrigation and Drainage Paper 24, United Nations Food and Agriculture Organization.

[19] United States Department of Agriculture, 1970, "Irrigation Water Requirements," Technical Release 21, USDA/Soil Conservation Service.

[20] Hershfield, D. M., 1961, "Rainfall Frequency Atlas of the U.S.," Hydrologic Service Division, Soil Conservation Serv'ce, U.S. Department of Agriculture, Washington, D.C.

[21] Dunin, F. X., 1976, "Its Simulation for Field Conditions," Chapter 8 in J. C. Rodda (ed.): Facts of Hydrology, pp. 199-227, Wiley, London.

[22] Komp, E. E., V. S. Frost, and J. C. Holtzman, 1983, "Reference Manual for the Radar Image Simulator," RSL Technical Report 581-2, University of Kansas Center for Research, Inc., Lawrence, Kansas.

APPENDIX A

DYNAMIC SOIL WATER ACCOUNTING MODEL

The purpose of a soil water-budget model within the context of realistic radar image simulation is to generate a distribution of near-surface (0-5 cm) soil moisture conditions at the spatial scale of the static terrain data base (100 m x 100 m) which responds to both static conditions (soil type, cover type, and surface slope) and dynamic conditions (crop stage, rain, and potential evaporation) on a time scale relevant to both the dynamics of the process and the orbital mechanics of an imaging satellite (daily basis). While many excellent water-budget models are available for various applications in agronomy and hydrology [11 to 15], no single model meets all the above criteria. Indeed, most such models require more detailed information on soil profile characteristics and weather conditions than is readily available for the simulation area. In addition, most models are designed to operate at a spatial scale much less than field size and over time increments significantly less than one day, or conversely, they are most appropriately applied to very coarse integration times on the order of weeks for a simple set of input parameters and at a macroscopic level much larger than field size.

Because of the large size of the data base (approximately 1,339,000 grid cells), it is necessary to tailor a model that emphasizes the surface horizon and requires a minimum of information as to soil profile and detailed local weather conditions, and yet is still sensitive to daily variation in soil moisture. A schematic of the final process model is shown in Figure A.1; it consists largely of the following components:

storm model,

surface runoff model,

crop development submodel,

evapotranspiration model, and

and interlayer redistribution model.

When given dynamic inputs of crop type, crop stage of development, rainfall, and potential evaporation, the model acts upon the static terrain model to yield daily projections of 0-5 cm soil moisture for each grid cell. It also governs the redefinition of canopy cover categories based on crop calendar changes or local flooding conditions, and these categories are then used as input to the radar simulation program's target/sensor interaction model.

A.1 Storm Model

Daily rainfall measurements as reported by 25 stations located in and around the test site were used as the basis for the storm model. Figure A.2 shows the location of the test site. Table A.1 shows the daily rainfall reported at each of these stations for the simulation period; May 18 through June 9. A grid map of estimated rainfall, with a resolution of 3 km by 3 km, was produced from measured rainfall data at these irregularly spaced recording stations

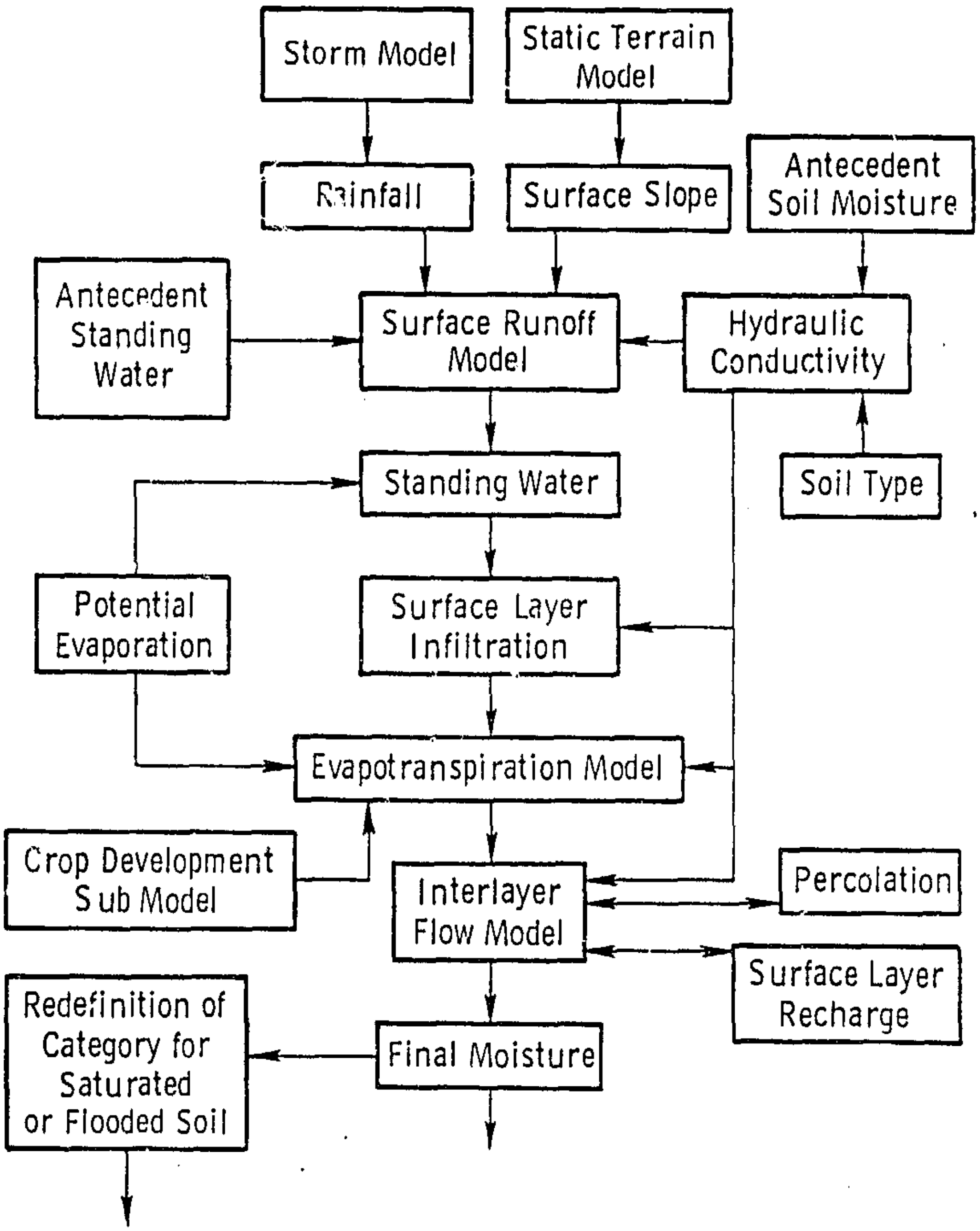

Figure A.1. Dynamic Soil Water Accounting Model (SWAM).

C-2

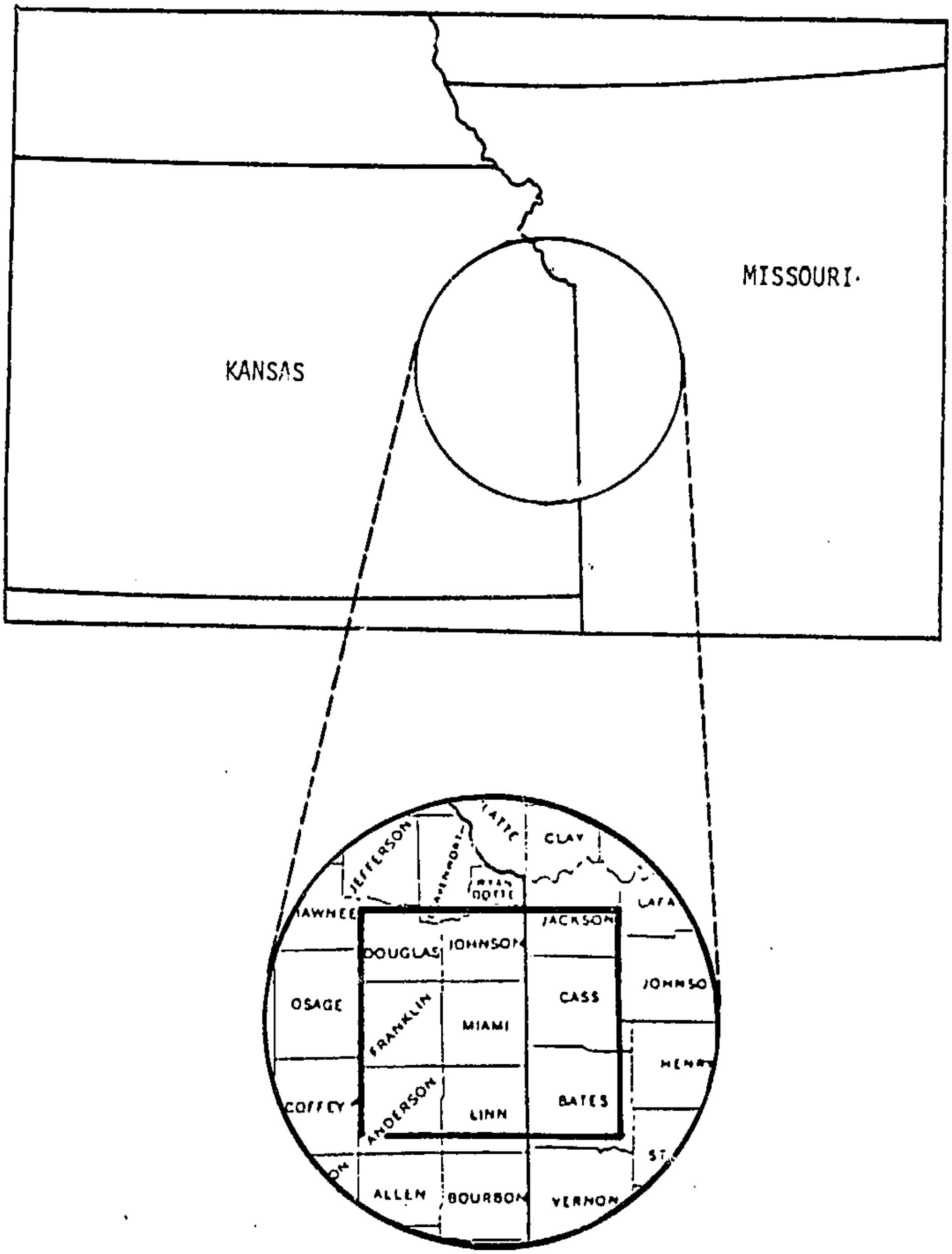

Figure A.2. Test site location.

	JULIAN DAY	TOPEKA USFO AF.	LEROY	WAVERLY	POMONA DAM	WILLIAMSBURG	LECOMPTON	CLINTON DAM	WORDEN	OTTAWA	GARNETT	LAURENCE	OSAWATOMIE	PAOLA	MOUND CITY	OLATHE	LACYGNE	KANSAS CITY	STILLWELL	LEES SUMI	BUTLER	APPLETON CITY	ELDORADO SP.	ODESSA	LEXINGTON	CLINTON	CM * EPAN	CM/HOUR RAIN INT
MAY 18	138	4.8	4.9	5.9	4.5	11.5	4.3	2.4	2.9	7.4	9.9	2.0	9.4	9.0	5.0	6.5	15.3	2.9	6.7	5.2	2.5	5.7	5.1	7.6	7.5	9.0	0.74	1.2
	139		5.1	1.9	0.4		1.7	2.7	2.2	1.3	0.0	2.5	0.9	2.3	0.2	1.5	1.1	0.1	2.0	1.4	11.0	0.1	0.5	1.7	1.0	0.6	0.31	1.7
	140																				1.0						0.48	
	141																										0.74	
	142	0.9																2.5									0.94	
	143				5.0		2.7		5.4	0.3	0.5	4.7	0.1	0.1	0.1	2.7		3.4	0.2	0.7		0.1		0.7	1.0	0.1	0.89	1.7
	144												0.0	0.3	4.0	2.5			0.1		2.2	1.3	1.1		0.7	0.9	0.6	3.6
	145	0.6					0.1											1.0									0.71	
	146			0.1			0.4			1.4															0.5		0.43	
	147																										0.42	
	148	0.4													0.6			0.0		1.0		1.1				0.5	0.35	2.3
	149		1.2	0.6	0.4	0.5	0.4	0.3	1.1	0.5	0.4	0.5	0.5	1.0		0.2	0.0		0.5	0.4			0.9	0.0	0.2		0.23	2.3
	150		0.6	3.0		1.2			2.1	0.3	0.3		0.2	0.1	4.4	2.7			0.1	0.1	0.2	0.0	0.3	3.5	0.4	0.1	0.38	3.6
	151			0.4													0.2				0.5		3.3			0.4	0.54	1.4
	152											NA											0.1				0.66	
	153	0.4	0.2	NA			0.3				0.5	NA	0.5	0.0	1.9	0.9		0.6	1.0	0.6		2.2					0.51	3.5
	154	2.1		NA	0.1	0.6	4.7	2.7	1.3	0.5		NA	0.5	0.5		0.5	1.0		0.3		2.1		0.2	1.4	0.6	3.3	0.58	3.6
	155	0.4	6.7	NA	2.4	0.1	0.6	1.1	2.7	0.2	4.2	NA	0.0		0.5	0.1	0.3	0.5	0.1			0.3	0.6				0.43	3.6
	156			NA								NA												0.1			0.40	
	157											NA															0.48	
	158		1.5								1.4	NA															0.62	
	159	0.3	1.1	0.4			0.2				0.2	NA			0.3												1.05	2.3
	160											NA															0.05	

* Epan : Mean of 11 stations for non-rainy days

Table A.1. Daily reported rainfall at 25 recording stations in and around the test site during the simulation period for 1981.

ORIGINAL PAGE IS OF POOR QUALITY

for every day during the simulation period that all or part of the test site received some rain. Figures A.3 and A.4 shows the amount of rain reported by each station on Julian day 144, and the estimated rainfall map for that day, respectively. These generated rainfall grid maps made available the total daily rainfall in cm received by each test site data base cell. An image representation of all rainfall grid maps has been shown on Figure 5.

Rainfall intensity is calculated as a daily constant from the minimum recorded daily storm duration according to

$$I_{day} = 10^{a_t} * D_{day}^{\,b_t} \tag{A.1}$$

where

I_{day} = daily constant intensity, cm/hr

D_{day} = daily minimum recorded duration, hrs.

t = storm type (2-year or 5-year), and

a and b are constant for each storm type.

The constants a_t and b_t are solved from a plot of local rainfall intensity-vs-duration curves for recurrence intervals of 2 or 5 years. For each day of the simulation, a rainfall event is classified as either a 2-year or a 5-year event based upon the maximum recorded rainfall at all gauging stations on that day. If net daily rainfall at any gauge exceeds a critical value M, then that day will be classed as a 5-year event and a_t and b_t will be used from the 5-year intensity-vs-duration curve; otherwise a_t and b_t will be used for a 2-year event. M is defined by

$$M = 10^{a} * D^{b+1}/(b+1) \tag{A.2}$$

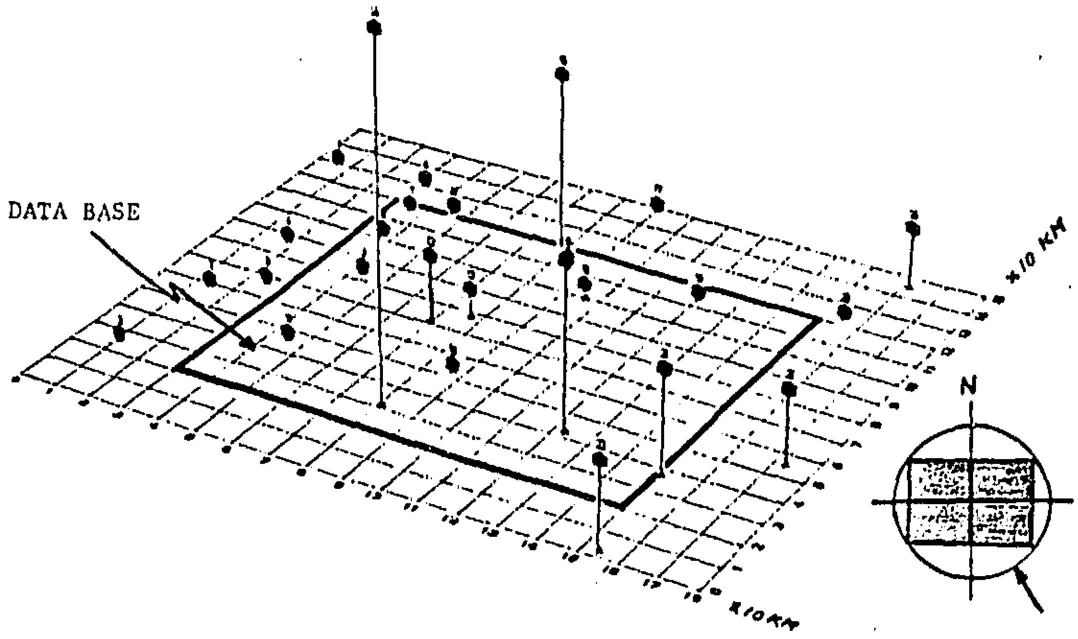

Figure A.3. Measured rainfall as reported on Julian day 144 at all stations in and around the data base (maximum rainfall is 4.8 cm).

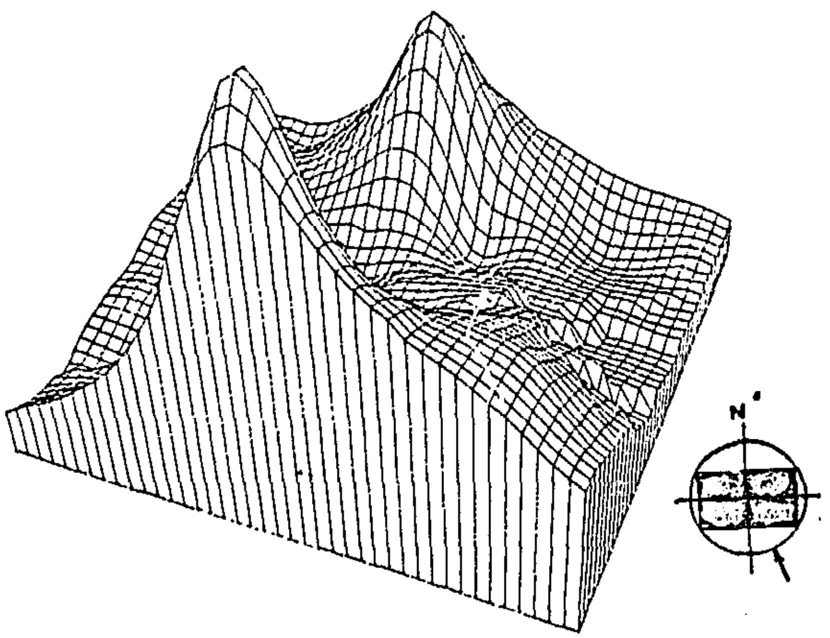

Figure A.4. Estimated rainfall on Julian day 144 for each 3 x 3 km area in the data base.

where a and b are 2-year coefficients. For the rainfall data given in Table A.1, the maximum net daily rainfall never exceeded M, therefore the 2-year coefficients were used in all precipitation events.

A.2 Surface Runoff Model

The surface runoff model considers only the net effect of local surface slope and does not explicitly account for water retention and impoundment by soil surface roughness, tillage practices, and the presence of terraces. The water available for drainage as lateral surface flow is equal to the sum of standing water remaining from the previous daily accounting period plus the incident rainfall in excess of that which can infiltrate the surface layer and the root layer. The drainage D is computed from remaining standing water and local surface slope by

$$D = SW * (1.1 - 0.8^{\alpha}) \qquad (A.3)$$

where

SW = standing water

α = the slope angle of the surface from horizontal in degrees.

The term $1.1 - 0.8^{\alpha}$ is defined as the drainage coefficient and is plotted versus surface slope (in percent) in Figure A.5.

A.3 Evapotranspiration Model

Evapotranspiration is calculated differently for cropped

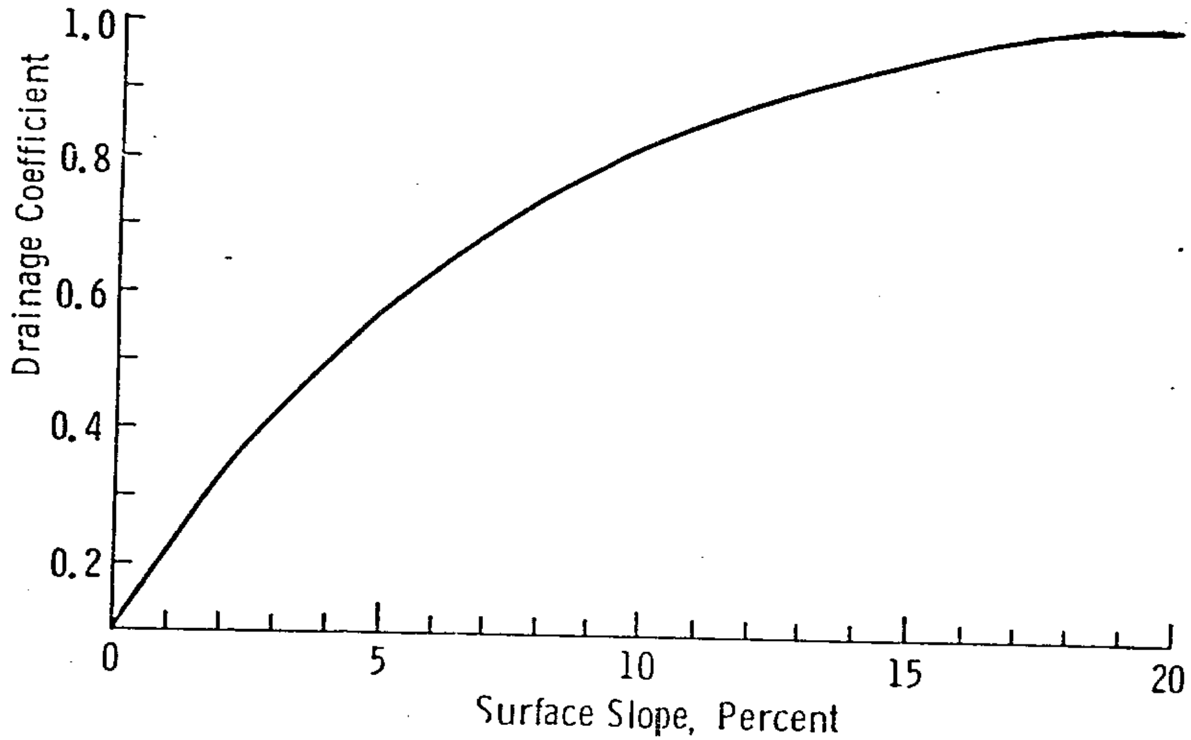

Figure A.5. Variation in drainage coefficient as a function of soil surface slope in the soil water accounting model (SWAM).

and bare soil surfaces. For bare soil surfaces, the actual evaporation is depleted solely from the soil surface layer, while for vegetated surfaces a static root distribution model removes 30 percent of the actual evapotranspiration from the 0-5-cm layer and removes the remaining 70 percent of actual evapotranspiration from the "root zone." For simplicity, the "root zone" is assumed to be one meter in depth and is treated as a constant with time and for all crops.

For bare soil, actual evaporation, AE, is computed from potential evaporation, PE, as limited by antecedent soil moisture in the surface layer and soil hydraulic properties. Accounting is performed on a daily basis using the mean daily pan evaporation recorded at 11 stations in the study area as shown in Table A.1 for 1981.

An experimental model is used to calculate actual evaporation from potential evaporation PE:

$$AE = PE * k_{soil} * k_{storm} \tag{A.4}$$

where

$$k_{storm} = (24 - T)/24, \tag{A.5}$$

k_{soil} = soil limiting coefficient

T = the duration of storm, and

$$PE = k_p * E_{pan}, \tag{A.6}$$

where

k_p = pan coefficient, and

E_{pan} = measured pan evaporation.

The soil limiting coefficient k_{soil} is defined by an experimental model [16] dependent upon PE and soil properties.

$$k_{soil} = A + B(MR) + C(MR)^2 + D(MR)^3 \tag{A.7}$$

where A, B, C, and D are empirically derived coefficients dependent upon PE, and MR is the moisture ratio. Regression fits to experimental data yield [16]:

$$A = -0.05 + 0.732/PE \tag{A.8}$$

$$B = 4.97 - 0.661\ PE \tag{A.9}$$

$$C = -8.57 + 1.56\ PE \tag{A.10}$$

$$D = 4.35 - 0.88\ PE \tag{A.11}$$

The moisture ratio MR is related to soil water retention characteristics via

$$MR = (\theta - WP)/(FC - WP) \tag{A.12}$$

where

θ = measured soil moisture,

WP = soil moisture at wilting point, and

FC = soil moisture at field capacity.

Assuming wilting point and field capacity to be defined as matric potentials of 15 bars and 1/3 bars, respectively, WP and FC can be defined from soil textural components using the approach of Clapp and Hornberger [17]

$$FC = \theta_s(\psi_s/333)^{1/b}, \text{ and} \tag{A.13}$$

$$WP = \theta_s(\psi_s/15{,}000)^{1/b} \tag{A.14}$$

where

θ_s = soil moisture at saturation,

ψ_s = matric potential at saturation, and

b = an empirically derived value related to soil texture.

For a given soil, θ_s is calculated from the soil bulk density profile and ψ_s and b are defined by A-horizon soil texture using values given in [17]. Thus, for a given day, the terms in Eq. A.4 are dependent on the antecedent soil moisture and the gross water-retention characteristics of each soil.

For vegetated soil, the actual evapotranspiration, ET_{crop}, is computed by a modification of the Blaney-Criddle formulation used in estimating crop irrigation requirements [18,19]. Although the method is designed for an effective integration period of weeks to months, the simplicity of its input requirements makes this a practical approach for such a large number of coarse grid cells. Basically, crop consumption of water over the rooting depth varies with temperature, length of day, available soil moisture, crop type, crop stage of growth, relative humidity, and windspeed. To simplify the formulation, average measured values of temperature, day length, relative humidity, and windspeed are assumed on a seasonal basis for the simulation area. The resultant expression for ET_{crop} becomes:

$$ET_{crop} = PE * k_{crop} * k_{storm} \tag{A.15}$$

where

k_{crop} = crop coefficient.

Crop coefficient as adjusted for mean local climate is plotted in Figure A.6 as a function of number of days after planting for several of the crop covers included in the data base. Crop consumption of the water is seen to be dependent on both crop and stage of crop development. Before the crop

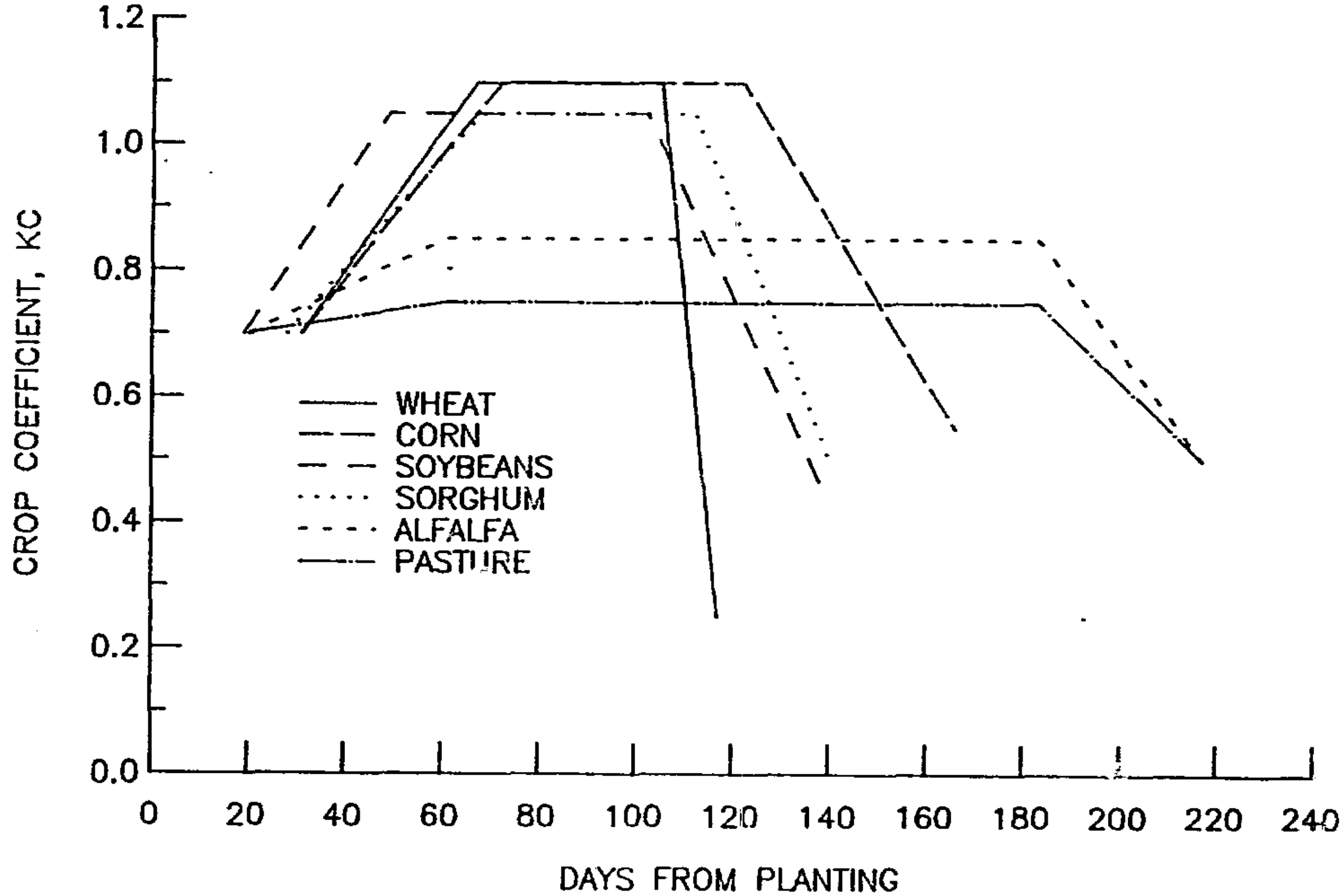

Figure A.6. Crop transpiration coefficient as a function of time from planting for several representative crops found within the simulation area.

ORIGINAL PAGE IS
OF POOR QUALITY

canopy has attained 20% ground coverage and again after harvest, the soil is treated as bare for both evapotranspiration and also for radar backscatter category.

A.4 Crop Development Model

The length of time required for a given agricultural field in the simulation data base to progress from one crop-development stage to the next is established from data gathered by the Statistical Reporting Service of the United States Department of Agriculture. The simulation area lies at the East Central reporting district of Kansas (No. 6). Figure A.7 presents a summary of mean crop development over a 10-year period as enumerated by AgRISTARS [20] for this crop reporting district. These percentages are used to define crop development stage within the simulation on a field-by-field basis. Thus, each distinct agricultural field in the data base is assigned one of the 10 planting dates. Hence, there are ten different absolute crop calendars possible for each crop type identified in Table 1.

Planting dates are randomly assigned to field codes for a specific crop based upon Figure A.7. This procedure results in the introduction of a significant source of between-field variance of soil moisture within a given crop type due to the effect of crop development stage on evapotranspiration. It also allows for a given field to have its taget classification changed in Table 1, since a medium-rough bare field becomes a cropped field after

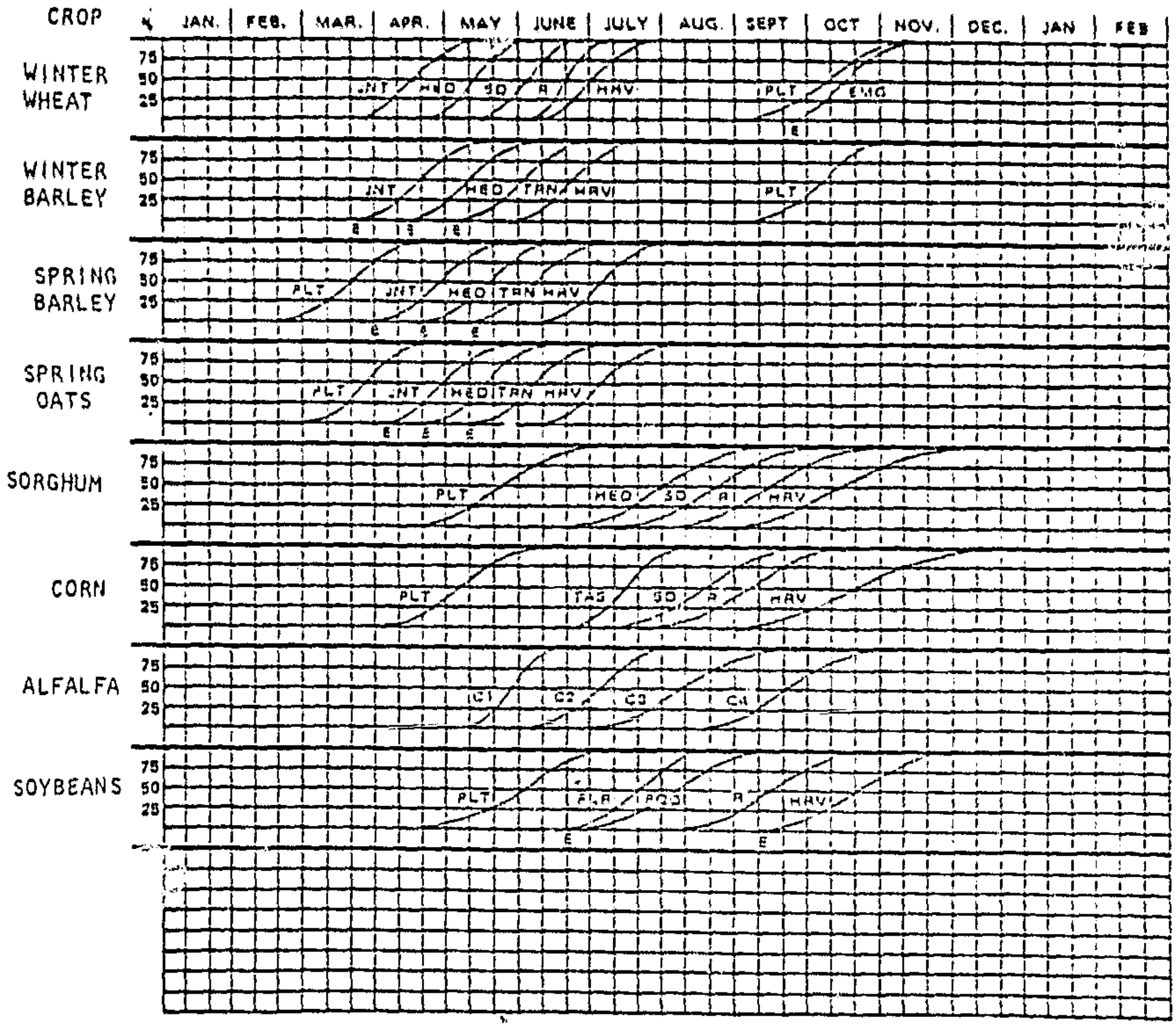

LEGEND

E	Under stage name, indicates rough estimate of date
EMG	Emergence
HED	Heading
HRV	Harvest
JNT	Jointing
PLT	Planting
R	Ripe
SD	Soft dough
TRN	Turning
FLR	Flowering
C	Cut
TAS	Tasseling

Figure A.7. Percent of crop are in development stage by specified date for Kansas crop reporting district 6 average crop calendars from 1963 to 1973 [20].

emergence, and finally reverts to bare soil status after harvest. As implemented, this procedure gives the data base a dynamic crop-category mix that can be modified to match regional agricultural practices such as double-cropping or dynamic soil surface roughness conditions.

A.5 Interlayer Water Redistribution

Infiltration of water into the surface layer, percolation of water into the root zone, and capillary recharge of surface layer moisture are controlled by the matric-potential profile as limited by soil structure.

A pixel's infiltration capacity during rainfall is given by [21]

$$i_r = t^{1/2}[2\ k_s\ \psi_f(\theta_s - \theta)]^{1/2} + k_s\ t/2 \qquad (A.16)$$

where

t = duration of rain event, hrs.

k_s = hydraulic conductivity at saturation

ψ_s = suction at field capacity

θ_s = prosity = $1 - \rho_b/\rho_s$

ρ_b = soil bulk density, g/cm^3

ρ_s = soil specific density = 2.65 g/cm^3 for all soils.

After rainfall ceases, infiltration proceeds at a rate defined by $k_s/2$ for the remaining time of the accounting period (24-t) or until all standing water is depleted. Thus, a pixel's infiltration capacity from standing water is defined as

$$i_{sw} = k_s/2 * (24 - t) \qquad (A.17)$$

and is limited by the amount of standing water. Hence, total infiltration into the surface layer of the soil, i_t, is determined by

$$i_t = i_r + i_{sw} \tag{A.18}$$

where

i_r < total rainfall received by the pixel

i_{sw} < standing water available.

Water will percolate from the surface layer (0-5-cm) into the root zone for all accounting periods where the surface layer's water content after infiltation exceeds the water content at field capacity (as determined by Equation A.13), such that final surface-layer's water content is reduced to less than porosity.

This is accomplished by first allowing excess water to drain from the root zone (5-100 cm depth). One third of the volumetric moisture in excess of root zone field capacity is allowed to drain gravitationally each day and hence is removed from further accounting periods. Then, assuming that the water content in the surface layer exceeds field capacity, the excess is permitted to percolate into the root zone at the minimum of either

$$R_i = \frac{T\ k_s}{2\alpha} \tag{A.19}$$

where

R_i = net percolation into the root zone,

α = a damping coefficient arbitrarily set to 48, and

T = duration of accounting period = 24 hours

or 1/3 of excess water is allowed to percolate

$$R_i = (\theta - FC)/3 \qquad (A.20)$$

where θ and FC are for the surface layer.

When evapotranspirative losses cause surface-layer water content to be reduced below wilting point, capillary recharge of the surface 5 cm of soil is allowed to occur during the night for a duration of 12 hours. The rate of the surface recharge is equal to $k_s/2$ and is arbitrarily limited to a maximum of 0.25 cm of water. Furthermore, capillary recharge is not allowed to raise surface layer water content above wilting point.

A.6 Within-Field Variability in Surface Soil Moisture

Prior to radar image simulation, the surface layer soil moisture values determined by the water-budget model for each 100-m by 100-m grid cell are randomized to approximate the natural variability in soil moisture measured within "homogeneous" fields. Randomization was performed on a grid-cell basis by a Gaussian random-number generator with a standard deviation of 6 percent M_{fs} [2].

A.7 Generation of Soil Moisture Distributions

The dynamic soil water accounting model (SWAM) was initialized on Julian day 138 and moisture distribution maps of the test site were produced for every day of the simulation period.

These moisture maps indicated the percent of the 1/3-bar water content M_{fs} in the 0-5 cm layer where

$$M_{fs} = 100 \times \theta/FC \qquad (A.21)$$

where

θ = measured soil moisture

FC = soil moisture at field capacity.

The resultant distributions were then examined and the three most closely approximating moderately dry, moist, and wet soil surface conditions were selected for radar image simulation. Image representation of 0-5-cm soil moisture distribution for Julian day 141, 150 and 160 are shown on Figure 6.

DEFINITIONS

PAUSDATE	An array which contains the Julian days on which the output moisture map needs to be saved.
STRTDATE	Julian day on which the process should begin.
STOPDATE	Julian day on which the process should stop.
RAINDATE	An array containing the Julian dates which all or part of the database received some rain.
ALLINTS	An array containing the mean rain intensity of each rainy day.
RAIN	Amount of rain received by a cell on a certain day in cm.
INTNSITY	Intensity of the rain for a cell in cm/hour.
DUR	Duration of the rain for a cell in hours
PERCENTS	In soil data subroutine. An array of percent probability of occurrence of soil bulk density associated with each of eight soil types present in our data base.
SFBULK	Quantized levels of surface layer (0-5 cm) bulk density associated with "PERCENTS".
RTBULK	Quantized levels of root layer (5-100 cm) bulk density associated with "PERCENTS".
B	An array containing b values for all 15 soil textures as estimated from Clapp & Hornberger, 1978.
FSUCTION	An array containing the suction ψ_f (at field capacity) for all 15 soil textures (see Clapp & Hornberger, 1978).
SSUCTION	An array containing the suction ψ_s (at saturation) for all 15 soil textures.
SHYDCOND	An array containing the hydraulic conductivity at saturation k_s for all 15 soil textures.

SATHC	Hydraulic conductivity at saturation.
PDATES	An array containing ten different planting dates for each crop type.
STAGEDAY	An array containing the number of days after the planting date which the crop advances to a new crop growth stage (five different stages) for each crop type.
KEQCONST	An array containing two parameters (slope and intercept) describing the change in K_{CROP} at each stage and for each crop type.
KCROP	Crop transpiration coefficient.
SW	Standing water (cm).
SWINF	Amount of standing water which infiltrates to the surface layer (cm).
RAININF	Amount of rain which infiltrates to the surface layer.
MPC	Water content expressed as a percent of field capacity.
DRAIN	Amount of excess water which is drained from the root zone (cm/cm).
SWRUNOFF	Amount of water runoff from standing water (cm).
RECHRG	Capillary recharge (cm).
ETO	An array containing the potential evaporation (cm) for every day of the simulation period.
SWEVAP	Amount of evaporation from standing water.
KSOIL	Bare soils evaporation coefficient.

The following variables are prefixed by "SF" or "RT" indicating the surface layer (0-5 cm) or root zone (5-100 cm), respectively.

BD	soil's bulk density
PROS	soil's porosity
FC	soil's water content at field capacity (cm/cm)
WP	soil's water content at wilting point (cm/cm)
WC	water content (cm/cm)
EVAP	amount of evaporation (cm)

```
C ----------------------------------------------------------------------
C                     UNIVERSITY OF KANSAS REMOTE SENSING LAB
C ----------------------------------------------------------------------
C PROGRAM SUITE : RADAR SIMULATION     REF. # : RSL REPORT 601-1
C ----------------------------------------------------------------------
C PROGRAM NAME: SWAM            AUTHOR: SAIED MOEZZI     DATE: MAY 1983
C LANGUAGE     : FORTRAN 77
C ----------------------------------------------------------------------
C PURPOSE :   THE PURPOSE OF PROGRAM SWAM (SOIL WATER ACCOUNTING MODEL)
C IS TO GENERATE A DISRIBUTION OF NEAR-SURFACE (0-5 CM) SOIL MOISTURE
C CONDITION AT THE SPATIAL SCALE OF THE STATIC TERRAIN DATA BASE WHICH
C RESPONDS TO BOTH STATIC CONDITIONS (SOIL TYPE, COVER TYPE, AND SURFACE
C SLOPE) AND DYNAMIC CONDITIONS (CROP STAGE, RAIN, AND POTENTIAL EVAPO-
C RATION) ON A DAILY BASIS.
C
C ----------------------------------------------------------------------
C                       PARAMETER DEFINITION
C  NAME              !                      DESCRIPTION
C ----------------------------------------------------------------------
C IROW1             ! FIRST ROW OF THE INPUT MATRIX TO BE PROCESSED
C IROW2             ! LAST  ROW OF THE INPUT MATRIX TO BE PROCESSED
C ICOL1             ! FIRST COLUMN CELL OF THE INPUT ROWS TO BE PROCESSED
C ICOL2             ! LAST  COLUMN CELL OF THE INPUT ROWS TO BE PROCESSED
C IOTCOL            ! NUMBER OF CELLS IN EACH OUTPUT ROW
C NCOL              ! NUMBER OF CELLS IN EACH INPUT ROW
C NPAUSE            ! NUMBER OF TIMES THAT PROGRAM SHOULD PAUSE DURING
C                   ! SIMULATION PERIOD FOR SAVING THE MOISTURE MAP
C                   !
C ----------------------------------------------------------------------
C                       SUBROUTINES REQUIRED
C    NAME           !                       DESCRIPTION
C ----------------------------------------------------------------------
C RAINFALL          !RETURNS THE AMOUNT OF RAIN (CM), DURATION (HOURS) AND
C                   !INTENSITY ( CM/HOUR ) FOR A GIVEN CELL ON A SPECIFIED
C                   !JULIAN DAY.
C INTRLAYR          !THIS ROUTINE CONTAINS ALL  4  WATER ACCOUNTING MODELS
C                   !EACH AS A SEARATE ENTRY. THESE ENTRIES ARE : SURFINF,
C                   !ROOTINF, RUNOFF AND RECHARGE.
C INITIALZ          !THIS ROUTINE IS USED FOR INITIALIZATION PROCESS AND
C                   !HAS TWO ENTRIES. THESE ARE: COMMENCE AND DAWN.
C EVAPORAT          !THIS ROUTINE SIMULATES THE EVAPORATION PROCESS FOR A
C                   !GIVEN CELL ON A SPECIFIED JULIAN DAY.
C CELLDATA          !THIS ROUTINE GETS ALL STATIC CONDITIONS OF A GIVEN
C                   !DATA BASE CELL.
C CROPDATA          !THIS ROUTINE GETS THE DYNAMIC CONDITIONS OF A GIVEN
C                   !DATA BASE CELL WHICH IS REGISTERED AS A CROP TYPE.
C SOILDATA          !THIS ROUTINE GET ALL THE REQUIRED INFORMATION
C                   !THAT IS BASED ON THE SOIL TYPE FOR A GIVEN CELL.
C GETFILES          !THIS ROUTINE OPENS ALL THE INPUT AN OUTPUT FILES.
C IOCALLS           !THIS ROUTINE CONTAINS TWO ENTRIES FOR READING AND
C                   !WRITING INPUT AND OUTPUT RECORDS. THESE ARE: READREC,
C                   !AND WRITDATA.
C UPDTHIST          !THIS ROUTINE IS USED FOR UPDATING A GIVEN HISTIGRAM.
C OTPTHIST          !THIS ROUTINE IS USED FOR WRITING OUT A GIVEN
C                   !HISTOGRAM.
COPNFIL             !EXTERNAL FUNCTION CALLED BEY 'GETFILES' ROUTINE
C                   !
C ----------------------------------------------------------------------
C
C
      PARAMETER ( IROW1=1,IROW2=1077,ICOL1=1,ICOL2=1245,IOTCOL=1245 )
      PARAMETER ( NPAUSE=4 , NCOL=1245 )
C
C
      INTEGER        PAUSDATE( NPAUSE ), FC( 14 ), HHMMSS( 3 )
      INTEGER        WATER, SOIL, ELEV, CATG, CAT, COL, ROW, DATE
      INTEGER        STRTDATE, STOPDATE, CROP, FIELD, DAY
      REAL           KCROP, INTNSITY, MFC
      CHARACTER*8    TYPE, TYPENOW
      LOGICAL        PAUSE
```

```
      COMMON /BUF3/ MFCOUT( NPAUSE, NCOL ), ICATOUT( NPAUSE, NCOL )
      SPECIAL COMMON BUF3
      COMMON /BUF4/ MFCHIST( NPAUSE , 256 ), ICATHIST( NPAUSE , 31 )
      SPECIAL COMMON BUF4
      COMMON  /BLOCK/
     & SATHC, SUCTION, SFPROS, RTPROS, SFFC, RTFC, SFUP,
     & SW, SFWC, RTWC, KCROP,
     & DAY, RAIN, DUR, INTNSITY, SLOPE, TYPENOW
      COMMON /FILCOD/ FC
      DATA  WATER/ 10 /, STRTDATE/ 138 /, STOPDATE/ 160 /
      DATA  PAUSDATE/ 140, 141, 150, 160 /
C
C
C
      WRITE(13,101) IROW1, IROW2, ICOL1, ICOL2
C
C     INITIALIZE ALL NECESSARY VARIABLES
C
      CALL COMMENCE
C
C     PROCESS EVERY CELL IN THE DATA BASE
C
      FOR  ROW=IROW1, IROW2
C
C     AFTER PROCESSING EVERY 100 RECORDS SEND A MESSAGE TO TO TERMINAL
C
      IF( MOD(ROW,10) .EQ. 0 ) THEN
      CALL TIME(HHMMSS)
      WRITE(11,103) ROW, HHMMSS
      END IF
      FOR  COL=ICOL1, ICOL2
C
C     GET REQUIRED INFORMATIONS FOR THE CELL BEING PROCESSED
C
      CALL CELLDATA( ROW,COL,ELEV,SOIL,CATG,SLOPE,TYPE,CROP,FIELD )
      IF( TYPE .EQ. 'NONAGRIC' ) THEN
C
C     THIS IS NOT AN AGRICULTURAL CELL THEREFORE SHOULD NOT BE
C     TREATED IN MOISTURE COMPUTATION. UPDATE THE OUTPUT ROW AND
C     START WITH NEXT CELL IN THE DATA BASE.
C
      FOR  IP=1, NPAUSE
      MFCOUT( IP , COL ) = 0
      ICATOUT( IP , COL ) = CATG
      CALL UPDTHIST( 0 , MFCHIST, IP, 0, 250 )
      ICAT = CATG / 10
      CALL UPDTHIST( ICAT, ICATHIST, IP, 0, 25 )
      END FOR
      ELSE
C
C     ELSE THIS CELL IS AN AGRICULTURAL TYPE, START THE MOISTURE
C     COMPUTATION AND CONTINUE FOR THE ENTIRE SIMULATION PERIOD.
C
C     GET MORE INFORMATION ABOUT THE UNDERLAYING SOIL
C
      CALL SOILDATA( SOIL, SFPROS, RTPROS, SFFC, RTFC, SFUP,
     &               SATHC, SUCTION )
C
C     INITIALIZE THIS CELL'S MOISTURE FOR DAY ZERO
C
      CALL  DAWN
C
      FOR  DATE= STRTDATE, STOPDATE
C
      DAY = DAY + 1
C
C     IF IT IS A RAINY DAY, THEN GET AMOUNT, INTENSITY AND THE
C     DURATION OF THE RAINFALL ON THIS GROUND CELL BEING PROCESSED
C
      CALL  RAINFALL( DATE, ROW, COL, RAIN, INTNSITY, DUR )
```

```
C
C       IF THE GROUND CELL IS REGISTERED AS A CROP THEN GET
C       KCROP AND CROP STAGE
C
        IF( TYPE .EQ. 'CROP    ' )  THEN
        CALL CROPDATA( CROP, FIELD, DATE, KCROP, TYPENOW )
        END IF
C
C
C       PROCESS ALL SOIL WATER ACCOUNTING MODELS
C
C       1: PONDING AND INFILTRATION INTO THE SURFACE LAYER (0 - 5 CM)
C
        CALL SURFINFL
C
C       2: PERCOLATION OF WATER INTO THE ROOT ZONE (5 - 95 CM)
C
        CALL ROOTINFL
C
C       3: STANDING WATER RUNOFF DUE TO LOCAL SLOPE
C
        CALL RUNOFF
C
C       4: EVAPOTRANSPIRATION
C
        CALL EVAPORAT
C
C       5: CAPILLARY RECHARGE OF THE SURFACE LAYER
C
        CALL RECHARGE
C
C
C       COMPUTE % OF FIELD CAPACITY OF SOIL MOISTURE BASED ON SURFACE
C       LAYER'S WATER CONTENT
        MFC = 100.0 * SFWC / SFFC
C
C
C       CHECK TO SEE IF THIS IS A PAUSE DAY, IF IT IS THEN RECORD
C       THE  COMPUTED 'MFC' AND  THE REASSIGNED CATEGORY.
C       (PAUSE DAY IS THE DAY THAT THE MOISTURE MAP MUST BE SAVED)
C
        PAUSE = .FALSE.
        FOR  IP=1, NPAUSE
        IF( DATE .EQ. PAUSDATE( IP ) )   THEN
        PAUSE = .TRUE.
        GOTO  100
        END IF
        END FOR
 100    IF( PAUSE ) THEN
C
C       APPLY A GAUSIAN DISTRIBUTION WITH COMPUTED 'MFC' AS THE
C       MEAN, AND 6% MFC AS THE STANDARD DIVIATION
C
        IMFC = NINT( RANN( MFC , 6.0 ) )
C
C       SET LOWER LIMIT OF % FIELD CAPACITY TO ONE
C
        IF( IMFC .LT. 1 ) IMFC=1
C
C       SAVE COMPUTED 'MFC' FOR THIS PAUSE DAY
C
        MFCOUT( IP , COL ) = IMFC
C
C       REASSIGNMENT OF THE REGISTERED CELL'S CATEGORY
C       1: CHANGE THE CATEGORY TO WATER IF THERE IS STANDINNG WATER
C          ON THIS GROUND CELL
C       2: CHANGE THE CATEGORY TO WATER IF SURFACE LAYER'S WATER
C          CONTENT EXCEEDS THE UNDERLAYING SOIL'S PROSITY
C       3: IF THERE IS NO STANDING WATER AND CELL IS REGISTERD AS A
```

```
C          CROP TYPE, THEN CHANGE THE CATEGORY TO BARE SOIL WHEN
C          BEFORE EMERGENCE OF THE CROP OR AFTER HARVEST
C
          IF( SW .GT. 0 ) THEN
          CAT = WATER
          ELSE
          IF( SFWC .LT. SFPROS ) THEN
          CAT = CATG
          IF((TYPE.EQ.'CROP    ') .AND.(TYPENOW.EQ.'SMTHBARE')) CAT = 210
          IF((TYPE.EQ.'CROP    ') .AND.(TYPENOW.EQ.'MEDMBARE')) CAT = 200
          ELSE
          CAT = WATER
          END IF
          END IF
          ICATOUT( IP , COL ) = CAT
          ICAT = CAT / 10
C
C         UPDATE THE HISTOGRAMS
C
          CALL  UPDTHIST( IMFC, MFCHIST, IP, 0, 250 )
          CALL  UPDTHIST( ICAT, ICATHIST, IP, 0, 25 )
C
          END IF
          END FOR
C
C         DONE WITH MOISTURE ESTIMATION FOR THIS CELL
C
          END IF
          END FOR
C
C         DONE WITH ALL THE COLUMNS OF THIS ROW
C         WRITE OUT THE COMPUTED MFC AND THE REASSINED CATEGORIES OF THIS
C         ROW TO THE OUTPUT FILES FOR ALL PAUSE DATES.
C
          CALL WRITDATA( 1. MFCOUT. IOTCOL )
          CALL WRITDATA( 2, ICATOUT, IOTCOL )
C
          END FOR
C
C         SOIL MOISTURE ESTIMATION IS DONE FOR THE ENTIRE DATA BASE
C         WRITE OUT A REPORT OF THE FINAL MOISTURE AND CATEGORY MAPS
C
          FOR  IP=1, NPAUSE
          WRITE(13,104) '  MFC    ',  PAUSDATE( IP )
          CALL  OTPTHIST( MFCHIST, IP, 0, 250 )
          WRITE(13,104) 'CATEGORY', PAUSDATE( IP )
          CALL  OTPTHIST( ICATHIST, IP, 0, 25 )
          END FOR
          CALL TIME(HHMMSS)
          WRITE(13,'(' COMPLETED AT    ',3A3)') HHMMSS
          WRITE(11,'(' COMPLETED AT    ',3A3)') HHMMSS
          WRITE(11,102)
          WRITE(13,102)
          STOP
  101     FORMAT(///,' S O I L   W A T E R   A C C O U N T I N G',
     &    '    P R O G R A M'//,' SWAM WAS PROCESSED ON THE DATA BASE'//
     &    ' ROW'I5,'  THROUGH  ROW'I5,'    ,    COL'I5'  THROUGH  COL'I5)
  102     FORMAT(' * * *  A L L   D O N E  * * *')
  103     FORMAT(' P R O C E S S E D   T H R O U G H   R E C O R D',5X,I4,
     &    3X,3A3)
  104     FORMAT('1',A8,' H I S T O G R A M   FOR JULIAN DAY'I5)
          END
```

```
C
C
C------RAINFALL
C
C
C       THIS ROUTINE READS THE RAINFALL DATA AND RETURNS THE AMOUNT
C       OF RAIN, DURATION, AND INTENSITY FOR A GIVEN CELL WITHIN THE
C       DATA BASE ON A SPECIFIED JULIAN DAY.
C       RAIN IS IN UNITS OF CENTIMETERS , INTENSITY IS IN CM/HOUR,
C       AND DURATION IS IN HOURS.
C
C
        SUBROUTINE RAINFALL( DATE, DBROW, DBCOL, RAIN, INTNSITY, DUR )
        IMPLICIT INTEGER ( A - Z )
        PARAMETER ( NDAY=13 , NRCOL=42 )
        COMMON /BUF5/ ROWRAIN( NRCOL,NDAY), RAINDATE( NDAY)
        SPECIAL COMMON BUF5
        DIMENSION FC(14)
        COMMON /FILCOD/ FC
        REAL   RAIN, DUR, INTNSITY, ALLINTS( NDAY )
        DATA  RECPTR / 0 /
        DATA   RAINDATE
     & / 138,139,143,144,148,149,150,151,153,154,155,159,161 /
        DATA  ALLINTS
     & / 1.2,1.7,1.7,3.6,2.3,2.3,3.6,1.4,3.6,3.6,3.6,2.3,2.3 /
C
C
C
C       READ RAINFALL DATA FOR ALL RAINY DAYS FOR THIS GROUND CELL
C
        RAINROW = ( ( DBROW - 1 ) / 30  + 1 )
        RAINCOL = ( ( DBCOL - 1 ) / 30  + 1 )
        WHILE( RECPTR .LT. RAINROW )
        FOR COL=1, NRCOL
        READ( FC(5), IOSTAT=IOS) ( ROWRAIN(COL,DAY),  DAY=1, NDAY )
        IF( IOS .NE. 0 )  GOTO 99
        END FOR
        RECPTR = RECPTR + 1
        END WHILE
C
C
C
C       CHECK IF THE DATE GIVEN WAS A RAINY DAY
C
        FOR  DAY=1, NDAY
        IF( RAINDATE( DAY ) .EQ. DATE ) GOTO 10
        END FOR
C
C       NO STORM ON THIS DAY, RETURN TO THE CALLING PROGRAM
C
        RAIN = 0.
        INTNSITY = 0.
        DUR  = 0.
        RETURN
C
C       A STORM OCCURED ON THIS DAY, GET THE AMOUNT OF RAIN RECIEVED
C       BY THIS CELL ON THE GIVEN JULIAN DAY
C
 10     RAIN = REAL( ROWRAIN( RAINCOL, DAY ) )/ 10.0
        INTNSITY = ALLINTS( DAY )
        DUR = RAIN / INTNSITY
        RETURN
C
 99     WRITE(11,'(1X,'ERROR **** WHILE READING RAINFALL ')')
        STOP
        END
>
```

```
C
C
C------INTRLAYR
C
C
C       THIS ROUTINE CONTAINS ALL 4 WATER ACCOUNTING MODELS, EACH
C       AS A SEPARATE ENTRY. THESE ARE 1-SURFACE INFILTRATION,
C       2-ROOT INFILTARION, 3-RUNOFF, 4-RECHARGE
C
        SUBROUTINE INTRLAYR
C
        INTEGER       FC( 14 ), DAY
        REAL          KCROP, INTNSITY, MAXRTINF, MINRTINF
        CHARACTER*8   TYPENOW
        COMMON  /BLOCK/
     &  SATHC, SUCTION, SFPROS, RTPROS, SFFC, RTFC, SFUP,
     &  SW, SFWC, RTWC, KCROP,
     &  DAY, RAIN, DUR, INTNSITY, SLOPE, TYPENOW
        COMMON /FILCOD/ FC
C
        ENTRY  SURFINFL
C       ---------------
C
C       COMPUTE AMOUNT OF 'RAIN' WHICH INFILTATES TO SURFACE LAYER
C
        IF( RAIN .GT. 0 ) THEN
        RI = SQRT( DUR ) * SQRT( 2*SATHC*SUCTION*( SFPROS-SFWC) ) +
     &       SATHC * DUR / 2
        RAININF = AMIN1( RAIN , RI )
        SW = SW + ( RAIN - RAININF )
        ELSE
        RAININF = 0
        END IF
C
C       COMPUTE AMOUNT OF 'STANDING WATER' WHICH INFILTRATES TO SURFACE
C       LAYER AFTER RAINFALL CEASES
C
        IF( SW .GT. 0 ) THEN
        SWI = SATHC * ( 24 - DUR ) / 2
        SWINF = AMIN1( SW , SWI )
        SW = SW - SWINF
        ELSE
        SWINF = 0
        END IF
C
C       TOTAL AMOUNT OF INFILTRATION TO THE SURFACE LAYER IS THE SUM
C       OF RAIN AND STANDING WATER INFILTARTION
C
        TOTALINF = RAININF + SWINF
C
C       COMPUTE WATER CONTENT PER CENTIMETER OF SURFACE LAYER
C
        SFWC = SFWC +  TOTALINF / 5.0
        RETURN
C
C
        ENTRY  ROOTINFL
C       ---------------
C
C       COMPUTE PERCOLATION  OF WATER FROM THE SURFACE LAYER INTO
C       THE ROOT ZOON ( 5-100 CM )
C
C       FIRST DRAIN THE EXCESS WATER OUT OF ROOT LAYER
C
        IF( RTWC .GT. RTFC ) THEN
        DRAIN = (RTWC - RTFC) / 3
        RTWC = RTWC - DRAIN
        END IF
C
C       THEN PERCOLATE
```

```
C
      IF( SFUC .GT. SFFC ) THEN
      SFUC1 = SFUC
      RTINF1 = 0.25 * SATHC
      RTINF2 = (SFUC - SFFC) / 3
      SFUC = AMIN1( SFUC1 , SFPROS )
      SFUC = AMAX1( SFUC-RTINF2 , SFUC1-RTINF1 )
      RTINF = (SFUC1 - SFUC) * 5
      RTUC = RTUC + RTINF/95
      ELSE
      RTINF = 0
      RETURN
      END IF
C
C     NOW CHECK THE SURFACE WATER CONTENT, IF IT EXCEEDS THE
C     PROSITY OF THE SOIL TYPE  MOVE THE EXCESS WATER TO THE
C     STANDING WATER
C
      IF( SFUC .GT. SFPROS ) THEN
      SWADD = ( SFUC - SFPROS ) * 5
      SFUC = SFPROS
      SW = SW + SWADD
      END IF
C
      RETURN
C
C
      ENTRY  RUNOFF
C     ------------
C
C
C     COMPUTE RUNOFF CAUSED BY THE SLOPE FOR 'STANDING WATER'
C
      IF( SW .GT. 0 ) THEN
      SURUNOFF = SW * ( 1.1 -  0.8 **SLOPE )
      SW = AMIN1( SW , SW-SURUNOFF )
      ELSE
      SURUNOFF = 0.
      END IF
      RETURN
C
C
      ENTRY  RECHARGE
C     ---------------
C
C     CAPILLARY RECHARGE IS ALLOWED TO OCCURE DURING NIGHT FOR A
C     DURATION OF 12 HOURS
C
      IF( SFUC .LT. SFUP ) THEN
      SFUC1 = SFUC
      RECHRG = 0.25
      SFUC = SFUC1 + RECHRG/5
      IF( SFUC .GT. SFUP ) THEN
      SFUC = SFUP
      RECHRG = (SFUC - SFUC1)  * 5
      END IF
      RTUC = ( 95 * RTUC - RECHRG ) / 95
      ELSE
      RECHRG = 0
      END IF
C
      RETURN
      END
>
```

ORIGINAL PAGE IS
OF POOR QUALITY

```
C
C
C------INITIALZ
C
C
C       THIS ROUTINE IS USED FOR INITIALIZING THE VARIABLES AS WELL
C       AS INITIAL MESSAGES TO THE TERMINAL AND OUTPUT REPORT FILE.
C
        SUBROUTINE INITIALZ
C
C
        INTEGER      DAYTIME( 2 ), DDMMMYY( 3 ), HHMMSS( 3 ), FC(14), DAY
        REAL         KCROP, INTNSITY
        CHARACTER*8  TYPENOW
        COMMON  /BLOCK/
     & SATHC, SUCTION, SFPROS, RTPROS, SFFC, RTFC, SFWP,
     & SW, SFWC, RTWC, KCROP,
     & DAY, RAIN, DUR, INTNSITY, SLOPE, TYPENOW
        COMMON /FILCOD/ FC
C
C
        ENTRY  COMMENCE
C       ---------------
C
C       AT THE BEGIMING WRITE OUT A MESSAGE TO THE TERMINAL AND
C       GET A SEED FOR RANDOM NUMBER GENERATOR FUNCTIONS BASED
C       ON THE COMPUTER CLOCK
C
        CALL DATE( DDMMMYY )
        CALL TIME( HHMMSS )
        CALL JDATE( DAYTIME )
        WRITE(11,101) HHMMSS, DDMMMYY
        WRITE(13,101) HHMMSS, DDMMMYY
        PRIMNO = DAYTIME( 2 )
        CALL IRANP( PRIMNO )
        RETURN
C
C
C
        ENTRY  DAWN
C       -----------
C
C       THIS ENTRY INITIALIZES THE MOISTURE CONTENT OF A CELL
C
        SW = 0
        DAY = 0
        SFWC = SFFC
        RTWC = RTFC
        RETURN
C
  101   FORMAT(///' TIME:  '3A3,'    ,    DATE:  '3A3)
        END
```

```
C
C
C------EVAPORAT
C
C       THIS ROUTINE SIMULATES THE EVAPOTRANSPITAION ON A GIVEN
C       DAY BASED ON THE DATA GATHERED. BARE SOIL, CANOPY COVERED
C       OR WATER COVERED CELLS ARE EACH TREATED DIFFERENTLY.
C
        SUBROUTINE EVAPORAT
C
        PARAMETER ( NSDAY= 24 )
C
        INTEGER FC( 14 ), DAY
        REAL    ET0( NSDAY ), MR, KSOIL, KSTORM, KSWEVAP, KCROP, INTNSITY
        REAL    A( NSDAY ), B( NSDAY ), C( NSDAY ), D( NSDAY )
        LOGICAL FRSTCALL
        CHARACTER*8  TYPENOW
        COMMON /DATA/ SWINF,RAININF,RTINF,SURUNOFF,RECHRG,SWEVAP,SFEVAP,
      & RTEVAP
        COMMON  /BLOCK/
      & SATHC, SUCTION, SFPROS, RTPROS, SFFC, RTFC, SFWP,
      & SW, SFWC, RTWC, KCROP,
      & DAY, RAIN, DUR, INTNSITY, SLOPE, TYPENOW
        COMMON /FILCOD/ FC
        DATA  FRSTCALL/ .TRUE. /
        DATA  ET0 / 0.48, 0.22, 0.31, 0.48, 0.61, 0.58, 0.40, 0.46,
      &             0.28, 0.27, 0.23, 0.15, 0.25, 0.35, 0.43, 0.33,
      &             0.38, 0.28, 0.31, 0.31, 0.40, 0.68, 0.55, 0.59 /
C
        IF( FRSTCALL ) THEN
        FRSTCALL = .FALSE.
C
C       COMPUTE THE CONSTANTST FOR KSOIL'S POLYNOMIAL EQUATIONS
C
        FOR  IDAY=1, NSDAY
        A( IDAY ) = -0.05  +  0.732 / ET0( IDAY )
        B( IDAY ) =  4.97  -  0.661 * ET0( IDAY )
        C( IDAY ) = -8.57  +  1.560 * ET0( IDAY )
        D( IDAY ) =  4.35  -  0.880 * ET0( IDAY )
        END FOR
        END IF
C
        PE = ET0( DAY )
        KSTORM = (24 - DUR) / 24.0
C
C       IF THE GROUND CELL IS A CANOPY THEN COMPUTE EVATRANSPIRATION
C       30% FROM SURFACE LAYER AND 70% FROM ROOT ZONE
C
        IF( TYPENOW .EQ. 'CANOPY  ' ) THEN
        EVAP = PE * KCROP * KSTORM
        SFEVAP = AMIN1( SFWC*5 , 0.30*EVAP )
        RTEVAP = AMIN1( RTWC*95 , 0.70*EVAP )
        SFWC = SFWC - SFEVAP/5
        RTWC = RTWC - RTEVAP/95
        IF( SW .GT. 0 ) THEN
        SWINF = AMIN1( SW , SFEVAP )
        SW = SW - SWINF
        SFWC = SFWC +  SWINF/5
        END IF
        RETURN
        END IF
C
C       IF THIS CELL IS COVERED BY STANDING WATER THEN COMPUTE
C       EVAPORATION OF STANDING WATER
C
        KSWEVAP = 1
        IF( SW .GT. 0 ) THEN
        EVAP = PE * KSTORM
        SWEVAP = AMIN1 ( SW , EVAP )
```

```
      SW = SW - SWEVAP
      KSWEVAP = ( PE - SWEVAP ) / PE
      PE = PE - SWEVAP
      END IF
C
C     COMPUTE EVPORATION FOR BARE SOIL
C
      IF( PE .GT. 0 ) THEN
      MR = ( SFWC - SFWP ) / ( SFFC - SFWP )
      IF( MR .LT. 0 ) MR= 0
      IF( MR .GT. 1 ) MR = 1
      KSOIL = A(DAY)  +  B(DAY) * MR  +  C(DAY) * MR*MR  +
     & D(DAY) * MR*MR*MR
      IF( KSOIL .LT. 0.05 )   KSOIL = 0.05
      IF( KSOIL .GT. 1.00 )   KSOIL = 1.00
      SFEVAP = PE * KSOIL * KSTORM * KSWEVAP
      SFEVAP = AMIN1( SFWC*5 , SFEVAP )
      SFWC = SFWC - SFEVAP/5
      END IF
C
      RETURN
      END
>
```

```
C
C
C------CELLDATA
C
C
C       THIS SOUBROUTINE GETS ALL THE AVAILABLE AND NECESSARY
C       INFORMATION ABOUT THE REQUSTED DATA BASE CELL.
C
C
        SUBROUTINE CELLDATA( RQUSTROW, RQUSTCOL, ELEV, SOIL, CATG,
     &                       SLOPE, TYPE, CROP, FIELD )
        IMPLICIT INTEGER ( A - Z )
        PARAMETER ( NCOL=1245 , NFIELD=10 )
        DIMENSION  CROPCODE( 10 ), FC( 14 )
        REAL       SLOPE, RESFEET
        CHARACTER*8 TYPE
        LOGICAL FRSTCALL
        COMMON /BUF1/  SOILS( NCOL ), ELEVS( NCOL ), CATGS( NCOL)
        SPECIAL COMMON BUF1
        COMMON /FILCOD/ FC
        DATA  RESFEET/ 328.08 /
        DATA CURNTROW / 0 /, FRSTCALL/ .TRUE. /
        DATA  CROPCODE/ 3, 5, 5, 4, 4, 3, 2, 2, 1, 6/
C       1-ALFALFA, 2-SOYBEAN, 3-WHEAT & OATS, 4-CORN, 5-SORGHUM, 6-PASTURE
C
C
C
C       WHEN CALLED FOR THE FIRST TIME OPEN ALL INPUT & OUTPUT FILES
C
        IF( FRSTCALL )   THEN
        CALL GETFILES
        FRSTCALL = .FALSE.
        END IF
C
C       IF THE ROW WHICH CONTAINS THE REQUESTED CELL IS NOT READ
C       YET, READ THE NEXT RECORD OF ALL THREE DATA BASE MAPS.
C
        IF( CURNTROW .LT. RQUSTROW ) THEN
        CURNTROW = CURNTROW + 1
        CALL  READREC( FC(2), SOILS, NCOL )
        CALL  READREC( FC(3), ELEVS, NCOL )
        CALL  READREC( FC(4), CATGS, NCOL )
        END IF
C
C       THE ROW WHICH CONTAINS THE REQUSTED CELL IS IN THE MEMORY
C       EXTRACT NECESSARY INFORMATION.
C
        ELEV = ELEVS( RQUSTCOL )
        SOIL = SOILS( RQUSTCOL )
        CATG = CATGS( RQUSTCOL )
C
        IF( RQUSTCOL .NE. NCOL ) THEN
        NEXTELEV = ELEVS( RQUSTCOL+1 )
        ELSE
        NEXTELEV = ELEVS( RQUSTCOL-1 )
        END IF
        SLOPE = ATAN( REAL( ELEV - NEXTELEV ) / RESFEET )
        SLOPE = ABS( SLOPE ) * 57.2958
C
C       DETRMINE THE SOIL TYPE FROM SOIL MAP CODES
C
        SOIL = SOIL / 30
C
C       DETEMINE THE TYPE OF THE CATEGORY (NON-AGRICULTURAL ,
C       BRAE SOIL OR CROP). IF IT IS A CROP TYPE FIND CROP.
C
        IF( (CATG .GE. 230)  .OR. (CATG .LE. 50) ) THEN
        TYPE = 'NONAGRIC'
        ELSE IF( (CATG .LT. 230) .AND. (CATG .GT. 150) ) THEN
        TYPE = 'BARESOIL'
```

```
        ELSE IF( (CATG .GE. 50 ) .AND. (CATG .LE. 150) ) THEN
        TYPE = 'CROP    '
        IC = CATG / 10 - 5
        CROP = CROPCODE( IC )
        FIELD = MOD( CATG , (CATG/10 * 10 ) ) + 1
        CATG = CATG /10 * 10
        END IF
C
C
        RETURN
        END
>
```

```
C
C
C------CROPDATA
C
C
C       THIS ROUTINE FINDS MORE INFORMATION ABOUT A CELL WHICH IS
C       REGISTERED AS CROP, SUCH AS CROP'S PLANTING DATE, CROP
C       CONSTANT K, AND ITS DYNAMIC TYPE BASED ON THE CROP CALANDER.
C
C
        SUBROUTINE CROPDATA( CROP, FIELD, DATE, KCROP, TYPENOW )
C
        PARAMETER ( NCROP=6 , NFIELD=10 , NSTG=5 )
        IMPLICIT INTEGER ( A - Z )
        DIMENSION PDATES( NCROP,NFIELD ), STAGEDAY( NCROP,NSTG )
        REAL      KEQCONST( NCROP, NSTG, 2), M, A, KCROP
        INTEGER   FC( 14 )
        CHARACTER*8 TYPENOW
        COMMON /FILCOD/ FC
C
        DATA (( PDATES( IC , IF ), IF=1, NFIELD), IC=1, NCROP)
C       1-ALFALFA,2-SOYBEANS,3-WHEAT & OATS,4-CORN,5-SORGHUM,6-PASTURE
     & /  62,  66,  69,  73,  71,  75,  78,  82,  87,  93,
     &   126, 134, 142, 149, 155, 158, 162, 167, 173, 186,
     &    54,  59,  62,  65,  68,  70,  74,  79,  84,  93,
     &   107, 112, 117, 122, 127, 130, 135, 142, 149, 161,
     &   120, 129, 134, 138, 143, 149, 155, 161, 169, 181,
     &    73,  73,  73,  73,  73,  73,  73,  73,  73,  73 /
C
        DATA  ((STAGEDAY( IC, IS ), IS=1, NSTG), IC=1, NCROP)
     & /  20,  61, 183, 217, 365,
     &    19,  49, 102, 139, 365,
     &    31,  67, 105, 117, 365,
     &    31,  72, 122, 166, 365,
     &    28,  68, 112, 140, 365,
     &    20,  61, 183, 217, 365/
C
        DATA  ((( KEQCONST( IC,IS,IK), IK=1,2), IS=1,NSTG), IC=1,NCROP)
     & / 0.0   , 0.7  , 0.004, 0.627, 0.0   , 0.85 ,
     &  -0.01  , 2.7  , 0.0  , 0.5  ,
     &   0.0   , 0.7  , 0.012, 0.478, 0.0   , 1.05 ,
     &  -0.016, 2.7   , 0.0  , 0.45 ,
     &   0.0   , 0.7  , 0.011, 0.356, 0.0   , 1.1  ,
     &  -0.071, 8.54  , 0.0  , 0.25 ,
     &   0.0   , 0.7  , 0.010, 0.398, 0.0   , 1.1  ,
     &  -0.013, 2.625, 0.0   , 0.55 ,
     &   0.0   , 0.7  , 0.009, 0.455, 0.0   , 1.05 ,
     &  -0.020, 3.25  , 0.0  , 0.5  ,
     &   0.0   , 0.7  , 0.001, 0.68 , 0.0   , 0.75 ,
     &  -0.007, 2.1   , 0.0  , 0.5  /
C
C
C.
        PLNTDATE = PDATES ( CROP , FIELD )
        CROPCNT = DATE - PLNTDATE
C
C       DETERMINE THE STAGE OF THIS CROP SUCH AS EMERGED, HARVESTED, ...
C
        FOR STAGE=1, 5
        IF( CROPCNT .LT. STAGEDAY( CROP, STAGE ) )  GOTO 10
        END FOR
 10     M = KEQCONST( CROP, STAGE, 1 )
        A = KEQCONST( CROP, STAGE, 2 )
        KCROP = A +  M * CROPCNT
C
C       TREAT ALL AS MEDIUM ROUGH BARE BEFOR EMERGENCE
C
        IF( STAGE .LT. 2 ) THEN
        TYPENOW = 'MEDMBARE'
        RETURN
>
```

```
      END IF
C
C     IF CROP STAGE IS AFTER EMERGENCE AND BEFOR HARVEST
C     THEN TREAT IT AS A CANOPY
C
      IF( STAGE .LT. 5 ) THEN
      TYPENOW = 'CANOPY  '
      RETURN
      END IF
C
C     AFTER HARVEST TREAT WHEAT, OATS AND ALFALFA AS SMOOTH BARE
C     AND TREAT ALL OTHERS AS MEDIUM ROUGH BARE
C
      IF( (CROP .EQ. 1) .OR. (CROP .EQ. 3) ) THEN
      TYPENOW = 'SMTHBARE'
      ELSE
      TYPENOW = 'MEDMBARE'
      END IF
C
      RETURN
      END
>
```

```
C
C
C------SOILDATA
C
C
C       THIS ROUTINE FINDS THE BULK DENSITY OF THE GIVEN SOIL
C       BASED ON THE BULK DENSITY DISTRIBUTION WITHIN THAT
C       SOIL, AND RETURNS OTHER REQUIRED INFORMATION ABOUT THE GIVE
C       SOIL SUCH AS WILTING POINT WATER CONTENT, FIELD CAPACITY
C       WATER CONTENT, HYDRAULIC CONDUCTIVITY AT SATURATION, ETC.
C
        SUBROUTINE SOILDATA( SOIL, SFPROS, RTPROS, SFFC, RTFC,
     &                       SFWP, SATHC, SUCTION )
C
C
        IMPLICIT INTEGER ( A - Z )
C
        PARAMETER ( NSOIL= 8 , NBD= 15 )
        REAL    SFBULK(NBD), B(NSOIL), FSUCTION(NSOIL), ALFA(NSOIL)
        REAL    RTBULK( NBD ), SSUCTION( NSOIL ), SHYDCOND( NSOIL )
        REAL    SFPROS, SATHC, SUCTION, SATSUCT, SFWP, SFFC, RTFC
        REAL    RTPROS, FBD, RTBD
        LOGICAL FRSTCALL
        COMMON /BUF2/  PROBABIL( NSOIL , 100 ), PERCENTS( NSOIL ,NBD )
        SPECIAL COMMON BUF2
C
        DATA ((PERCENTS(IS, IBD), IBD=1, NBD), IS=1,NSOIL)
     & /  0,  0,  0,  0,  0,  7,  7, 22, 22, 14, 14, 14,  0,  0,  0,
     &    0,  0,  0, 11, 26, 26, 26, 11,  0,  0,  0,  0,  0,  0,  0,
     &    2,  3,  3,  8, 18, 20, 17, 11, 12,  3,  3,  0,  0,  0,  0,
     &    0,  0,  1,  9, 22, 25, 14, 11,  9,  5,  2,  2,  0,  0,  0,
     &    0,  0,  0, 18, 18, 28, 18, 18,  0,  0,  0,  0,  0,  0,  0,
     &    1,  1,  1,  7, 18, 22, 23, 15,  7,  4,  1,  0,  0,  0,  0,
     &    0,  0,  0,  7, 19, 18, 30, 15,  7,  4,  0,  0,  0,  0,  0,
     &    0,  0,  0,  0,  0,  0,  0,  0,  0, 15, 31, 23,  8, 15,  8 /
C
        DATA  SFBULK/ 0.818, 0.888, 0.957, 1.03, 1.10, 1.17, 1.24, 1.30,
     &                1.37 , 1.44 , 1.51 , 1.58, 1.65, 1.72, 1.79 /
        DATA  RTBULK/ 1.10, 1.15, 1.20, 1.25, 1.30, 1.35, 1.40, 1.45,
     &                1.50, 1.55, 1.60, 1.65, 1.70, 1.75, 1.80 /
C
        DATA  B
     & /  9.77,  6.66,  7.21,  6.81,  6.22,  6.81,  6.66,  4.26 /
        DATA  FSUCTION
     & / 21.49, 13.91, 12.90, 13.18, 16.03, 13.18, 13.91,  3.22 /
        DATA  SSUCTION
     & / 31.20, 34.67, 30.76, 33.08, 39.25, 33.08, 34.67, 10.14 /
        DATA  SHYDCOND
     & / 0.814,  2.33,  2.02,  2.31,  2.39,  2.31,  2.33, 58.36 /
        DATA    FRSTCALL/ .TRUE. /
C
C
C       SET UP THE PROBABILITY ARRAY FOR BULKDENSITY DETERMINATION
C       OF EACH SOIL TYPE. (ONLY AT FIRST CALL)
C
        IF( FRSTCALL ) THEN
        FRSTCALL = .FALSE.
        FOR  IS=1, NSOIL
        ALFA( IS ) = 1 / B( IS )
        END FOR
        FOR  IS=1, NSOIL
        START = 1
        STOP = 0
        FOR  BDCODE=1, NBD
        PERC = PERCENTS( IS , BDCODE )
        IF( PERC .NE. 0 ) THEN
        STOP = STOP + PERC
        FOR  I=START, STOP
        PROBABIL( IS, I ) = BDCODE
        END FOR
>
```

```
      START = START + PERC
      END IF
      END FOR
      IF( STOP .NE. 100 ) WRITE(11,'(1X,'STOP=',I4,I6)')STOP,IS
      END FOR
      END IF
C
C     GET THE BULK DENSITY ACCORDING TO THE PROBABILTY FOR THIS SOIL
C     FOR BOTH SURFACE LAYER (0-5 CM) AND ROOT LAYER (5-95 CM)
C
      RANDOM =IRAN( 1 , 100 )
      BDCODE = PROBABIL( SOIL, RANDOM )
      SFBD = SFBULK( BDCODE )
      RTBD= RTBULK( BDCODE )
C
C     CALCULATE THE WATER CONTENT OF EACH SOIL TYPE AT WILTING POINT
C     AND FIELD CAPACITY. SPECIFIC BULK DENSITY IS 2.65 FOR ALL SOILS
C
      SFPROS = 1 -  SFBD / 2.65
      RTPROS = 1 -  RTBD / 2.65
      SFFC =  SFPROS *  ( SSUCTION( SOIL ) / 333.0 ) ** ALFA( SOIL )
      RTFC =  RTPROS *  ( SSUCTION( SOIL ) / 333.0 ) ** ALFA( SOIL )
      SFWP =  SFPROS *  ( SSUCTION( SOIL ) / 15000 ) ** ALFA( SOIL )
      SUCTION = FSUCTION( SOIL )
      SATHC = SHYDCOND( SOIL )
      RETURN
      END
>
```

```
C
C
C------GETFILES
C
C       THIS ROUTINE OPENS ALL THE INPUT AND OUTPUT FILES AND
C       ASSIGNS AN AVAILABLE UNIT (FILECODE) ON WHICH THE FILE
C       WILL BE OPENED.
C
        SUBROUTINE GETFILES
C
        INTEGER*1  FILENAME( 17 )
        INTEGER    FC( 14 ), ERRCODE
        LOGICAL    ERR
        COMMON /FILCOD/ FC
C
C
        WRITE(11,104)
        READ(12,102) FILENAME
        CALL OPN( FC(1), FILENAME,'OLD','FOR',ERRCODE,ERR)
        IF( ERR ) THEN
        WRITE(11,101) FILENAME, ERRCODE
        STOP
        END IF
        READ(FC(1),*) NUMFILES
        FOR  I=2,NUMFILES+1
        READ(FC(1),102) FILENAME
        CALL OPN(FC(I),FILENAME,'OLD','UNF',ERRCODE,ERR)
        IF( ERR ) THEN
        WRITE(11,101) FILENAME, ERRCODE
        STOP
        END IF
C       WRITE(11,103) FILENAME, FC(I)
        END FOR
        RETURN
 101    FORMAT(1X,'ERROR ****  WHILE OPENINIG '17A1,'ERRCODE='I3)
 102    FORMAT(17A1)
 103    FORMAT(1X,17A1,'WAS ASSIGNED TO'I4)
 104    FORMAT(1X,'ENTER NAME OF THE FILE WHICH CONTAINS INPUT',
     &  ' AND OUTPUT FILE NAMES')
        END
>
```

```
C
C
C------IOCALLS
C
C
C       THIS ROUTINE HAS TWO ENTRIES USED IN READING AND WRITING
C       FROM AND TO THE I/O FILES
C
        SUBROUTINE IOCALLS
C
        IMPLICIT INTEGER ( A - Z )
        PARAMETER ( NWRD =1245 , NPAUSE=3 )
        DIMENSION RECORD( NWRD ), MATRIX( NPAUSE, NWRD )
        INTEGER  FC( 14 )
        COMMON /FILCOD/ FC
C
C
C
        ENTRY  READREC ( FILECODE, RECORD, NWORDS )
C       --------------
        BUFFER IN ( FILECODE, RECORD, B, NWORDS, IO )
        CALL STATUS( FILECODE )
        IF( IO .NE. 2 ) THEN
        WRITE(11,101) FILECODE, IO
        STOP
        END IF
        RETURN
C
C
        ENTRY  WRITDATA ( IDENT , MATRIX, NCOL )
C       ---------------
C
        IF( IDENT .EQ. 1 )   OTFILE=FC(6)
        IF( IDENT .EQ. 2 )   OTFILE=FC(10)
        FOR  IP=1, NPAUSE
        FOR  COL=1, NCOL
        RECORD( COL ) = MATRIX( IP , COL )
        END FOR
        BUFFER OUT( OTFILE, RECORD, B, NCOL, IO )
        CALL STATUS( OTFILE )
        IF( IO .NE. 2 ) THEN
        WRITE(11,102) OTFILE, IO
        STOP
        END IF
        OTFILE = OTFILE + 1
        END FOR
        RETURN
C
 101    FORMAT(1X,'ERROR **** WHILE READING FROM UNIT'I4,'  STATUS',I4)
 102    FORMAT(1X,'ERROR **** WHILE WRITING TO UNIT 'I4,'   STATUS='I4)
        END
>
```

```
C
C
C-------UPDTHIST
C
C
C       THIS ROUTINE'UPDATES THE HISTOGRAMS
C
        SUBROUTINE UPDTHIST( VAL, HIST, INDEX, MIN, MAX )
        IMPLICIT INTEGER ( A - Z )
        PARAMETER ( NPAUSE=3 )
        DIMENSION  HIST( NPAUSE, MAX )
C
C
C       UPDATE MIN, MAX VALUES OF DATA
C
        HIST( INDEX , 1 ) = MIN0( HIST( INDEX , 1 ) , VAL )
        HIST( INDEX , MAX-MIN+5) = MAX0( HIST( INDEX , MAX-MIN+5), VAL )
C
C       UPDATE THE TOTAL NUMBER OF VALUES COUNTED
C
        HIST( INDEX , MAX-MIN+6) = HIST( INDEX, MAX-MIN+6 )+1
C
C       UPDATE THE FREQUENCY COUNT FOR THIS VALUE
C
        VAL = MAX0( MIN0( MAX+1 , VAL), MIN-1)
        HIST( INDEX, VAL-MIN+3 ) = HIST( INDEX, VAL-MIN+3 ) + 1
        RETURN
        END
>
```

```
C
C
C------OTPTHIST
C
C
C       THIS ROUTINE TAKES A GIVEN HISTOGRAM ARRAY CONTAINING THE
C       FREQUENCIES AND WRITES OUT THE PERCENTS AND CUMULATIVE
C       PERCENTS FOR EACH DATA VALUE.
C
        SUBROUTINE OTPTHIST( HIST, INDEX, MIN, MAX )
C
        IMPLICIT INTEGER ( A - Z )
        DIMENSION  HIST( 3, MAX )
        REAL  TOTAL, SUM
C
C
        TOTAL = HIST ( INDEX , MAX-MIN+6 )
        SUM = HIST( INDEX , 2 )
C
C       WRITE OUT INFORMATION ON DATA POINTS ENCOUNTERED WHICH
C       WERE LESS THAN THE INDICATED MINIMUM VALUE
C
        WRITE(13,100) MIN, HIST( INDEX, 2 ), SUM/TOTAL, SUM/TOTAL
C
C       WRITE OUT PERCENTS AND CUM PERCENTS FOR ALL VALUES FROM
C       INDICATED MINMUM VALUE THROUGH MAXIMUM VALUE
C
        FOR  PTR= 3, MAX-MIN+3
        COUNT = HIST( INDEX, PTR )
        SUM = SUM + COUNT
        IF( COUNT .NE. 0 ) THEN
        WRITE(13,101) MIN+PTR-3, COUNT, COUNT/TOTAL, SUM/TOTAL
        END IF
        END FOR
C
C       WRITE OUT INFORMATION ON DATA POINTS ENCOUNTERED WHICH
C       WERE LARGER THAN THE INDICATED MINIMUM VALUE
C
        COUNT = HIST( INDEX, MAX-MIN+4 )
        SUM   = SUM + COUNT
        WRITE(13,102) MAX, COUNT, COUNT/TOTAL, SUM/TOTAL
C
C       WRITE OUT TOTAL NUMBER OF VALUES, MIN VALUE AND MAX VALUE
C       THAT WAS ENCOUNTERED
C
        WRITE(13,103) TOTAL, HIST( INDEX , 1 ), HIST( INDEX , MAX-MIN+5)
        RETURN
C
  100   FORMAT(/9X,'RANGE',14X'COUNT',7X,'PERCENT'10X'CUM PERCENTS',
     & //5X,'<'I7,5X,'-',5X,I8,5XE14.7,5XE14.7)
  101   FORMAT(7X,I6,5X,'-'5X,I8,5XE14.7,5X,E14.7)
  102   FORMAT(5X,'>',I7,5X,'-',5X,I8,5XE14.7,5XE14.7)
  103   FORMAT(2XF10.1,' TOTAL VALUES COUNTED'5X'MIN AND MAX VALUES'
     & ' ENCOUNTERED = 'I9,2XI9)
        END
```